Cytoskeleton dynamics and cell remodelling during *Arabidopsis thaliana* lateral root development

Dissertation

Submitted to the
Combined Faculty of Natural Sciences and Mathematics
of the Ruperto Carola University Heidelberg, Germany
for the degree of
Doctor of Natural Sciences

Amaya Vilches Barro

Heidelberg, 2018

Dissertation

Submitted to the

Combined Faculty of Natural Sciences and Mathematics

of the Ruperto Carola University Heidelberg, Germany

for the degree of

Doctor of Natural Sciences

Presented by

Amaya Vilches Barro, Master of Science

Born in Madrid, Spain

Oral-examination: 26th October

Cytoskeleton dynamics and cell remodelling during *Arabidopsis thaliana* lateral root development

Referees: Prof. Dr. Alexis Maizel

Prof. Dr. Karin Schumacher

Table of contents

Summary

Plants are characterized by an unparalleled ability to adapt to their environment by forming organs post-embryonically. In contrast to animal cells, plant cells are encaged in a rigid extracellular matrix, the cell wall, which glues cells tightly to their neighbours. The presence of the cell wall precludes cell migration and determines that plant morphogenesis relies on the ability of cells to control the direction of growth and the orientation of cell division. The microtubule and actin cytoskeletons play an essential role in the control of these processes. Cortical microtubules guide the deposition of cellulose fibrils in the cell wall and in consequence dictate the shape and growth direction of the cell. Actin is essential for the establishment and maintenance of cell polarity and together with microtubules orchestrates cell division.

The root system is formed by the continuous growth of root tips and branching of lateral roots. This enables anchoring and efficient absorption of water and nutrients. The branching of lateral root starts with the coordinated division of two pericycle founder cells located in the outer most layer of the main root vasculature. During this phase, called lateral root initiation (LRI), founder cells swell synchronously and their nuclei migrate towards the common cell wall Once nuclei are asymmetrically localized, founder cells divide asymmetrically originating two small daughter cells in the centre and two long daughter cells at the flanks.

In this work, we combined cytoskeleton tissue-specific markers and confocal live imaging to determine the role of the cytoskeleton in the coordination of the swelling and nuclear migration of founder cells during LRI. We observed that founder cells expand more in the central domain than in the periphery, a process amplified by the asymmetric positioning of the nucleus and pursued after the first asymmetric cell division (ACD). We observed that after ACD, microtubules reorganise in a parallel array at the periphery and remain more isotropic in the central domain. Genetic and pharmacological perturbation of microtubule organization, support a model in which the graded organization of microtubules constraints radial expansion at the periphery and allow fast expansion of the central cells. We detected that before cell division actin bundles reorganize in a polarized mesh around the nucleus.

Pharmacological disruption of actin network revealed that actin is essential for the migration of the nucleus, the asymmetry of cell division and cell expansion. Auxin is an essential regulator of LRI that controls in particular the expression of LBD16, a transcription factor involved in the polar migration of nuclei during LRI. Expression of the repressor LBD16-SRDX abolishes nuclear migration and asymmetric cell division. We observed that cytoskeleton polarity and organization are disrupted in the LBD16-SRDX background, where asymmetric cell expansion is also impaired.

After initiation, founder cells divide and expand to form a dome shaped primordium (LRP) in response to the spatial accommodation of the overlaying endodermis. In a second part of this work, we observed that disturbing microtubule dynamics hinders the spatial remodelling of the endodermis and delays the growth of the LRP. We found that microtubule organization in the endodermis is dependent on SHY2-mediated auxin signalling and shows a cell face-determined pattern.

In conclusion, our results evidence the importance of cytoskeleton dynamics during LRI and the spatial accommodation of the endodermis and reveal a role for auxin signalling in these processes

Zusammenfassung

Pflanzen zeichnen sich durch eine beispiellose Anpassungsfähigkeit an ihre Umwelt aus, indem sie postembryonale Organe bilden. Im Gegensatz zu tierischen Zellen sind pflanzliche Zellen in der Zellwand eingehüllt, die die Zellen fest mit ihren Nachbarn verbindet. Das Vorhandensein der Zellwand schließt Zellmigration aus und bestimmt, dass die Pflanzenmorphogenese von der Fähigkeit der Zellen anhängt, die Wachstumsrichtung und die Ausrichtung der Zellteilung zu kontrollieren. Die Mikrotubuli und Aktin-Zytoskelette spielen eine wesentliche Rolle bei der Steuerung dieser Prozesse. Kortikale Mikrotubuli leiten die Ablagerung von Zellulosefibrillen in der Zellwand und bestimmen somit die Form und Wachstumsrichtung der Zelle. Aktin ist essentiell für den Aufbau und Erhalt der Zellpolarität und orchestriert zusammen mit Mikrotubuli die Zellteilung. Das Wurzelsystem wird durch das kontinuierliche Wachstum der Wurzelspitzen und der Verzweigung der Seitenwurzeln gebildet. Die Verzweigung der Seitenwurzel beginnt mit der koordinierten Teilung von zwei Perizykel-Gründerzellen, die sich in der äußersten Schicht der Hauptwurzelvaskulatur befinden. Während dieser Phase, der sogenannten lateralen Wurzelinitiierung (engl. „LRI“), schwellen die Gründerzellen synchron an und ihre Zellkerne wandern in Richtung der gemeinsamen Zellwand. Sobald die Kerne asymmetrisch lokalisiert sind, teilen sich die Gründerzellen asymmetrisch, wobei zwei kleine Tochterzellen im Zentrum und zwei lange Tochterzellen an den Flanken entstehen.

In Dieser Arbeit kombinierten wir zytoskelettspezifische Marker und Konfokale Live-Bildgebung, um die Rolle des Zytoskeletts bei der Koordination der Schwellung und Kernmigration von Gründerzellen während der LRI zu bestimmen. Wir beobachteten, dass Gründerzellen in der zentralen Domäne mehr expandieren als in der Peripherie, ein Prozess, der durch die asymmetrische Positionierung der Kerns Verstärkt und nach der ersten asymmetrischen Zellteilung (engl. „ACD“) verfolgt wird. Wir beobachteten, dass sich Mikrotubuli nach der ACD in einer parallelen Anordnung an der Peripherie reorganisieren und im zentralen Bereich isotroper bleiben. Genetische und pharmakologische Störungen der Mikrotubuli-Organisation unterstützen ein Modell, bei dem die abgestufte Organisation der Mikrotubuli die radiale Expansion an der Peripherie einschränkt und eine schnelle Expansion der Zentralzellen ermöglicht. Wir haben festgestellt, dass sich vor der Zellteilung Aktinbündel in einem polarisierten Netz um den Kern herum reorganisieren. Pharmakologische Störungen des Aktin-Netzwerks zeigten, dass Aktin für die Migration des Zellkerns, die Asymmetrie der zellteilung und Zellausdehnung unerlässlich ist. Auxin ist ein wesentlicher Regulator LRI, der insbesondere die Expression von LBD16 kontrolliert, einem Transkriptionsfaktor, der an der polaren Migration von Zellkernen während der LRI beteiligt ist. Die Expression des Repressors LBD16-SRDX hebt die Kernmigration und die asymmetrische Zellteilung auf. Wir beobachteten, dass Zytoskelettpolarität und -organisation im LBD16-SRDX-Hintergrund gestört sind, wo auch die asymmetrische Zellausdehnung beeinträchtigt ist. Nach der Initiierung teilen sich die Gründerzellen und expandieren zu einem kuppelförmigen Primordium (LRP) als Reaktion auf die räumliche Akkomodation der überlagerten Endodermis. In einem zweiten Teil dieser Arbeit wurde festgestellt, dass eine störende Mikrotubuli-Dynamik die räumliche Remodelleriung der Endodermis behindert und das Wachstum des LRP verzögert. Wir fanden heraus, dass die Mikrotubuli-Organisation in der Endodermis von SHY2-vermittelten Auxin-Signalen abhängt und ein zellgesichtsbestimmtes Muster zeigt.

Unsere Ergebnisse belegen die Bedeutung der Zytoskelett-Dynamik während der LRI und der räumlichen Akkomodation der Endodermis und zeigen eine Rolle für die Auxin-Signalisierung in diesen Prozessen

1 Introduction

1.1 Cellular basis of morphogenesis in plants

To understand the mechanics of plant growth, it is important to review first the fundamental properties of plant cells. In contrast to animals, plants cells are encased in a rigid but elastic cell wall that counteracts the internal turgor pressure. Therefore at a cellular level, plant growth depends on the balance between two mechanical forces: the internal turgor pressure pushing from the inside of the cells and the rigid but expandable cell wall, that prevents plant cells from bursting [1].

The cell wall cement cells with their surrounding neighbours. Therefore, while at cellular level, mechanical stress is originated by turgor pressure, at the tissue level mechanical stresses derive from the growth of adjacent cells [2] or differential cell expansion and proliferation rates of neighbouring tissues [3].

Differential growth between neighbour cells creates local tensions and compressions, which feedback on molecular effectors at a cellular level, like microtubules, which align with supra cellular tensions, derived from organ shapes [4, 5].

Interphase microtubules or cortical microtubules (CMT) in plants are associated to the plasma membrane, where CMT guide for the deposition of cellulose at the cell wall [6]. The orientation of cellulose microfibrils in one direction reinforces the cell wall and cell growth occurs on the perpendicular direction [1]. Therefore the orientation of CMT directly impacts on the direction of growth [7].

Similar to CMT, the auxin efflux transporter PIN1 is also responsive to mechanical deformations [8]. In the shoot apical meristem (SAM) PIN1 localizes at the plasma membrane that is parallel to the orientation of CMT [9]. Ablation of cells at the SAM creates circumferential pattern of stress, which result in circumferential orientation of CMT and relocation of PIN1, indicating that PIN1 and CMT are under the control of a common upstream element [1, 9].

Pharmacological-induced changes of cell wall stiffness have a direct impact on the polar organization of PIN1 [10]. These observations suggest that the orientation of CMT and the stiffness of the cell wall directly influence the direction of polar auxin transport (PAT).

PAT is determinant for the creation of auxin gradients and the formation of auxin maxima, which are instrumental for organ growth in plants [11].

At a cellular level, auxin directly impacts on cell wall softening by inducing changes in the apoplastic pH or activating the activity of cell wall remodelling enzymes (see below, [12]). Auxin also acts via Rho of Plants (ROPs) in orientation of CMT at a cellular level helping to create local constraints of cell expansion and thereby shaping cells (See bellow)[13].

In sum, there is a feedback loop between mechanical stresses derived from growth and biochemical gradients. Both act on regulatory networks at the cellular level and regulate the collective behaviour of cells at a tissue level [1].

In the following section I will focus on directional cell expansion and asymmetric cell division, making specially stress on the role of cytoskeleton and their molecular regulators.

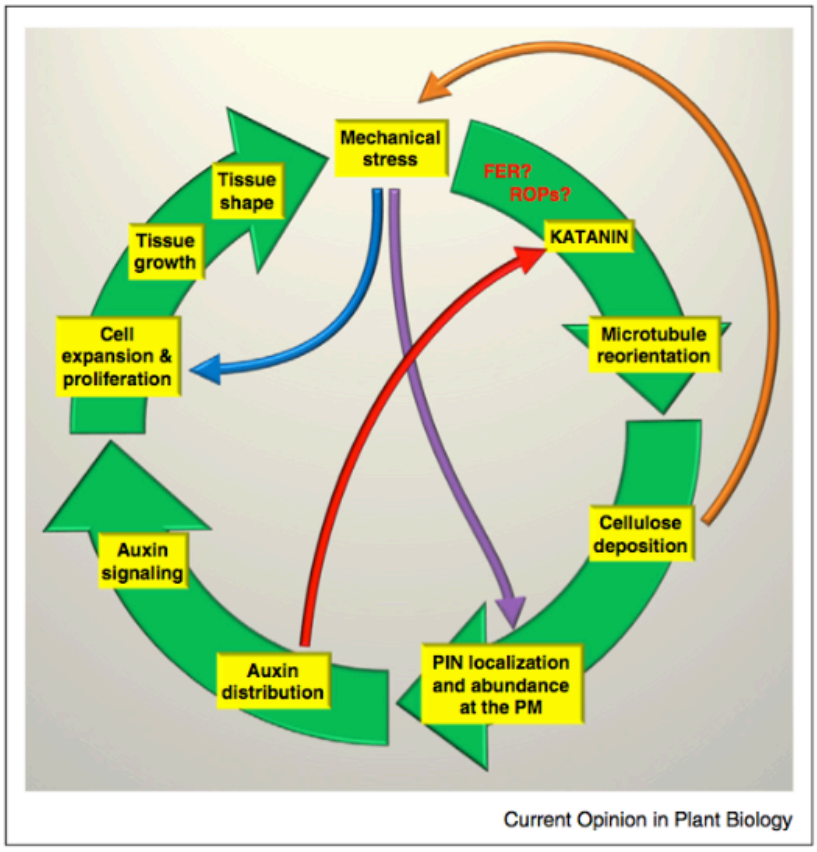

Fig. 1 Mechanical feedbacks in plant development. Adapted from [1]

1.1.1 Directed cell growth

Cell wall remodelling enables directional (or anisotropic) cell expansion to determine final cell shapes [14]. Cell expansion is achieved by local increase of cell wall (CW) extensibility [12]. The extension of cell walls requires a change in the biochemical composition and arrangements of cell wall polysaccharides, which is achieved by modifications of the chemical bounds between cell wall components mediated by the cell wall remodelling (CWR) enzymes. In order to grow, cell need to expand their cell wall irreversibly a process that also requires de-novo synthesis and deposition of new polysaccharides in the extracellular matrix [15-17].

1.1.1.1 Cell wall remodelling

There three classes of cell wall polysaccharides: cellulose, pectin and hemicellulose.

(I) Cellulose is a linear homopolysaccharide that can make up long and stiff microfibrils, which are interconnected by hemicellulose and pectin, constituting the load-bearing scaffold of the cell wall.

(II) Pectins, like homogalacturonan, are rich in galacturonic acid. Pectins are secreted in the cell wall in highly esterified forms. In the wall they become de-esterified allowing their polymerization by crosslinking with Ca^{+2}. Making linkages with glycoproteins and other carbohydrates, pectins can control the stiffness or flexibility of the cell wall.

(III) Xyloglucans and xylans are the most abundant hemicelluloses in cell walls. Depending on the level of acetylation, xyloglucans can be cross-linked to other cell wall components, like cellulose.

Cell wall components are assembled in the Golgi and are secreted in the cell surface. Once incorporated at the cell wall, polysaccharides are exposed to modifications by CWR

enzymes, which control cell wall properties and cell growth. [12, 14, 16, 18]. The best known of these proteins are:

(I) The A-TYPE EXPANSIN (EXPA). Expansins mediate cell wall loosening by modifying the interaction between xyloglucans and cellulose. Expansins mediate low-pH dependent cell wall loosening, yet they don't exhibit enzyme activities [19]. This mechanism could be responsible for the "acid-growth" hypothesis, which postulates that cell wall expands at acidic pH. By loosing the cell wall structure, EXPAs make other polysaccharides more expose to modifications.

(II) XYLOGLUCAN ENDOTRANSGLYCOSYLASE / HYDROLASES (XTHs) cleave and relegate xyloglucan backbones to incorporate fragments into the wall.

(III) Cell wall stability can be reduced by the degradation of pectins by polygalacturonase and cleavage by pectin lyases. Pectin can be also demethylesterified by PECTIN METHYL ESTERASES (PME) allowing its crosslinking with other pectins or cell wall proteins and thereby affecting cell wall elasticity. PME inhibitors counteract their activity and induce cell wall loosening. However, PME are also involved in cell wall loosening Therefore the interplay between PME and their inhibitors can fine-tune local expansion and growth and at the same time provide structural support.

Auxin promotes acidification of the apoplast and activates CWR, like EXPAs [20]. Auxin signalling is also behind the ROP/RIC/KATANIN signalling pathway that controls microtubule organization [13]. Moreover, auxin not only induces the activity, but also the transcriptional activation of CWR genes [16, 21]. Affecting rigidity of the cell wall affects the plasma membrane location of auxin transporters, closing the feedback loop between cell wall properties and auxin signalling [22].

Recently, it has been reported that cell wall and microtubule organization are connected in an auxin-independent manner [16]. Like this, CWRs can affect microtubule organization and induce cell expansion and outgrowth [23]. Also the surveillance of the status of the cell wall by receptors like the receptor-like kinase FERONIA, are transmitted into cellular responses, via ROP signalling, which control microtubule organization [24, 25]. Together, these observations show that auxin transport and signalling, cell wall dynamics and microtubule organization are intimately coordinated to regulate growth and proliferation.

1.1.1.2 Microtubules, cell wall properties and cell polarity

Microtubules are cylindrical hollow structures of ~24nm of diameter, that consist of 13 protofilaments held together by lateral interactions. Each protofilament is made out of alternation of alpha- and beta-tubulins monomers. Microtubules have a very dynamic nature, constantly switching between polymerization and depolymerization, their length ranging from few nanometres to several microns. This property is called dynamic instability [26, 27].

In contract with animals and fungi, plants lack organizing centres. Consequently microtubules during the interphase are arranged dispersed in a 2D space in close interaction with the cell cortex. For this reason, interphase microtubules are called cortical microtubules (CMT). CMT have the ability of collective self-orientation by mutual collision and re-growing. In a two dimensional space the probability of collisions is very high. Depending on the angle with which the plus-end of growing microtubule collisions with the lateral domain of another microtubule, this will undergo shrinkage or will continue growing. In general, shallow angles of collision favour microtubule growth, allowing the formation of parallel arrays of growing microtubules [27]. Not only self-organization but also hormonal gradients and mechanical stretching or compression are able to induce changes in CMT orientation [9, 28-30]. The protein KATANIN is a microtubule-severing protein than participates in the self-organization

of CMT in parallel arrays. Katanin mutants display randomly organized CMT, decreasing the ability of cells to counteract mechanical stresses [28]

Microtubule associated proteins (MAPs) are involved in several signalling pathways that determine the optimal organization of CMT [31]. Many MAPs mediate the anchorage of CMT to the plasma membrane. The plasma membrane-bound phospholipase D (PLD)[32]; the microtubule-binding protein CLASP [33] or the phosphatidic acid-bound MT-bundling protein, MAP65 [34], count among the best well known.

However, the slight detachment of CMT in the mutants of these genes, suggest that other proteins should redundantly participate in the interaction of cortical microtubules with the plasma membrane [26, 35].

The interaction between CMT and the plasma membrane-embedded cellulose synthase (CESA) complex, mediated by the cellulose synthase interactive protein1 (CSI1), also provides anchorage for CMT to the plasma membrane [36]. The major role of CMT in interphase cells is guiding the movement of the CeSa complexes, as they synthesize ß-1,4-glucan chains[6]. Glucan chains are packed together by lateral hydrogen bonds in cellulose microfibrils. Microfibrils provide the mechanical resistance of the cell wall to external stresses and internal turgor pressure. According to the microtubule-microfibril alignment hypothesis, parallel oriented microfibrils control cell expansion and their organization is determined by the orientation of CMT. In growing plant cells, CMT align perpendicular to the axis of cell expansion, directing the assembly of cellulose microfibrils, which constrain radial expansion [37].

Microtubules, in interaction with other proteins are also involved in the creation of plasma membrane domains. The association of CMT with the establishment of plasma membrane domains is regulated by the interaction with the Rho-GTPases in plants (ROPs), which act as signalling switches[38].

The association of ROPs to the plasma membrane depends on their lipid–based post-transcriptional modifications [35]. Among the ROPs, ROP2 and ROP6 in interaction with the target-effector ROP-interactive CRIB motif–containing1 (RIC1) regulate the interaction of CMT with the plasma membrane and by activating KATANIN, induce the formation of CMT bundles [13].

Recently the IQD protein family has been described as signalling linkers between Ca^{+2} signalling and CMT dynamics or stability [39, 40]. Plasma membrane domains created by the interaction between microtubules and membrane-associated proteins participate in the formation of the pitted pattern of the secondary cell wall of xylem vessels. IQD13, ROP11/MID11/KINESIN13A establish a signalling bridge to create local plasma membrane domains, necessary for the proper development of xylem vessels [41].

1.1.1.3 The role of actin in cell wall remodelling and cell polarity

The building blocks of actin filaments are monomeric 42-KDa adenosine triphosphate (ATP)-binding proteins, called G-actin, which have the ability of self-assembly or addition to existing F-actin filaments. After nucleation, via the formation of a homo/ hetero-trimer complex, actin filaments elongate in a process that requires the addition of ^{ATP}G-actin to the growing plus end of the new actin-trimmer or a pre-existing filament.

The versatile and dynamics functions of actin rely on its organizational switch between monomeric globular (G)- and filamentous (F)-actin. Actin interacts with more than 72 proteins in plants, the actin-binding protein superfamily. These proteins are important regulators for the structural organization of actin filaments but also link actin to different cellular processes like cell division elongation, establishment of cell polarity and movement, endocytosis and vesicle trafficking.

ATP hydrolysis and the activity of the actin-depolymerizing factor (ADF) drive the depolymerisation of the actin filament at the ^{ADP} F-actin end in a process called “treadmilling”. The balance between these two processes of growth and depolymerisation control the direction of F-actin filaments [42].

Important regulators of actin activity and organization are the formin proteins, the networked (NET) superfamily and phospholipase D (PLD). Formins, which are important organizers of actin nucleation, elongation and severing, mediate also the association of actin to the plasma membrane. PLDs catalyse the hydrolysis of plasma membrane phospholipids, like phosphatidylcholine, to produce phosphatic acid (PA). PDL binds at the plasma membrane with actin filaments and microtubules for the creation of specific plasma membrane domains. Last but not least, the actin-bind NET superfamily controls the association of actin to the plasma membrane and the plasmodesmata [35].

Actin is essential for the delivery of Golgi vesicles with cell wall material and enzymes to the expanding membrane in tip-growing cells, like pollen tube and root hairs. In these cells actin creates a polar domain with fine F-actin at the tip and actin cables along the growing axis, which act as tracks for cytosplasmic streaming of vesicles, which will fuse to the plasma membrane. As important regulators of cell polarity, ROPs participate in the polarization of actin organization and vesicle transport in tip-growing cells. Consequently, morphological defects on pollen tube growth and pavement cell expansion are directly related to ROP-associated actin defects [38, 43, 44].

Polar localization of the auxin efflux transporters is achieved by the constitutive cycling between the plasma membrane and the endosomal compartments in an actin-dependent manner [45, 46] Indeed, chemical alteration of the actin cytoskeleton has a direct effect in the polar distribution of PIN proteins [47]. A positive feedback loop has been reported in pavement cells in which ROP2-mediated stabilization of actin microfilaments facilitate PIN export at lobe regions. In turn, accumulation of auxin at lobes, induce the expression of ROP2 to maintain PIN1 plasma membrane association [46, 48].

Membrane contact of actin with the plasma membrane is important for cell wall formation, not only by regulating the exocytosis of vesicles or inducing accumulation of auxin efflux transporters (see below [49]); also actin interacts with CMT influencing the distribution of cellulose synthesis complexes at the plasma membrane [50]

The interaction between actin and microtubules is not always synergic. In fact, the ROP/RIC-mediated actin and microtubule mutual inhibition allow the formation of local plasma membrane domains in tip-growing cells as well as in the pavement cells [43].

1.1.2 Cell division orientation

The presence of the cell wall around cell plants implies that after division, plant cells need to build a new cell wall between the two daughter cells. Already long time ago, it

became clear that the position of the new cell wall is dependent on the geometry of the cell (Reviewed by[51]). Modern cell-division models propose that in longitudinal cells the cell division occur in shortest distance that divides a mother cell in two halves. However, in polygonal cells the division plane is rather random and can be influenced by surrounding mechanical forces [52]. These rules however only apply for symmetric dividing cells [51, 53]. Asymmetric cell divisions override cell geometry and the division plane is determined by polar cues (Shao and Dong 2016).

1.1.2.1 Formative division in plant development

In contrast with symmetric cell divisions, asymmetric cell division allows the formation of different cell types, while proliferative divisions allow additional growth [54].

Symmetry breaking usually precedes asymmetric cell division. Asymmetry of daughter cells is not necessary geometric with unequal partition of volume upon division. Equally sized cells can acquire different cell fates through positional or external cues. Therefore, we can distinguish between two kinds of factors that cause asymmetry during cell division; intrinsic and extrinsic factors.

Intrinsic factors are polarizing cues in the mother cell. These cells generally produce daughter cells with different sizes. Extrinsic factors are external factors that after division induce different fates in daughter cells [54].

In plants, the presence of the cell wall favors the acquisition of different fates by extrinsic factors, like positioning with respect to a molecular gradient and cellular communication. Some examples in of mobile factors that control cell division and cell fate decisions are WOX5 during the division of columella stem cells [55] in the root apical meristem (RAM), or TARGET OF MONOPTEROS7 (TMO7) during the division of the hypophysis in the embryo [56].

However, a number of cells in plant development produce daughter cells with distinct cell sizes, whose asymmetry is determined by polarization of proteins in the mother cells before cell division. This is the case of the polar localization of the intrinsic regulator BREAKING OF ASYMMETRY IN THE STOMATAL LINEAGE (BASL), which is instrumental for stomatal asymmetric division (See bellow) [54, 57].

The interaction of cell-cycle regulators and proteins necessary for the establishment of division plane determine the polar migration of the parental nucleus and the asymmetric position of the new cell wall. The cytoskeleton plays an important role during cell division. Here I describe how actin and microtubules participate in cell division and how are they coordinated by molecular regulators, to facilitate asymmetric division in plant cells.

1.1.2.2 The role of microtubules during cell division

In contrast with animal cells, cell division in vascular plants requires the formation of the preprophase band (PPB) prior division [51]. The PPB is a structure formed by microtubules and actin that marks the plane of cell division in G2, before mitosis. Although PPB is not required in all plant species and, the PBB ensures the robustness of cell division and the lack of PPB results in aberrant division planes [53, 58].

Several protein localize to the PPB. The PPB, dissembles during the prophase at the beginning of the mitosis, but several molecular markers remain at the plasma membrane site, where later the new cell plate will be formed. Among these regulators are TONNEAU1 (TON1) and TON2/ FASS-containing protein phosphatase PP2A. Together with TON1 and TON2, the TON1-recruiting motif (TRM) forms the (TON1/TRM/PP2A) TTP complex, which is essential for proper PPB assembly and division-plane establishment [59]. The TRM mutants grow properly, but fail to form the PPB, showing aberrant cell division planes [58].

Before the PPB completely disappears microtubules organized in the perinuclear spindle, whose main axis is perpendicular to the PPB orientation. The presence of the PPB is

important for the bipolarity and orientation of the spindle, which show aberrant orientations when the PPB is missing. The spindle dissembles at anaphase to form a bipolar microtubule array, which in late telophase will pull daughter chromosomes apart, towards the spindle poles. At telophase and during completion of cytokinesis the bipolar microtubule array is transformed into the phragmoplast. The phragmoplast guide the deposition of Golgi derived vesicles and expands centrifugally towards the region at the plasma membrane where the molecular markers for the former position of the PPB can be found [26]. Microtubules play a very important role during cell division and especially for the definition of the cell plane positioning. In symmetric dividing cells, the PPB is formed in the middle of the cell, where the nucleus migrates and divides.

Other mechanisms participate in the determination of the cell plane during asymmetric dividing cells. One of these molecular effectors has been discovered in the asymmetric division of stomatal precursor cells [57]. In Arabidopsis, the polar localization of the protein BREAKING OF ASYMMETRY IN THE STOMATAL LINEAGE (BASL) before cell division, predicts the position of the division cell plane [60]. BASL activates a mitogen-activated protein kinase (MAPK) signalling cassette, which is known to regulate microtubule dynamics, through phosphorylation of MAP65 microtubule-bundling factor [61]

Auxin signalling can influence symmetry breaking during cell division. Dominant negative mutations of the auxin-signalling repressor BODENLOS (BDL)/IAA12, revert asymmetric divisions in embryo development, rendering them symmetric [62]. Similarly, when the transcription repressor LBD16-SRDX is expressed in dividing cells during lateral root initiation, cell division is symmetric and lateral root formation is abolished [63]. However, it still remains unknown how auxin signalling may orient cell division plane.

1.1.2.3 The role of actin during cell division

Although the mitotic machinery is traditionally associated with microtubules, treatment with actin destabilizing drugs, induce defect in the orientation of the division cell plane, delay or even halt cell division, suggesting that actin plays a role in cell cycle progression [51, 64].

The PPB is a region of interaction for actin and microtubules. Different proteins like, formins, kinesins and myosins mediate actin-microtubule interactions at the PPB [51]. Later during metaphase, actin forms a cage-like structure, between the spindle and the cortex of the cell, which is though to maintain the correct axis during metaphase. During cytokinesis actin drives the transport of Golgi vesicles to the growing phragmoplast [64].

Actin also plays an important role in asymmetric division of subsidiary mother cells (SMC) during stomata development. The PAN1/ROP polarity module is thought to participate in the formation of polarized actin patch, affecting nuclear migration and asymmetric positioning of the cell division plane. An alternative hypothesis suggests that ROP-mediated actin nucleation and vesicle trafficking indirectly promotes cell wall loosening and local cell expansion. Local changes in the mechanical properties of the cell wall could induce microtubule reorganization and PPB formation [57]. Independently of the possible mechanism behind, actin polar patch formation is essential for establishment of asymmetric cell division in SMC.

Actin it is intimately associated with the nuclear envelope and participates in nuclear movements during asymmetric cell division. The actin-depolymerizing drug LatB blocks nuclear migration before the first asymmetric division of the zygote and renders cell division symmetric [65]. The SUN (SAD1/UNC84) and KASH (Klarsicht/ Anc/ Syne-1 homology) associates actin cytoskeleton to the outer membrane of the nuclear envelope, controlling the shape of the nucleus. Moreover, in combination with Myosin XI-I, KASH proteins control the movement of the vegetative nucleus from the pollen grain to the tip of the pollen tube during fertilization [66].

1.2 Lateral root formation

Lateral roots (LR) are formed post-embryonically from a small group of founder cells, located deep in the parental root. LR formation is a good system to study how cell growth and cell division coordinate to ensure the robust *de novo* formation of an organ. The formation of LR in Arabidopsis offers several advantages: first, the simple anatomy of Arabidopsis roots, consisting of single layers of epidermis, cortex and endodermis around the vascular tissue [67] and their optical transparency, allows easy imaging. Second, the continuous development of LR and their ordering along the primary root, with the younger stages close to the root tip, provides with numerous observations at different developmental phases. Third, mechanical or gravity-induced bending of the primary root, as well as exogenous treatment with auxin can induce LR development. This allows us to follow the development of a new LR, even before any sign of division.

Lateral root development is regulated by the action of different plant hormones [68]. From all of them auxin plays the most relevant role and is the best studied, being auxin signalling and auxin transport essential regulators of LR development at all developmental phases. Genetically- or chemically-induced perturbations on auxin signalling or transport have a direct effect on the number and the development of LR [67] [11, 68]. Therefore a short introduction about auxin signalling and transport is given in this chapter.

1.2.1 Auxin signalling

The transcriptional regulators, auxin responsive factors (ARFs) and AUX/IAA proteins mediate auxin-dependent gene regulation. In Arabidopsis there are 23 members of the ARF family. All ARFs bind to auxin-responsive elements (AuxREs) in the promoters of auxin responsive genes. ARFs can form homo and heterodimers with other ARFs and depending on the amino acid sequence of the middle region, ARFs can work as transcriptional activators or repressors of auxin responsive genes.
AUX/IAA proteins form heterodimers with ARFs, repressing their transcription-regulatory activity. In Arabidopsis there are 29 members of the transcriptional repressors AUX/IIAA family. These can also form homodimers with other AUX/IAA.

Auxin binds to a co-receptor complex formed by one of the six TRANSPORT INHIBITOR RESPONSE 1/AUXIN SIGNALLING F-BOX (TIR1/AFB) receptor protein encoded in Arabidopsis and one AUX/IAA repressor. Upon binding the co-receptor, auxin induces the targeting of AUX/IAA to Skp1-Cullin-F-box/Transport Inhibitor Response 1 (SCF^{TIR1}), leading to ubiquitiation of AUX/IAA proteins and proteolysis by the 26S proteasome. Degradation of AUX/IAA proteins liberates ARFs to regulate expression of auxin-responsive genes. Gain-of-function mutations of the domain II block the binding to SCF^{TIR1} resulting in constant inactivation of ARF function [69] and affect LR development at different developmental phases.

Also chromatin remodelling mediates auxin gene transcription regulation as ARFs and AUX/IAA heterodimers can bind TOPLESS (TPL), which recruits HISTONE DEACETYLASES (HDACs), resulting in tightly, packed chromatin. Degradation of AUX/IAA allows the interaction of SWI/SNF to ARFs, enabling chromatin unpacking by HISTONE ACETYLTRANSFERASE (HAT) activity and gene activation by the access of additional transcription factors (Review by [70]). ARFs expression is also regulated posttranscriptionally by micro RNAs (miRNAs) and transacting small interfering (tasiRNAs). These small RNA help to fine tune or increase the robustness of auxin signalling (Review by [70]).

Auxin-dependent transcriptional responses take between minutes and hours. However, auxin can also activate fast non-transcriptional developmental responses. The rapid auxin signalling processes are mediated by the activation of ion transporters at the plasma membrane (PM). Auxin modulates H^+ flux inducing pH changes and Ca^{+2} influx, increasing cytosolic Ca^{2+} as part of the fast auxin-induced responses [71]. Recently two

studies show that the receptor SCFTIR1/AFB not only mediates transcriptional activation of auxin -responsive genes in the nucleus via the proteosomal degradation of AUX/IAAs, but also is necessary for mediating fast developmental responses [72, 73]. The rapid auxin-dependent growth inhibition of epidermal cells in the inner side of the bend is mediated by SCFTIR1/AFB and auxin accumulation by AUX1, allowing root bending following the gravity vector [73]. The IAA/H^+-symporter, AUX1 drives the fast influx of auxin and protons (two H^+ per one IAA^-), leading to the depolarization of the plasma membrane. Cytosolic auxin is perceived by SCFTIR1/AFB, which together with cyclic nucleotide-gated channel CNGC14 activates Ca^{+2} channels, induces an increase on cytosolic Ca^{+2} levels [72].

1.2.2 Auxin transport

Auxin transport and local auxin biosynthesis play an important role in creating auxin gradients and maxima at cellular and tissue level [74]. Auxin gradients are essential for creating growth axis during embryonic development, maintenance of stem cells in meristems and tropic responses [75].

Auxin can be synthesized in leaves and cotyledons and transported in a long-distance pathway, like carbohydrates and other hormones, along the sieve elements and companions cells towards the root tip, which is one of the major sink tissues. However, auxin is also locally synthesized in the roots, contributing to the maintenance of gradients and maxima, necessary for proper root development. In the root tip or in the young lateral root primordia (LRP) where cells are not differentiated, auxin moves through the apoplast (Reviewed by [76]). The acid pH in the apoplast favours the protonated form of auxin, which can cross PM. Auxin influx is also aided by the action of the auxin uptake carriers of the AUX1/LIKE-AUX1 (AUX/LAX) family. De-protonated auxin in the cytoplasm cannot diffuse through the PM. Auxin efflux is driven by two classes of efflux carriers: the phosphoglycoproteins members of the B-subfamily ATP BINDING CASSETTE transporter family (ABCB/PGS) and the PIN-FORMED (PIN) [75].

The role of AUX/LAX and PIN transporters in the maintenance of PAT during LRP development has been extensively described [11, 77, 78]. Because of their importance for LRP development, I will focus in the molecular mechanisms controlling the polar localization of these two transporter families. Disrupting expression of AUX1 reduces the number of lateral roots whereas loss of LAX3 function affects LR emergence [77, 78].

AUX1 polar localization in protophloem cells at the root meristem depends on subcellular trafficking between the endoplasmic reticulum and the PM regulated by actin, the plant RHO-like small GTPases, Rho Of Plants (ROPs) and their activators ARF guanine nucleotide exchange factors (GEFs) [49].

ROPS act as molecular switches, need the interaction with GEFs to change from the GDP-bound inactive form, to the GTP-bound active form. In the embryo and early seedling development, the ROP activator GEF1 controls the polar distribution of AUX1 and the differential accumulation of PIN7 and PIN2, playing an essential role in controlling development at these stages [74].

Auxin efflux is also mediated by ABCB/PGS transporters, which were observed to interact with the auxin transport inhibitor N-1-naphthylphthalamic acid (NPA). Their location at the PM is dependent on the interaction with actin and the ABCB chaperone TWISTED DRAWF 1 (TDW1)[79].

Directional cell-to cell transport of auxin is controlled by the polar localization of PIN proteins at the PM. Mutation of different PIN proteins affects the number or the position of LRs [11]. PM localization of PIN proteins depends on their sequence polar targeting signals and their phosphorylation status, which is controlled by the PINOID kinase and the protein phosphatase2A (PP2A) [80].

The rapid redirection of auxin transport allows fast developmental responses. This is achieved by the rapid relocation of PINs from one cell side to the other (Reviewed by [75].

PINs are constantly moving between the PM and the endosomal compartments in constitutive cycles of clathrin-dependent endocytosis and ARF-GEF GNOM-dependent exocytosis to the PM [81]. Accordingly, affecting GNOM-dependent location of PIN at the PM reduces the number of LR (Reviewed by [82]). PINs are also targeted to degradation in the vacuole. The retromer components SORTING NEXIN1 (SNX1) and VACUOLAR PROTEIN SORTING29 (VPS29) participate in the transport of PIN proteins for degradation in the vacuole [83], which is also dependent of the microtubule network and gibberellin (GA) action [84].

Long-PINs like, PIN1, PIN2, PIN4 and PIN7 are responsible of polar auxin transport, whereas the so-called short-PINs, like PIN5 and PIN6, with reduced hydrophilic loop, are mostly located at the endomembrane system. PIN5 localizes to the ER, where it has been suggested to control intracellular auxin gradients (Reviewed by [85]. Similarly as the short-PINs, another protein family of auxin transports, PIN-likes (PILS), is found in the ER and work as internal auxin homeostasis regulation. Reduction or up regulation of PILS leads to alteration of LR formation, among other developmental effects (Reviewed by [86]).

1.2.3 Lateral root patterning

The formation of a lateral root starts when a small group of pericycle cells undergo a coordinated program of cell division to form a new LRP.

The pericycle is the outermost layer of the vascular tissue. It is made of a mixed population of cells: the phloem-associated pericycle and the xylem-associated pericycle, also called the xylem pole pericycle (XPP) cells. In contrast with the quiescent phloem-associated cells, XPP cells, adjacent to the protoxylem, leave the root apical meristem maintaining their meristematic activity and therefore are considered like a “meristem continuum” of the primary root [87]. The association with the xylem pole seems to be essential for the ability of XPP cells to divide. Mutation that disrupts the patterning of the xylem poles, affects the ability of their adjacent pericycle cells to form LRP [88].

XPP cells maintain cytological characteristics of meristematic cells, like dense cytoplasm, small vacuoles and big nuclei [87]. Besides, XPP cells are mitotically active along the life span of the plant, however these occasional divisions are mostly proliferative and do not lead to the formation of a new lateral root [89]. Although originally it was thought that dedifferentiation of XPP cells preceded the entrance in cell cycle, soon it was proved that these cells leave the root apical meristem in the G1 phase, and auxin induce the transition from G1 into S and G2 phase, prior division [90].

Lateral roots are formed acropetally and the younger developmental stages are found close to the root tip (reviewed by [91]). Even though all XPP cells are mitotically active, only a small group of XPP cells are able to originate LR. The process by which XPP acquire this condition is called priming and occurs in the root apical meristem. Priming of XPP cells determines the distance between two LRs and their right-left arrangement. The spatial distribution of LRP along the primary root is also called rhyzotaxis (reviewed by [91]).

Priming is detected as recurrent expression of the auxin-transcription reporter DIRECT REPEAT5 (DR5) at protoxylem cells adjacent to the XPP cells that will form a LRP. It has been suggested that signals go from the xylem into XPP cells to prime them for LR formation (Reviewed by [92].

The expression of many genes, like *ARF7* and *LATERAL ORGAN BOUNDARIES DOMAIN16 (LBD16)* (see below), was observed to oscillate in phase and antiphase with the DR5 reporter and the region where this process occurs is called the oscillation zone (OZ) [93, 94]. The PLETHORA (PLT) AP2-transcription factors PLT3, 5 and 7 control rhyzotaxis [95]. Activated by ARF7 and ARF19 (see below), the combined activity of these three PTLs determines the position of LRP to avoid that LR grow adjacent or close to each other [95].

Local auxin biosynthesis in the lateral root cap (LRC) contributes to LRFC specification. Auxin is formed from the precursor indole-3-butiric acid (IBA) in the outer cell of

the root cap and then transported into the OZ [96]. Programmed cell death (PCD) of LRC cells at the start of the elongation zone is coupled in time with DR5 oscillation and LRFC specification [97]. It is suggested that PCD of outer LRC cells releases auxin into the epidermis and causes an auxin maximum in the OZ, contributing to gene-oscillation frequency. (Reviewed by [98]).

1.2.4 Lateral root founder specification

Although several cells undergo oscillating gene expression, only pairs of abutted cells originate a LRP, the so-called lateral root founder cells (LRFC) (reviewed by [99]). After the priming event, once cells leave the OZ, some XPP cells undergo LRFC specification in an auxin-dependent manner and can be seen as static points with fixed DR5 expression. This occurs close to the meristem, however, external addition of auxin can also induce LRFC specification in the differentiation zone [100]. An early marker of LRFC directly activated by auxin is GATA23. Its expression correlates with the gene expression oscillation at the meristem and is under the control of the AUX/IAA protein IAA28 [101].

Environmental cues, like water availability biases the position of LRFC specification and LRP progression in a process called hydro patterning (Bao, Aggarwal et al. 2014). Similar to hydro-patterning, root waving upon avoidance of an obstacle or induced by gravity, also affects rhizotaxis (reviewed by [102]). The root curvature is associated with the formation of LRP at the convex side of the bending. However, only when mechanical bending occurs close to the root tip it induces the formation of a new LRP [103], indicating that bending needs to occur close to the meristem, where LRFC are specified.

Sharp bending of the root close to the meristem induces changes in auxin transport. When the gravity vector changes the differential elongation of cells in the convex vs. the concave side originates a root bend. Auxin accumulates in the concave side of the bending thanks to the relocation of PIN1 and PIN2 transporters and inhibits cell elongation at the concave side. In contrast, cells in the convex side elongate faster and stretch [103].

A computational model predicted that stretching of cells at the outside/ convex side leads to accumulation of auxin in these cells. Accumulation of auxin in XPP cells in the outer side is depending on AUX1, priming them as future LRFC and promoting the formation of a new LRP [104]. Accumulation of auxin induces an increase in cytosolic Ca^{+2} and blocking Ca^{+2} channels prevents the formation of LRP at the convex side. What indicates that Ca^{+2} signalling is important for specification and LR formation at the bending [82].

1.2.5 Lateral root initiation.

During the canonical lateral root initiation (LRI), two abutting LRFC increase in volume and their nuclei migrate towards the common cell wall. This is followed by an asymmetric anticlinal cell division, with two small daughter cells in the centre and two big daughter cells at the flanks. Alternative to the canonical LRI, one-cell initiation is also observed. In the later, one XPP cell divides in the middle and the two daughter cells divide asymmetrically [67, 89].

A tight control of the progression of cell division is essential for the formation of a LRP, as disrupting the expression of cell cycle genes leads to the absence or the overproduction of LRP. The maintenance of XPP mitotic activity and their ability to produce LR depends on the presence of a nuclear protein, ABERRANT LATERAL ROOT FORMATION4 (ALF4), controls the expression of *CYCLIN B1;1* (*CYCB1;1*). Accordingly, the mutant *alf4* does not produce lateral roots [105]. Recently it has been reported that ALF4 inhibits the E3 ligase $SCF^{TIR,}$ which is responsible of the degradation of the AUX/IAA repressors. The authors propose that the lack of LRP in *alf4* is derived from the increased levels of Aux/IAA proteins [106]

Auxin induces the expression of G1/S regulator CYCLIN D3;1 (*CYCD3;1*). However, the sole activity of cell cycle genes without functional auxin signalling does not lead to LRP

formation. Ectopic expression of CYCD3;1 in the auxin signalling mutant *slr-1* (see below) is not sufficient to induce the formation of LRP and cells undergo uncontrolled cell proliferation, but do not form LRP [107].

Cell division activation by auxin also depends on CYCLIN-DEPENDENT KINASES (CDKs), whose activity is dependent on many regulators like cyclins (e.g. CYCA2;1) and inhibitors of the G1 and S phase, like members of the INTERACTOR OF CYCLIN-DEPENDENT KINASE (CDK)/ KINASE-INHIBITORY PROTEIN (KIP)-RELATED PROTEIN (ICK/KRP) family. CDKA;1 and the CYCA2;1 are constitutively expressed in XPP cells [87]. As negative regulators of CDKs, auxin inhibits the expression of KRP2 and KRP1 and enhances their turnover, increasing CDKA;1-CYCD2;1 complex activity and inducing cell division [108].

Auxin maxima, visualized by DR5 expression, are created in LRFC before the asymmetric cell division. Accumulation of auxin is achieved by auxin influx mediated by AUX1 [104]. As the LRP develops DR5-GUS staining is confined to central cells and latter it forms a maximum at the tip of the LRP [11].

The auxin efflux transporters, PINs are expressed in LRP in all stages of the development and contribute to establishment of the auxin maximum at the tip of the lateral root primordium [11]. PIN1 is present at the transversal cell wall in earlier stages. Later, PINs relocate in the periclinal cell wall towards the root tip to accumulate auxin at the LRP tip [11]. Localization of PIN1 at the plasma membrane is essential for cell division during LRI. The hormone cytokinin counteracts auxin and blocks cell division during LRI [109]. However, cytokinin does not block LRI at the transcriptional level but rather through a rapid post-transcriptional regulation of PIN1. Cytokinin mediates specific PIN1 targeting to the vacuole for degradation, blocking auxin efflux and progression of LRI [110].

Local biosynthesis of auxin also helps in the increase of cytosolic auxin by the expression of auxin biosynthetic gene *YUCCA4* in LRFC (reviewed by [91]). MEMBRANE_ASSOCIATED KINASE REGULATOR4 (MAKR4) is activated by IBA and IAA and is expressed in LRFC before cell division. Los-of-expression of MAKR4 reduces the number of LR but not the number of founder cells [97].

Auxin signalling plays an essential role in every step of LRP development. SOLITARY ROOT (SLR)/IAA14 is the major regulator of LRI. Upon auxin-dependent targeting for degradation of SLR, ARF7 and ARF19 activate the expression of a plethora of auxin-responsive genes [69]. Directly controlled by ARF7/ARF19 is the transcription factor *LATERAL ORGAN BOUNDARIES DOMAIN 16* (*LBD16*). Repression of LBD16 block nuclei migration and cell division asymmetry [63]. LBD33/LBD18 are also expressed during LRI, where they control the expression of the G1/S transition-regulator E2Fa [111].

The AUX/IAA protein, SHORT HYPOCOTYL2/SUPPRESSOR OF HY2 (SHY2)/IAA3, regulates LRI downstream of SLR/IAA14-ARF7-ARF19 module. SHY2 supresses LBD16 and the gain-of-function mutation, *shy2-101*, increases the number of LRI sites and LDB16 expression [112]. Another important auxin-signalling module for LRI is the MONOPTEROS (MP)/ARF5-BODENLOS (BDL)/IAA12 pair. Disrupting of this auxin-signalling module renders LRP very close to each other or even fused [113].

It has been suggested that symplastic connectivity might allow the transport of inhibitory signals coming from the initiated LRFC to repress LRI in neighbouring cells, in a non-cell autonomous manner [114]. The symplastic connection through plasmodesmata (PD) between XPP cells is controlled by the deposition of callose at PD. The PLASMODESMATA-LOCALIZED ß-1,3-GLUCANASE1 (PDBG1) is expressed in XPP cells and LRP under the control of the SLR-signalling pathway. PDBG1 and PDBG2 are involved in callose turnover and the mutants accumulate more callose at the PD. Interestingly, the mutants *pdbg1* and *pdbg2* show more LRI sites than wild type and its overexpression reduces LRI density. In line with this observation, the membrane-localized receptor-like kinase ARABIDOPSIS CRINKLY4 (ACR4) is expressed in the small daughter cells after the asymmetric cell division for non-cell autonomous restriction of LRI in neighbouring cells [115]. Also some small

peptides act as negative regulators of LRI. GOLVEN/root growth factor/CLE-like (GLV/RGF/CLEL) inhibits pericycle divisions when over-expressed (Fernandez 2015) and loss-of-expression of the small peptide RAPID ALKALINIZATION FACTOR-LIKE34 (RALFL34) increases LR density [116].

Environmental signals can influence LR formation (reviewed by [117]. The MADS-box transcription factor AGL21 induces LR formation integrating signals from other hormones like abscisic acid (ABA) and methyl jasmonate (MeJa) or nutrient deficiency [118]. Nitrate deficiency and ABA can also modulate LR development [119].

The expression of WOX7 is activated by sugar and mediates LR inhibition under high-sugar conditions. The member of the WUSCHEL related homeobox (WOX) family transcription factor, WOX7 is primarily involved in LRI and expressed in all stages of LRP development where it inhibits LR development by repressing CYCD6;1 [120].

After the first asymmetric cell division, subsequent anticlinal and periclinal cell divisions originate a two-layered primordium. The proper transition from stage I to II and subsequent cell divisions are redundantly controlled by the transcription factors PLT3, 5 and 7. These genes control as well the formation of the auxin maximum at the LRP in later stages. Moreover, PLT transcription factors control the expression of the tissue-specific regulators WOX5, SCARECROW (SCR) AND SHORT-ROOT (SHR) in LRP, determining tissue patterning in LRs [121].

The central cells divide more actively than the flanking cells, which will conform the boundaries of the LRP. Cell division at the boundaries is controlled by APETALA2/ETHYLENE- RESPONSIVE ELEMENT BINDING PROTEIN (AP2/EREBP) transcription factor, PUCHI. At initial developmental stages PUCHI is expressed in the whole LRP. As LRP development continues PUCHI expression is restricted to the flanking cells, where it restricts cell division. Loss-of-function *puchi-1* has additional divisions at the boundaries, creating a wider and flatter LRP[122].

New studies have described the spatiotemporal dynamics that ensures the formation of a LRP [123, 124]; these studies determined that the first asymmetric division is tightly regulated and defines the core of the primordium[123]. In contrast the next rounds of divisions are less deterministic and follow a non-stereotyped order. Yet, these divisions follow some rules: first, they tend to divide following the ‘shortest-wall’ principle; second, they tend to alternate the orientation of division with each new round of division and third, the outer layer, generated from periclinal divisions, tends undergo periclinal divisions before the inner layer [123].

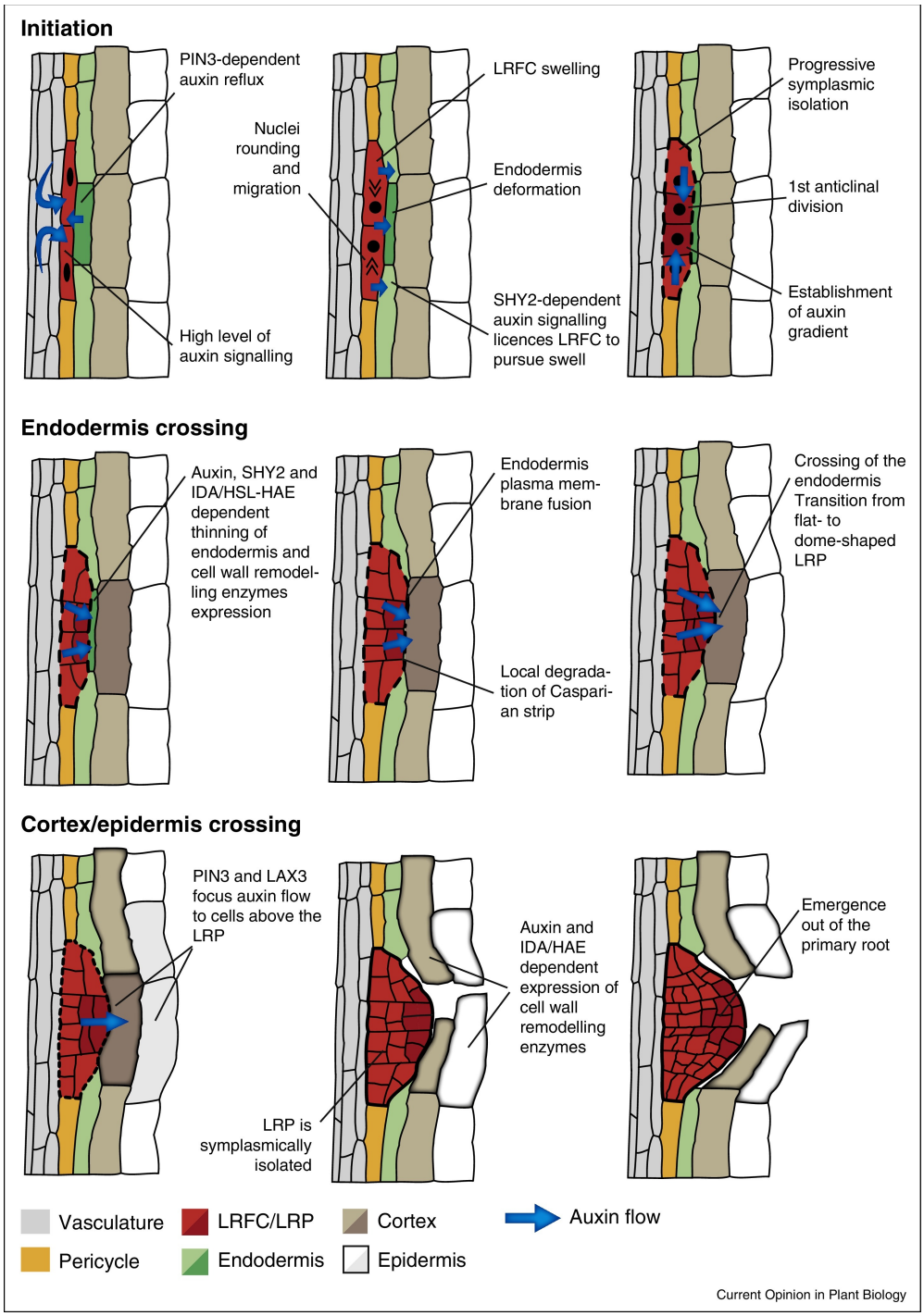

Fig. 2 Phases of lateral root formation in *Arabidopsis thaliana*.

For each phase (initiation, crossing of the endodermis and of the cortex/epidermis), the main events are indicated. Tissues are color coded, darker shade indicates high level of auxin signalling (Adapted from [125]

1.2.6 Lateral root development: the interplay with the endodermis

Shortly before cell division, nuclei of two abutting founder cells need to migrate towards the common cell wall. Concomitantly with nuclei migration, founder cells also increase in volume [2]. SHY2 is expressed in founder cells during LRI but also in the endodermis, where it controls emergence [112]. Tissue-specific expression of the gain-of-function mutant *shy2-2* in the endodermis, blocks swelling of founder cells and cell division.

This effect is exclusive for the endodermis, as expression of *shy2-2* in the cortex and epidermis had no effects on LRI.

The endodermis differs from other root tissues in the presence of the Casparian strip (CS), which acts as apoplastic diffusion barrier and is made of non-extendable and non-degradable ligning (Reviewed by [126]). The CS firmly glues endodermal cells together, which in contrast with the cortex and the epidermis cannot separate from each other to allow the emergence of the LRP. To enable LRP emergence the endodermis undergoes a dramatic local loss-of-volume until opposite membranes fuse together. Also the CS is only locally remodeled. The spatial accommodation of the endodermis is controlled by SHY2. Tissue-specific expression of *shy2-2* in the endodermis, not only blocks LRI but also emergence throw the endodermis. Whereas ectopic treatment with auxin can resume cell divisions in CASP1pro::*shy2-2*, the endodermis remains stiff and LRP cannot cross it and become flattened [2].

Recently it has been suggested that the proliferative activity of XPP cells is constraint by the mechanical interaction of the endodermis. Single-cell ablation of endodermal cells induces cell division in the naïve (no founder cell-specified) pericycle cells, however these divisions do not give rise to a LRP. Auxin is essential for controlling the cell division plane orientation and ablation of single endodermis cells in the presence of auxin, rescues formative cell divisions [127].

Auxin transport from the endodermis is also necessary for LRI. The auxin efflux transporter PIN3 is expressed in the elongation zone and the root apical meristem, where it mediates root bending upon gravistimulation. However, in the differentiation zone PIN3 expression can only be observed in endodermis cells overlying LRFC during LRI. PIN3 appears only in the vascular side of the endodermis after DR5 auxin-signalling reporter can be detected in LRFC. Genetic disturbance of PIN3 expression drastically reduces DR5 expression in founder cells and delays LRI. Hence, PIN3-mediated auxin reflux from the endodermis into the pericycle is necessary for LRI [128].

Reactive oxygen species (ROS) has been detected between the endodermis and the cortex cells overlying a growing LRP. ROS produced by RESPIRATORY BURST OXIDASE HOMOLOGS (RBOHs) have been suggested to facilitate cell wall remodelling and assist during LRP emergence; Accordingly, loss-of-function of RBOHs cause a delay in LR emergence. Interestingly, authors show that treatment with H_2O_2 restores endodermis spatial accommodation and emergence through the cortex and epidermis in the CASP1pro::*shy2-2* [2], *aux1* and *lax3* mutants (see below) [129].

1.2.7 Lateral root emergence: crossing overlying tissues

Changes in cell shape or cell separation of the overlying tissues requires the activity of CWR enzymes. Auxin activates CWR enzymes, including the PECTIN METHYL ESTERASE1 (PME1), the ALPHA-EXPANSIN1 (EXP1) and the PECTIN LYASES (PL), PLA1 and PLA2, which are suggested to participate during LRP emergence [130] It activity modifies the mechanical properties of the overlying tissues and allow LR emergence. Accordingly, the expression of a dominant negative mutation of AXR3/IAA17, *axr3-1* in the tissues overlying a growing LRP block LRP emergence and LRP remain flattened [124].

Auxin activates the small peptide INFLORESCENCE DEFICIENT IN ABSCISSION (IDA) and its receptors HAESA (HAE) and HAESA-LIKE2 (HSL2). Together they conform a signalling pathway that controls the expression of CWR enzymes, XTH23/XYLOGLU- CAN ENDOTRANSGLYCOSYLASE6 (XTR6) and the expansin EXP17 during lateral root emergence [131]. Defects in the IDA/HAE/HSL2 signalling pathway delays the crossing throw the endodermis.

Other small peptides act negatively on LR emergence. Overexpression or ectopic treatment with CLAVATA3/EMBRYO SURROUNDING REGION (CLE), which also regulates LR

development by mediating the phosphorylation of ARFs, and C-TERMINALLY ENCODED PEPTIDEs (CEPs) reduces the number of emerged LRP (Reviewed of [116]).

The auxin signalling pathway ARF7-ARF19/LBD16-LBD18 is not only important for LRI, but also it controls the expression of expansins EXPA14 and EXP17 in the overlying tissues; Accordingly, lacking LBD16/LBD18 significantly reduces the number of emerged LR [132-134].

Systemic cell wall softening during LR emergence would render the plant susceptible for pathogen attacks. For this reason, auxin movement and signalling needs to be specifically canalized in the few cells overlying the growing LR. To achieve this the signalling pathway ARF3/LBD18-LBD29 activates the expression of the auxin influx transporter LAX3 in the overlying tissues. The combined activity of LAX3 and PIN3 contributes to restrict of auxin transport into few cells, where LAX3 activates the expression of CWR, AIR, XTR6 and PLA2, allowing cell separation during LR emergence [77, 135, 136].

Cell wall remodelling as well as loss-of-turgor pressure in the overlying tissues are both necessary for the accommodation of the overlying tissues to the growth of LRP. The PLASMA MEMBRANE INTRINSIC PROTEIN (PIP) family mediates water movements throw the PM. Auxin controls the expression of these proteins during LR emergence. Loss-of-turgor pressure is presumably achieved by down-regulation of PIP2;1 whereas PIP2;8 is up-regulated at the base oft he LRP [137]. TONOPLAST INTRINSIC PROTEINS (TIPs) are expressed in the whole root with the exception of the epidermis. The triple mutant *tip1;1,tip1;2,tip2;1* shows LR emergence delay, indicating the importance of water movements to allow LRP outgrowth [138].

2 Aims of the thesis

The postembryonic formation of a lateral root begins with the anticlinal asymmetric division of a pair of adjacent founder cells in the vascular tissue of the primary root. This process is called lateral root initiation (LRI) and is characterized by the synchronous swelling of founder cells and the migration of nuclei towards the common cell wall before the first round of asymmetric cell division, these elements are crucial for the proper morphogenesis of the lateral root [2, 101, 123] Auxin is an essential regulator of LRI and development. The transcription factor LBD16/ASL18 is a primary target of the auxin-signalling pathway and it controls nuclei migration and asymmetry of cell division during LRI [63].

As the founder cells swell and divide to form a lateral root primordium (LRP), the overlying endodermis must actively accommodate the growth of the new LR [2]. The endodermis is characterized by the presence of the Casparian strip, a lignified structure that prevents the LRP to simply pass in between endodermis cells. As a consequence the endodermis undergoes a dramatic local loss-of-volume until opposite membranes fuse together and open a gap in the endodermis through which the primordium can grow [2]. Auxin signalling is required for the spatial accommodation of the endodermis. The expression of the dominant negative version of SHORT HYPOCOTYL2/IAA3 (SHY2) in the endodermis prevents cell shape remodelling and LRI cannot take place [2]

2.1.1 In this context this work aimed at answering four essential questions:

2.2 How do actin and microtubules control cellular events during LRI?

Microtubules and actin are key regulators of cell shape, nuclei migration and cell division. To describe the dynamics of actin and microtubules during LRI we performed two-photon live microscopy using founder cell specific marker lines and a quantitatively analysed microtubules and actin dynamics. Making use of pharmacological and genetics perturbations we revealed the contribution of the cytoskeleton to LRI.

Our results show that both microtubules and actin are highly dynamic during LRI. We found that the polar organization of the cytoskeleton licences the asymmetric expansion of the founder cells that prefigures the dome shape aspect of the LRP.

2.3 Does auxin signalling control cytoskeleton dynamics during LRI?

We then studied how perturbing the auxin-induced polarity of founder cells influences the dynamics of the cytoskeleton. For this, we crossed the repressor line LBD16-SRDX [63] with our cytoskeleton markers and performed live imaging of LRI. Our results revealed that in absence of polarity, the cytoskeleton looses its polar organisation and founder cell swell symmetrically.

2.4 Do microtubules play a role in the spatial accommodation of the endodermis?

To test whether microtubules dynamics contribute to the spatial accommodation of the endodermis we analysed lateral root emergence in the katanin mutant (*bot1-7)*, in which cortical microtubules (CMT) dynamics are impaired [139]. We performed live imaging with an endodermis specific CMT reporter in wild type and mutant plants. Our results show that altering CMT dynamics negatively impacts on the endodermis remodelling and lateral root emergence.

2.5 Does auxin signalling control cytoskeleton dynamics in the endodermis?

We monitored CMT reorientation in the endodermis upon treatment with exogenous auxin and observed that microtubules reorganize differently depending on the cell side. As microtubules reorient in response to mechanical stresses [4, 9, 29], we performed CMT imaging in the endodermis of lines in which auxin signalling was either blocked in the endodermis or in the pericycle. We observed that auxin induction of CMT reorientation in the endodermis requires SHY2-dependent signalling regulation.

3 Results

3.1 Auxin-dependent cytoskeleton dynamics control the first asymmetric division in LRI

3.1.1 The dome shape is established by asymmetric swelling during the first formative division

Lateral root initiation (LRI) can be visualised when founder pericycle cells increase in volume, the nuclei migrate towards one end and cells divide asymmetrically [101, 123]. Although the role of auxin in regulating these processes has been extensively studied [63, 101, 140], the temporal coordination between changes in cell geometry, nuclear migration and cell division has only been studied in a few instances [2, 141].

In order to describe and analyse these events more carefully, we made use of a quadruple marker line (sC111; according to the code of the lab) that marks plasma membrane with PIP1;4 [142], founder cell identity with GATA23 [101], cell division with RPS5A [143] and auxin maxima with DR5 [144].

LRI was triggered in sC111 by gravistimulation (180° inversion of the plate), setting our temporal reference t=0h. After 4h cells did not show any hints of initiation. Here, we will call cells prior to LRI as naïve pericycle.

Approximately 6h to 7h after gravistimulation we could detect the coordinated migration of nuclei in pairs of founder cells towards their common cell wall. During this phase of migration founder cells increase in volume [2] but this swelling is readily more pronounced in the central region where the two abutting founder cells share a wall, than on the periphery (Fig. 1A-C).

Once nuclei are asymmetrically positioned, the nuclei round up and founder cells divide asymmetrically. From the first asymmetric cell division (ACD) the asymmetry in swelling progressively increased with each round of division, with the small daughter cells in the centre expanding much faster than the peripheral edge of the big daughter cell (Fig. 3B and C).

In sum, we observe that pairs of founder cells expand co-ordinately and asymmetrically during the phase of nuclear migration preceding the first ACD. We noticed that the asymmetry in swelling increases once the nucleus is asymmetrically localized in founder cells, with the region surrounding the nucleus expanding faster than the periphery, which remains almost unchanged.

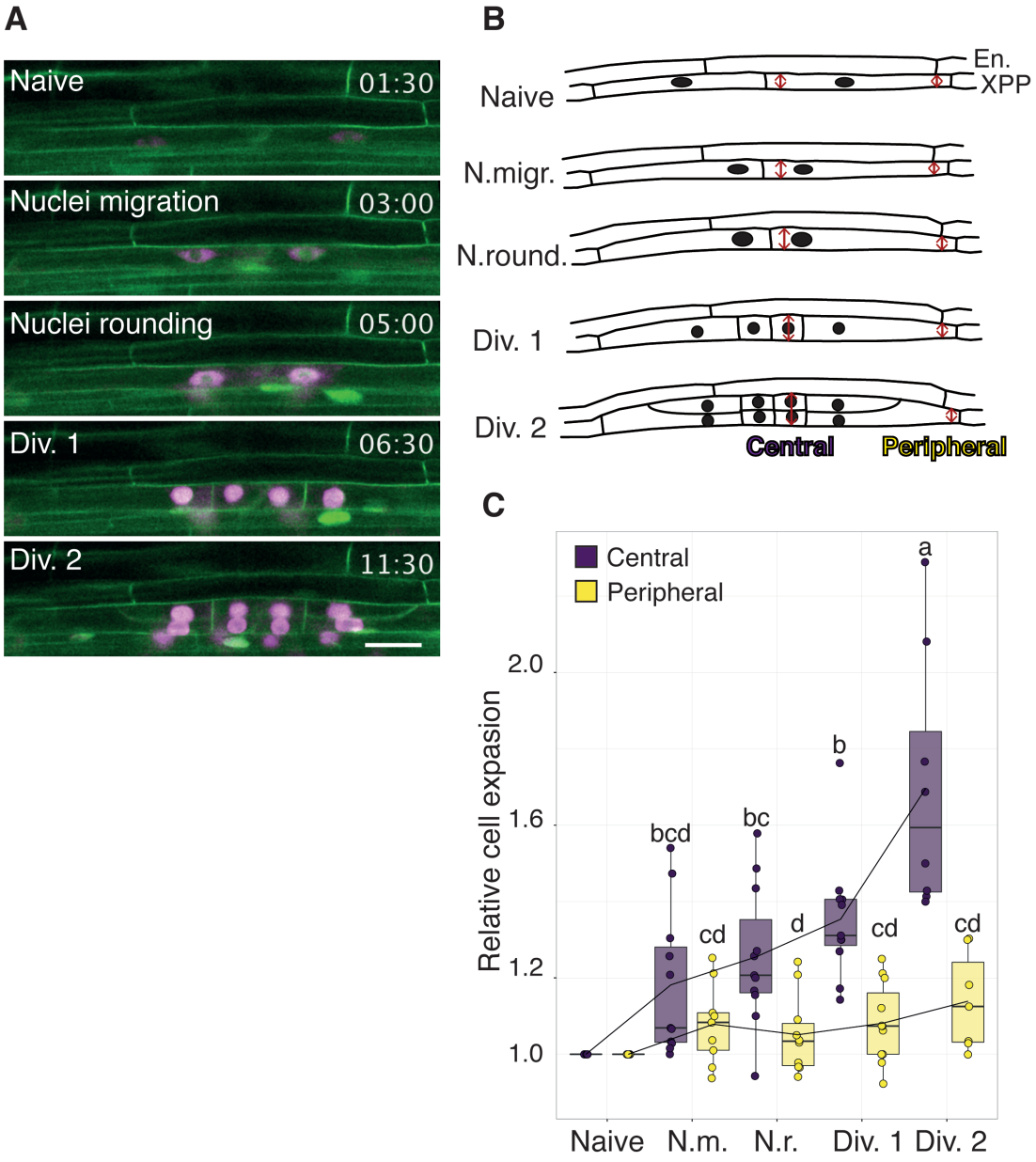

Fig. 3 Asymmetric expansion of founder cell coincides with the polar migration of nuclei.

A) Confocal sections of roots taken at different time points after gravistimulation. The different phases of lateral root initiation are indicated. Naïve pericycle cells show no obvious sign of initiation, then nuclei migrate, round up and cell divide asymmetrically (Div.1). Later, cells undergo a second round of divisions (Div.2), when a two-layered primordium is formed. Images were taken every 30 min after 4h gravistimulation in the marker line sC111. Scale bar 20 μm.

B) Schematic representation of the events depicted in (A). In the central domain cells swell faster and form the tip of the dome and whereas at the periphery swelling is constrained.

C) Quantification of the founder cells expansion in the peripheral and central domains during LRI. Boxplots represent the distribution of cell width at the central (purple) or peripheral (yellow) positions at the indicated phases: naïve founder cells, after nuclei migration (N.m), after nuclei rounding (N.r), after the first ACD (Div.1) and after the second division (Div.2). Five independent roots and 11 cells were imaged and cell width measurements were normalized to the initial cell width (Naïve). Groups with the same letters do not differ from each others (Tukey test; alpha=0.05).

3.1.2 CMT reorient in founder cells during LRI and show a gradient of organization

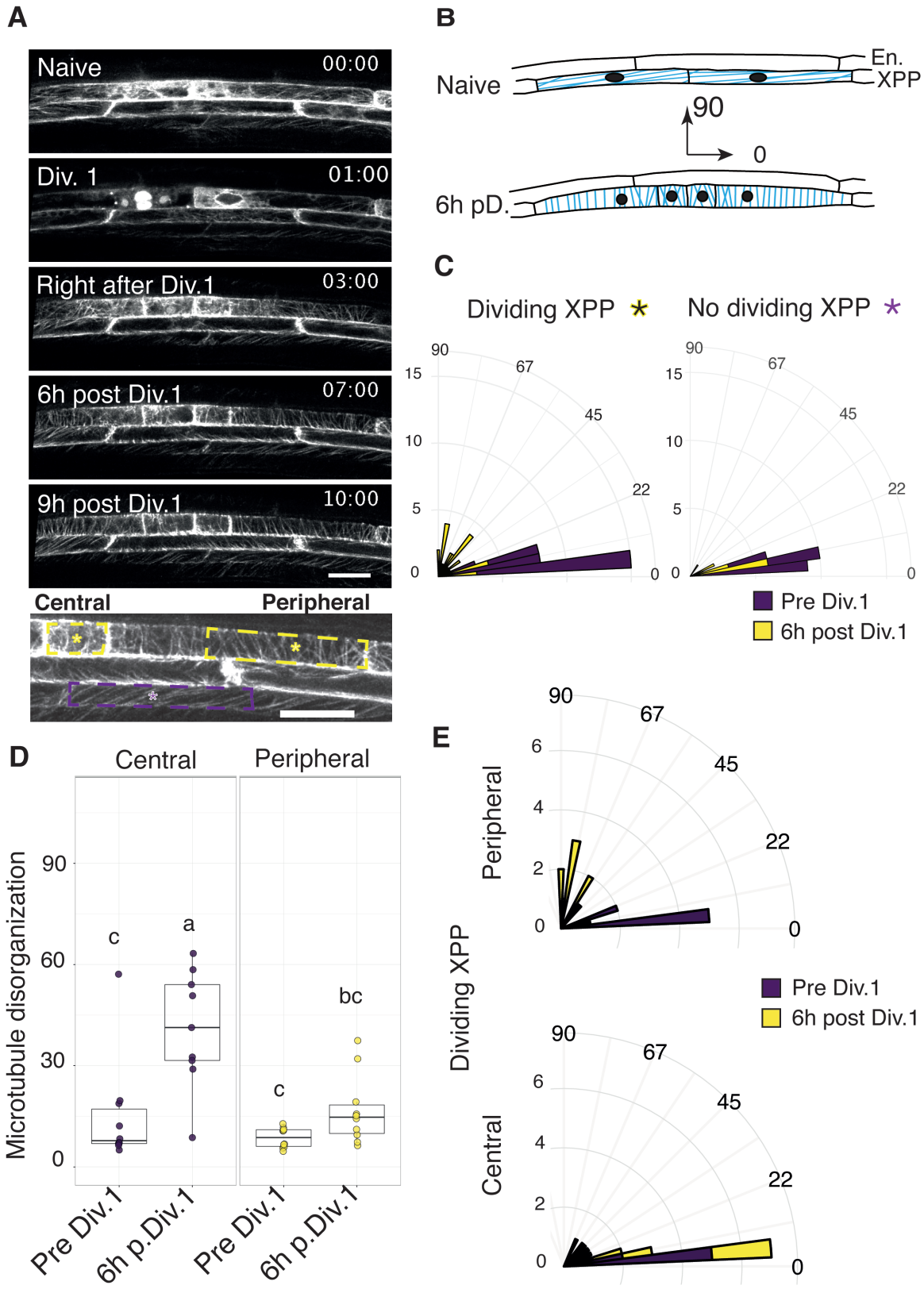

Fig. 4 Cortical microtubules reorient in founder cells during LRI and show a graded organization from the centre to periphery

A) Two-photon confocal sections of the microtubule marker GATA23*pro*::GFP:MBD (upper part) live imaged after 6h gravistimulation, 30min time intervals. In the lower part the magnification shows daughter cells after first ACD, founder cells are labelled with a yellow asterisk/box and non-dividing cells with a purple asterisk/box. Yellow box marks the position used for microtubule analysis with Fiji (Fibril Tool). The central and peripheral domains are indicated, corresponding to the small and the big daughter cell, respectively. Scale bar is 20 μM.

B) Schematic representation of the organization of CMT (in blue) seen in A. Before the first asymmetric division (pre Div.1) microtubules line with the longitudinal cell-axis. 6h after the first division (6h pD.) microtubule orientation is transversal to the longitudinal cell-axis. Endodermis (En) and Xylem pole pericycle cells (XPP) are indicated.

C) Polar plot of microtubule orientation (0° to 90°) in dividing and non-dividing cell at two time points: previous cell division in purple (Pre Div.1.) and 6h after cell division in yellow (6h post Div.1). Concentric circles in polar plots (Y axis) indicate the number of measurements of a specific orientation.

D) Measure of microtubule disorganization in dividing cells at the central (purple) and peripheral position (Yellow). The higher the score the more disorganized. Different letters show significant differences among groups (Tukey Test; alpha=0.05,in n =10 dividing_cells).

E) Polar plot of microtubule orientation (0°-90°) in dividing cells at the central and the peripheral position before cell division (purple, Pre Div.1) and 6h after cell division (Yellow, 6h post Div.1).

In plants directional cell growth is largely determined by the organization of cellulose fibrils and local action of cell wall remodelling enzymes, both dependent on the organization of cortical microtubules (CMT) [6, 16, 145]. The observation that founder cells undergo differentially local expansion, prompted us to look at the organization of CMT in founder cells.

To image CMT dynamics during LRI we took advantage of the line GATA23*pro*::GFP:MBD, in which the MAP4-Binding Domain is tagged with GFP and predominantly expressed in founder cells. We observe that in naïve pericycle cells, previous to initiation, CMT arrange helicoidally along the long axis of the cells (Fig. 2 A). Just after nuclei migration and before cells begin ACD, we observed that CMT disorganize around the nucleus. Right after the first ACD, CMT reorganize in transversal parallel bundles. Reorientation of CMT begins at the peripheral edge of the big daughter cell and progressively propagates along the cell towards the centre. Approximately 6h after cell division is the time where transversal bundles became more obvious in our observations (Fig. 4 B). In adjacent non-dividing cells, CMT orientation barely changes even 6 hours after the first ACD (Fig. 4 C). We observed that CMT are heterogeneously organized between daughter cells (Fig. 4 A). 6h after division microtubule of the small daughter cell are more disorganized with no predominant orientation (Fig. 4D, central). To the contrary, in the periphery of the big daughter cells CMT remain organized and form close-to-transversal bundles (Fig. 4 D and E, peripheral).

Taken together, our observations indicate that CMT reorient in founder cells during LRI and display a graded organization from the centre to periphery.

3.1.3 The *bot1-7* mutant fails to form dome-shaped primordia

Our results show that founder cells swell asymmetrically during LRI with the central part expanding more than the periphery, prefiguring the future LRP dome-shaped appearance. Concomitantly, CMT show a gradient in organization, more heterogeneous in the central domain than the periphery.

In order to see whether affecting microtubule organization would have an impact on cell swelling and dome-shape formation, we analysed the development of lateral root primordia (LRP) in the mutant *botero1-7* (*bot1-7*)[146]. The mutant *bot1-7* is an allele of *KATANIN*, a gene encoding for a microtubule-severing protein, important for the reorganization of CMT [7].

Roots of 7 day-old wild type (Col-0) and *bot1-7* seedlings were cleared for microscopic analysis of the shape and the number of LRP [147]. We observed that rate of lateral root

formation is severely reduced in *bot1-7* (Fig.S 1. The *bot1-7* mutant is affected in cell growth and production of lateral roots

We saw that LRI is affected (Fig. 5) in *bot1-7*. In particular we could not observe any pronounced asymmetric swelling. At stage II, where the dome-shape becomes obvious in wild type, LRP in *bot1-7* show aberrant shapes and in some cases the central part of the primordium collapses in the centre.

In conclusion, these results suggest that proper organization of the CMT network is necessary for early establishment of asymmetric swelling, prefiguring the future dome-shape of the primordium.

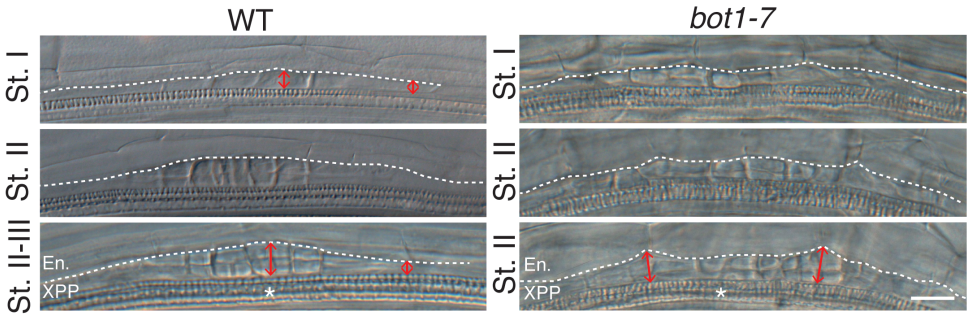

Fig. 5 The *bot1-7* mutant fails to form dome-shaped primordia in early developmental stages.

Pictures of lateral root primordia in cleared roots of wild type (WT) and *bot1-7*. In *bot1-7*, early stages differ in shape and cell organization from LRP in wild type (Col-0). Stage I (St.I) one-cell layer, stage II (StII) two-cell layer, stage III (StIII) three-cell layer. The contour of the primordia is highlighted with dashed line in white, between the endodermis (En.) and xylem pole perycicle cells (XPP). The white asterisk indicates the position of the xylem pole. Red arrows in wild type show the central and the peripheral regions of the primordium. Red arrows in *bot1-7* show the two highest points, but these are not at the central area of the primordium as in wild type. Scale bar 20 μm

3.1.4 CMT reorganization in parallel bundles is necessary for asymmetric swelling

The previous results support the hypothesis that CMT reorganization and asymmetric cell swelling are linked. To further substantiate this idea, we followed CMT dynamics in the *bot1-7* during LRI. We crossed *bot1-7* with a microtubule reporter line with specific expression in the XPP cells, XPPpro::CITRINE:TUA6 [148].

We performed live imaging on 7-day old seedlings of XPPpro::CITRINE:TUA6 in the *bot1-7* background after 6h gravistimulation. As previously reported in other tissues, CMT failed to reorganize in parallel bundles in the pericycle even 13h after the first ACD (Fig. 6 A). Although in *bot1-7* the orientation of the cell division plane is affected, forming oblique cell walls, the first division was still asymmetric.

Interestingly, we could not measure any asymmetry in the swelling of the founder cells (Fig. 6 B and C). In contrast to wild type, in *bot1-7* the peripheral edge of the big daughter cell expands concomitantly with the central part, leading to an ‘en bloc’ swelling of the founder cells (Fig. 6 C).

In conclusion, CMT fail to reorganize in parallel bundles during LRI in *bot1-7* and their orientation remains disorganized along the whole cell length in founder cells, which expand symmetrically (‘en bloc’). These observations suggest that the organization in parallel bundles at the peripheral edge might be necessary to constrain cell expansion and suggest that the gradual organization of CMT allows different local growth rates resulting in asymmetric cell geometry.

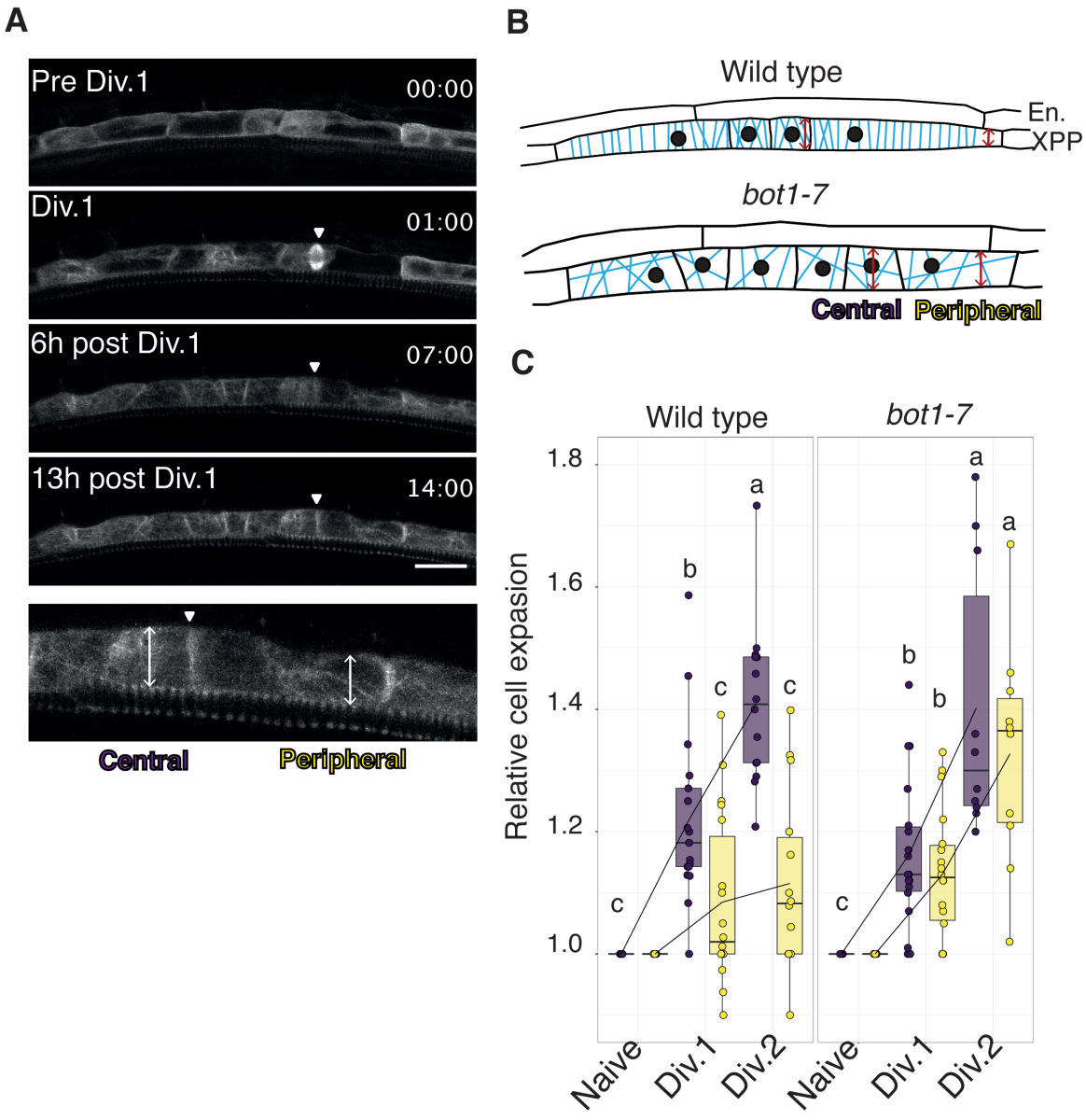

Fig. 6 Asymmetric swelling is impaired in the *bot1-7* mutant, where CMT cannot organize in parallel bundles.

A) Two-photon confocal sections of the *bot1-7* mutant expressing the microtubule marker XPPpro::CITRINE:TUA6. Live imaging was performed after 6h gravistimulation every 30 min. The white triangle marks the first ACD. On the lower part, a magnification after 20h of gravistimulation (14:00) shows the organization of CMT in the mutant. The white arrows show the positions (central and peripheral) at which cell swelling was measured. Scale bar is 20 μM

B) Schematic representation of the events in A for WT and *bot1-7*. Red arrows indicate central and peripheral regions, the CMT are depicted in blue.

C) Quantification of the founder cells expansion in the peripheral and central domains during LRI in WT and *bot1-7*. Boxplots represent the distribution of cell width at the central (purple) or peripheral (yellow) positions at the indicated phases: naïve founder cells, after the first asymmetric division (Div.1) and after the second round of division (Div.2). At least 18 cells were imaged and analysed in each genotype. Measurements were normalized to the initial cell width (Naïve). Groups with the same letters do not differ from each others (Tukey test; alpha=0.05).

3.1.5 Altering CMT polymerization with pharmacological treatments disrupts asymmetric swelling

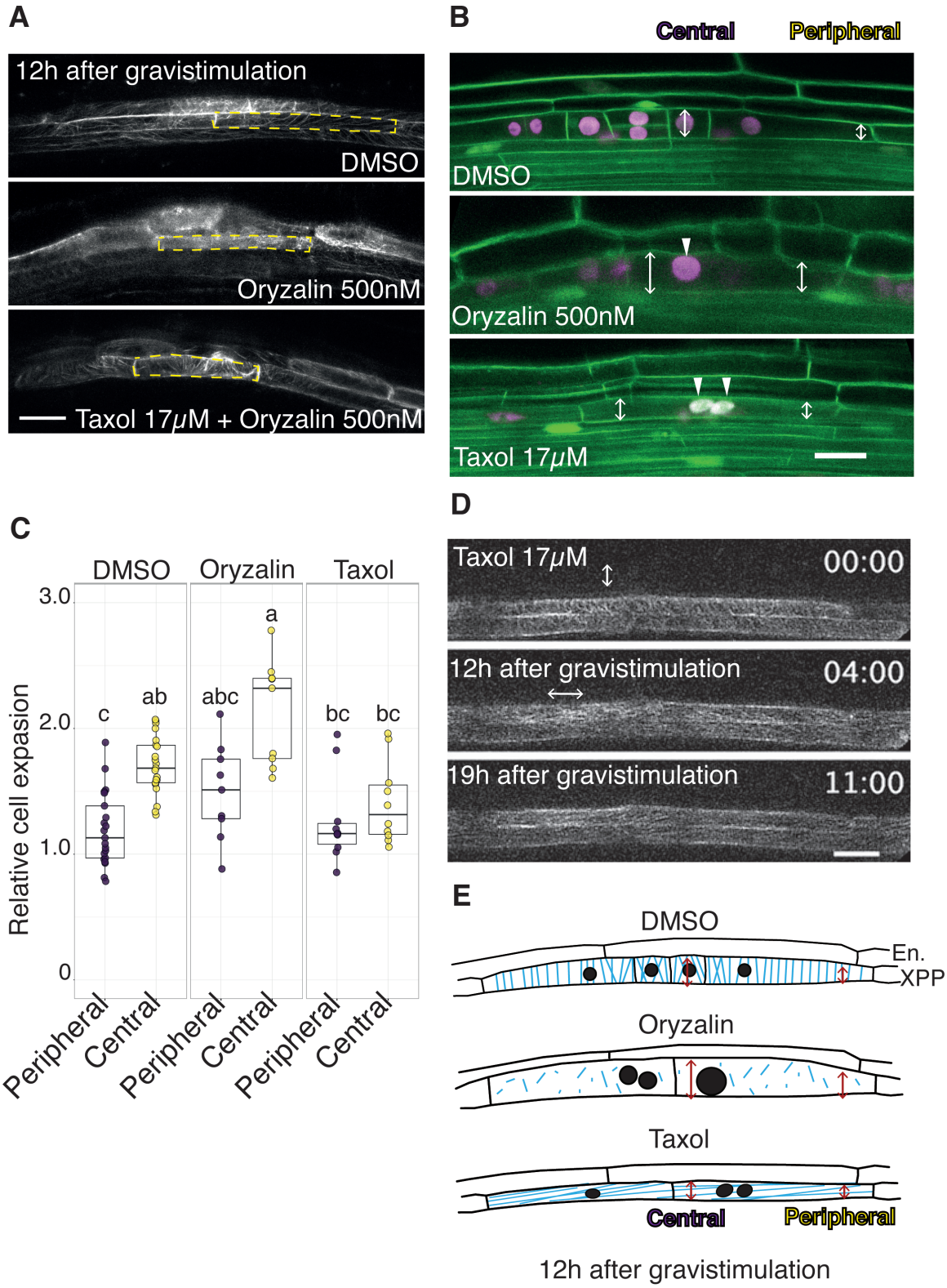

Fig. 7 The tubulin-binding drugs, oryzalin and taxol, show opposite effects on cell swelling during LRI.

A) Confocal sections of GATA23pro::GFP:MBD expressed in LR primordia treated with oryzalin and taxol. Roots were gravistimulated for 12h in the presence of DMSO, oryzalin (500nM) and oryzalin (500nM) with taxol (17μM). In the yellow box CMT fibrils are visible in DMSO, whereas they disappear upon oryzalin treatment. Taxol counteracts the depolymerioing effect of oryzalin and fibrils are visible.

B) Confocal sections of LRP upon oryzalin and taxol treatment. The reporter line sC111 was live imaged under the indicated pharmacological treatments. Images represent LRI after the first ACD (t=12h post gravistimulation). White triangles mark the position of the nuclei and white arrows mark the position (central or peripheral) where cell width was measured.

C) Quantification of founder cell swelling (t=12h post gravistimulation) at the peripheral (purple) or central (yellow) domains, in the presence of DMSO, oryzalin and taxol. The cell width in dividing founder cells was normalized to the one of in non-dividing cells on the other side of the xylem pole. Different letters indicate significant differences between groups (Tuckey test, alpha=0.05; n_{DMSO}=23, n_{TAXOL}=10, $n_{ORYZALIN}$=9 cells were analysed).

D) Confocal sections of the GATA23pro::GFP:MBD showing the effects of taxol on microtubule organization after 8h, 12h and 19h post gravistimulation (00:00, 04:00 and 11:00). White arrows show the main orientation of the fibrils.

E) Schematic representation of the effect of oryzalin (destabilizing) and taxol (stabilizing) on CMT (blue) and cell swelling (Red arrows; central and peripheral domain) in founder cells after 12h of gravistimulation. Endodermis (En.) and Xylem pole perycicle cells (XPP). Scale bar 20μM.

To further test the idea that CMT dynamics impact on the ability of founder cells to swell asymmetrically, we analysed ACD and cell swelling during LRI in roots treated with oryzalin or taxol, two compounds that respectively inhibit or stabilize CMT polymerization.

A final concentration of 500nM oryzalin was observed to specifically depolymerize CMT (Fig.S 2) without abolishing cell division during LRI (Fig. 7 A). Differently, a concentration of 17μM taxol was necessary to stabilize CMT in the pericycle and induce alterations in LRP formation (Fig. 7A; Fig.S 3).

We observed that oryzalin treatment increases cell swelling in the central and the peripheral domains and consequently induced loss of asymmetry (Fig 5B, C). On the contrary, fixing microtubules with taxol precluded the central part to expand and also leaded to a loss in asymmetric expansion (Fig. 7 C).

Taxol treatment was observed to block CMT dynamics, which did not reorganize in transversal bundles. Live imaging of the microtubule marker GATA23pro::MBD:GFP in the presence of taxol showed that 8h after gravistimulation microtubules remained transversally oriented, presumably after cells abandoned the elongation zone. Later we could observe that CMT turned 90° their orientation and remained parallel to the root axis (Fig. 7 D).

In summary, the results show that disorganization of CMT promotes cell expansion, whereas stabilization of microtubules impairs swelling and drastically reduces asymmetry in cell geometry. These results support our hypothesis that CMT organization dynamics during LRI has an impact on the grade of expansion of founder cells.

3.1.6 Tissue-specific destabilization of CMT in founder cells phenocopies LRP defects induced by katanin mutation and pharmacological treatments

Although both pharmacological as genetic alteration of microtubule organization show an effect on asymmetric cell swelling, we could not discard the possibility that pleiotropic effects, derived from affecting microtubules in all tissues, could have an impact on the expansion of founder cells.

For this reason we first attempted to modify katanin expression in specific tissues with two approaches: overexpression and down-regulation with artificial microRNAs (ami$R_{KATANIN}$). Although three different ami$R_{KATANIN}$ were created, only one effectively down-regulated the expression of KATANIN in tobacco leaves (Fig.S 4). We cloned this ami$R_{KATANIN}$ downstream of four different promoters: UBIQ10pro [149], for ubiquitous expression in the whole plant, XPPpro *[148]* for expression in the xylem pole pericycle cells, CASP1pro [150], for

expression in the endodermis and GATA23pro [101], for specific expression in founder cells (Fig.S 5).

We also cloned the coding sequence of *KATANIN* tagged with GFP (3xHA:KATANIN:GFP) downstream of the same four promoters that we use for the knockdown lines. By co-infiltration in tobacco plants with a microtubule marker line, we verified that 3xHA:KATANIN:GFP show microtubule-severing activity and could efficiently depolymerize microtubules, as previously showed by [139] (Fig.S 4).

Ubiquitous expression of the transgenic protein as well as the ami$R_{KATANIN}$ lead to similar growth defects as *bot1-7* (Fig.S 6). However, neither tissue-specific knockdown lines (Fig.S 7), nor tissue-specific-over-expression of 3xHA:KATANIN:GFP (Fig.S 5) showed any effect in the number or the shape of LRP. Crossing the *bot1-7* with the overexpression lines could neither rescue the whole-plant growth defects, nor the low number of LRP of the mutant (Fig.S 8).

The absence of a clear phenotype in the tissue-specific lines did not allow us to draw any conclusion about the role of CMT during LRI. For this reason, we pursued with a new strategy, adapting a previously described method to induce CMT depolymerisation in single cells. PHS1 (PROPYZAMIDE-HYPERSENSITIVE) is an atypical kinase that phosphorylates alpha-tubulin and is responsible of CMT destabilization under cold stress conditions. A truncated version of PHS1 with only 69kDa, PHS1ΔP, has a strong microtubule-depolymerizing activity [151].

PHS1ΔP was inducible-expressed from tissue-specific promoters using the glucocorticoid-inducible two-components system pOP/LhG4 [152]. We used 3 different promoters: XPPpro (XPPpro>>PHS1ΔP), for pericycle cells, LBD16pro (LBD16pro>>PHS1ΔP) for founder cells [63] and CASP1pro (CASP1pro>>PHS1ΔP), for the endodermis. The constructs were expressed in the microtubule-reporter line GATA23pro::MBD:GFP and the sC111 reporter line (Fig. 3A). After 24h gravistimulation of GATA23pro::MBD:GFP in presence of dexamethasone (DEX10μM) we observed that in LBD16pro>>PHS1ΔP, CMT were effectively depolymerized exclusively in the growing primordium and not in adjacent XPP cells (Fig. 8 A). No effects on CMT were observed when mock (DMSO) inductions were performed.

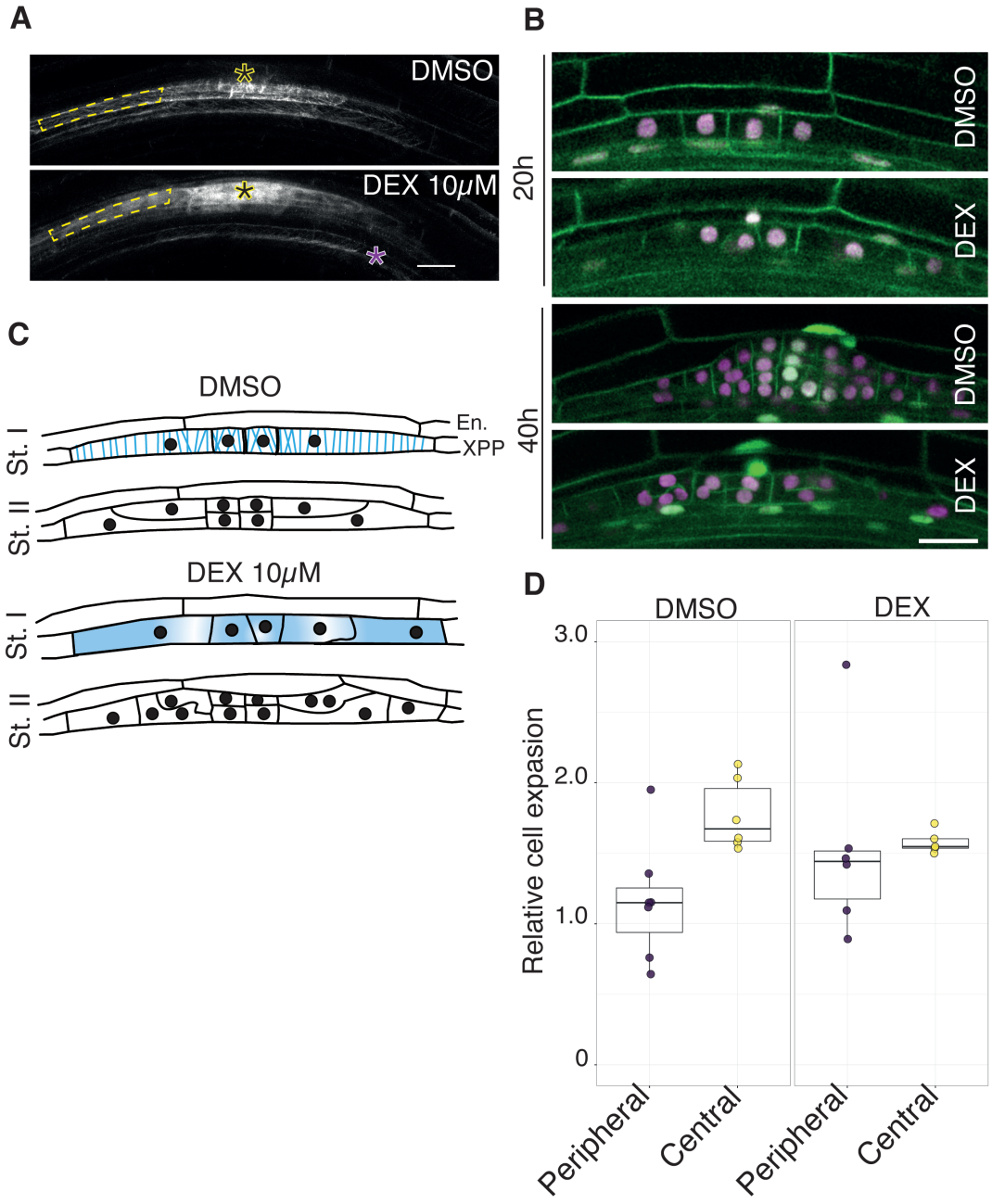

Fig. 8 Tissue-specific depolarization of microtubule in the pericycle originates the same LRP phenotype as in *bot1-7*.

A) Confocal sections of roots expressing LBD16pro::LhG4:GR:6xOP:PHS1ΔP:mCherry in GATA23pro::MBD:GFP. Images were taken after 24h gravistimulation in induction (DEX 10μM) and control conditions (DMSO) of T1 lines. Notice in the highlighted area with yellow dashed line the presence of fibrils in DMSO, whereas in the DEX treatment CMT have disappeared. The effect on microtubule stability is specific of dividing cells (yellow asterisk), whereas in non-dividing cells (purple asterisk) microtubule fibrils are not affected. Scale bar 20 μm.

B) Confocal sections of LBD16pro>>PHS1ΔP in the sC111 background were imaged 20h and 40h post gravistimulation in inducing (DEX 10μM) and control (DMSO) conditions. Scale bar 20 μm.

C) Schematic representation of the events depicted in (B). Notice CMT (blue) destabilization in DEX10μM.

D) Quantification of cell swelling 20h post gravistimulation in the peripheral (purple) or central (yellow) domains, upon induction of LBD16pro>>PHS1ΔP (DEX10μM) or control conditions (DMSO). Cell width in dividing cells was normalized to cell width in non-dividing cells in the opposite xylem pole. (N_{DMSO}= 6 , N_{DEX}= 6).

We then tested the effect of LBD16pro>>PHS1ΔP on asymmetric cell expansion of founder cells and LRP shape. We transferred seedlings to induction or control medium and gravistimulated them for 20h and 40h (Fig. 8 B). 20h after gravistimulation we detected oblique and aberrant cell division planes in young primordia when PHS1ΔP was induced. However, still ACD could be detected, as previously observed in *bot1-7*.

We measured relative cell expansion of founder cells and found that in contrast with control conditions (DMSO), asymmetric swelling was lost and cells swell 'en bloc' under induction of PHS1ΔP (Fig. 8C and D). After 40h of gravistimulation the LRP development was strongly delayed compared to control conditions and the shape resembled the "collapsed" primordia observed in the *bot1-7* (Fig. 8 B and C).

These results corroborate the idea that functional microtubule dynamics are essential for asymmetric cell expansion of founder cells. Together these results indicate that the increasing organization of the CMT towards the periphery restricts radial expansion in this domain, favouring asymmetry in cell swelling and the establishment of a dome-shaped primordium.

3.1.7 Loss of asymmetric division in LBD16-SRDX results in symmetric swelling and homogeneous organization of CMT

Auxin is the major regulator of LRP formation: many auxin signalling modules regulate different developmental phases of LRP formation, like priming at the root meristem or initiation and growth in the differentiation zone (Reviewed in [153]. In addition, it has been also reported that auxin induces differential cell growth, by regulating CMT and actin dynamics via Rho GTPases (Reviewed by [44]).

LRI is controlled by the *SOLITARYROOT* (*SLR*)/IAA14-ARF7/19 auxin module [69, 107]. In the dominant negative mutant, *slr1*, XPP cells do not divide and LRI is blocked. Downstream of SLR/IAA14, ARF7 and ARF19 activate the expression of the transcription factor *LATERAL ORGANS BOUNDARIES-DOMAIN 16 / ASYMMETRIC LEAVES2-LIKE18* (*LBD16/ASL18*) [63, 154]. The expression of the dominant repressor LBD16-SDRX blocks polar nuclear migration and asymmetric cell division. *LBD16* is therefore considered an important regulator for the establishment of asymmetry during LRI [63].

To test cell swelling and CMT dynamics when founders cells divide symmetrically we crossed LBD16-SRDX to the GATA23pro::GFP:MBD reporter. We observed CMT dynamics in F1 seedlings 8h post-gravistimulation. Alike the situation in wild type, in LBD16-SRDX CMT organized in transversal parallel bundles after cell division (Fig. 9 A and B). However, in LBD16-SRDX founder cells divided symmetrically and the differential organization of CMT between daughter cells is lost. Highly organized transversal parallel bundles could be indistinctly detected in both daughter cells. This organization is kept even 12h after cell division (Fig. 9 C and D).

Unlike wild type, in LBD16-SRDX, cell expansion is symmetric among daughter cells, which swell to the same extent (Fig. 9 E). In contrast to wild type, parallel bundles of CMT could be also observed in non-dividing cells in LBD16-SRDX. Reorientation of CMT in non-dividing cells occurred 6h after cell division and is also maintained after 12h of gravistimulation (Fig. 9A).

These results indicate the asymmetric organization of CMT among daughter cells is dependent on the transcriptional activity of LBD16. We could hypothesised that LBD16 regulates the expression of a gene (or genes) that act as a polarizing factor and induce the gradient of organization of CMT from the centre to the periphery.

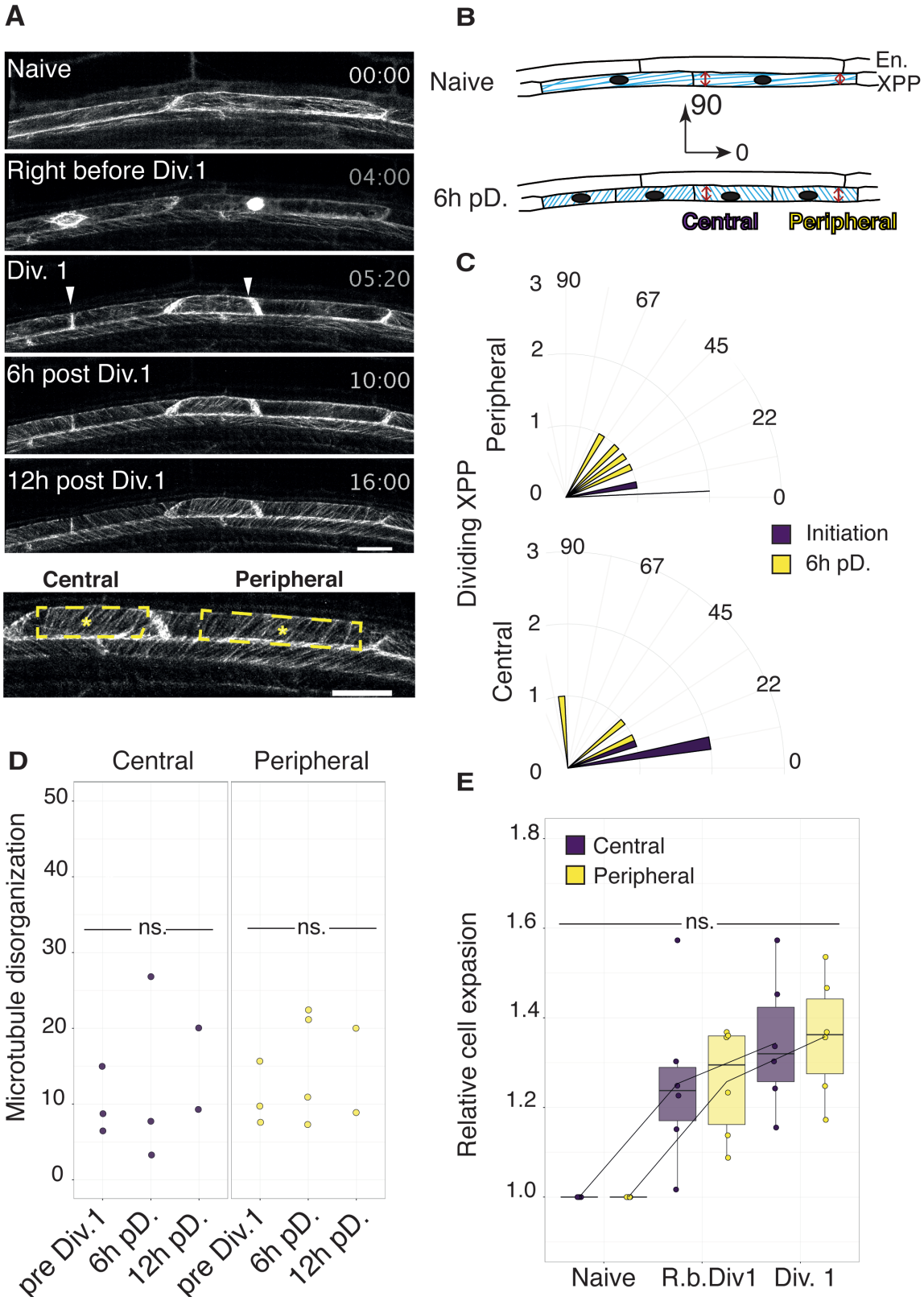
A
Naive
00:00
Right before Div.1
04:00
Div. 1
05:20
6h post Div.1
10:00
12h post Div.1
16:00
Central
Peripheral
B
Naive
En.
XPP
90
0
6h pD.
Central
Peripheral
C
Dividing XPP
Peripheral
Central
3
2
1
0
90
67
45
22
0
Initiation
6h pD.
D
Central
Peripheral
Microtubule disorganization
50
40
30
20
10
0
ns.
ns.
pre Div.1
6h pD.
12h pD.
pre Div.1
6h pD.
12h pD.
E
Relative cell expasion
1.8
1.6
1.4
1.2
1.0
Central
Peripheral
ns.
Naive
R.b.Div1
Div. 1

Fig. 9 Cell swelling is symmetric in the LBD16: SRDX background and microtubules reorient homogeneously.

A) Two-photon confocal sections of the GATA23pro::GFP:MBD in the LBD16-SRDX background live imaged after 8h of gravistimulation. Naïve cell show no obvious sign of initiation; Right before division nuclei round up and microtubule concentrate around the nucleus. Then cells divide once (Div.1) and microtubule progressively increases 6h and 12h after division. White triangles mark the position of cell divisions. Yellow dashed line marks the position used for microtubule analysis with Fiji (Fibril Tool).

B) Schematic representation of microtubule (blue) reorientation depicted in (A). In naïve cells CMT line with the longitudinal cell-axis. 6h after the first division (6h post Div.1) microtubule orientation is transversal to the longitudinal cell-axis. Red arrows indicate the position where swelling was measured in the central and the peripheral cell. Endodermis (En) and Xylem pole pericycle cells (XPP) are indicated.

C) Polar plot of microtubule orientation (0° to 90°) at the central or peripheral domain of dividing cells at two time points: previous cell division in purple (Naïve) and 6h after cell division in yellow (6h pD.). Concentric circles in polar plots (Y axis) indicate the number of measurements of a specific orientation.

D) Measure of microtubule disorganization in dividing cells at the central (purple) and peripheral position (Yellow). The higher the score the more disorganized. No significant differences were found among groups. (Tukey Test; alpha=0.05,in n =3 dividing_cells).

E) Quantification of the founder cells expansion in the peripheral and central domains in LBD16-SRDX. Boxplots represent the distribution of cell width at the central (purple) or peripheral (yellow) positions at the indicated phases: naïve founder cells, right before the first asymmetric division (R.b.Div.1) and after the first division (Div.1). At least 8 cells were imaged and analysed. Measurements were normalized to the initial cell width (Naïve). No significant differences were found among groups (Tukey test; alpha=0.05).

3.1.8 After the first asymmetric division actin reorganizes in a polarized mesh that surrounds the nucleus

LBD16 controls the asymmetric migration of nuclei before the ACD of the founder cells [63]. Consequently, upon perturbation of LBD16 activity founder cells divide symmetrically, originating two equally sized cells. In addition, we observed that when LBD16 transcription activity is inhibited, CMT orient in transversal parallel bundles in both daughter cells, which also experience comparable level of expansion.

Microtubules are often associated with directional control of cell growth, however another important component of the cytoskeleton, actin, has also been associated with polar cell expansion and nuclear migration in different developmental processes (reviewed by [44, 66, 155].

To determine the role of actin cytoskeleton during LRI we first set to document actin dynamics in the tissue-specific marker line LBDD16pro:: GFP:ABD2 (kindly donated by Tatsuaki Goh). We observed that before division, thick actin bundles are longitudinally oriented along pericycle cells. Once nuclei are asymmetrically positioned, actin reorganizes in a dense mesh surrounding the nucleus. This actin mesh is heterogeneously distributed, being almost absent at the peripheral edge (Fig. 10 A and B, Fig. 12 A (DMSO)). Right before division actin can be detected at the pre prophase band. When the new cell wall is formed, actin remains associated to the nucleus, occupying the whole cell volume in the small daughter. In contrast, in the big daughter cell, actin accumulates close to the nucleus and remains excluded from the periphery. While the actin mesh becomes increasingly disorganized and fluorescence intensity progressively dimmers after ACD, in non-dividing cells actin bundles remain unaltered (Fig. 10 A, B and D).

Our observations of actin dynamics during LRI show that, similarly as CMT organization, actin shows a polarized gradient of organization. Actin mesh accumulates at the central domain, where it spatially correlates with the region of maximal expansion. Moreover actin is intimately associated with the nucleus and is completely absent in the peripheral domain of the young primordium.

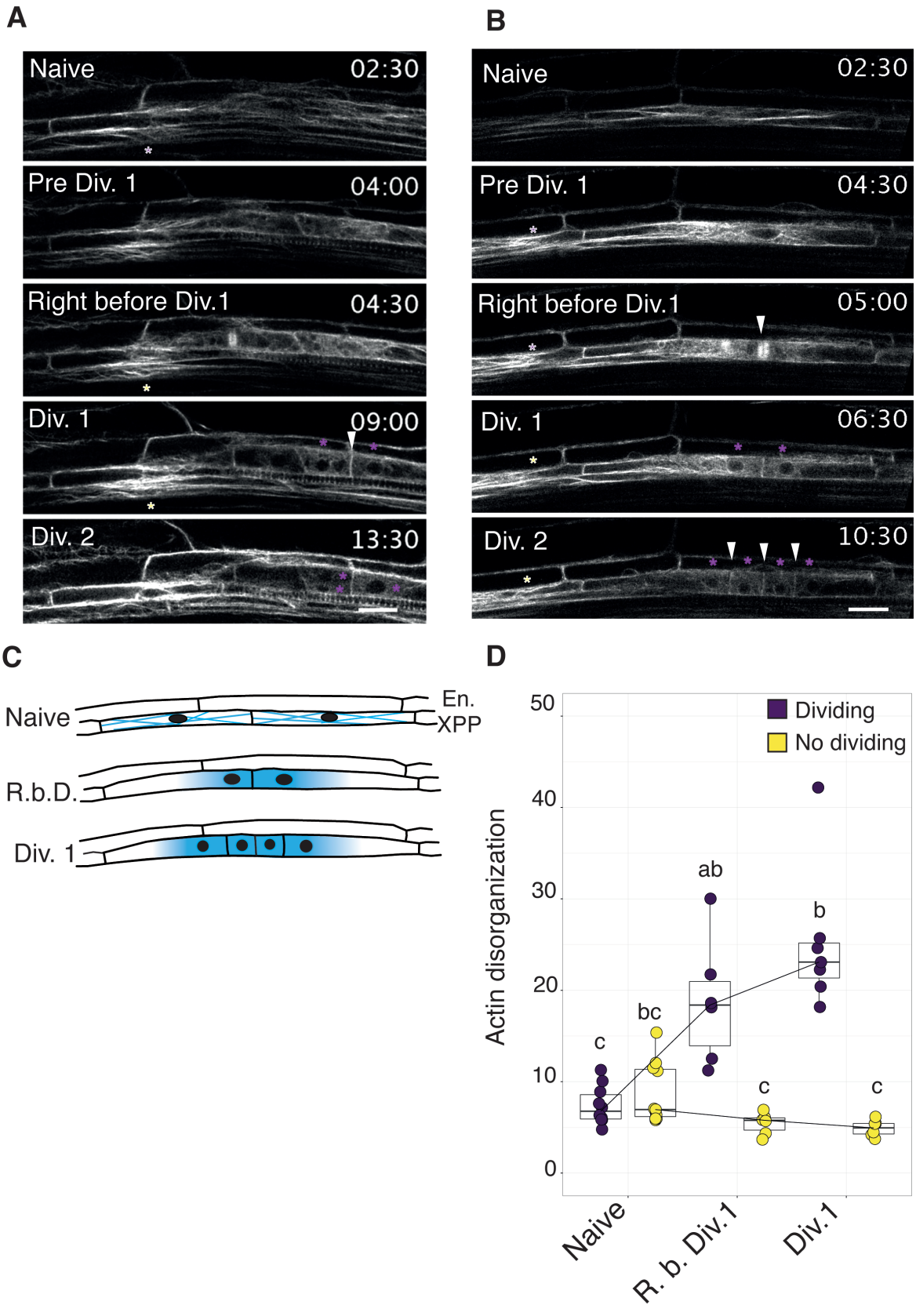
A
Naive
02:30
Pre Div. 1
04:00
Right before Div.1
04:30
Div. 1
09:00
Div. 2
13:30
B
Naive
02:30
Pre Div. 1
04:30
Right before Div.1
05:00
Div. 1
06:30
Div. 2
10:30
C
Naive
En.
XPP
R.b.D.
Div. 1
D
Dividing
No dividing
Actin disorganization
50
40
30
20
10
0
ab
b
bc
c
c
c
Naive
R. b. Div.1
Div.1

Fig. 10 Actin reorganization in a polarized mesh around the nucleus is exclusive from founder cells during ACD

A) Confocal sections of LBD16pro::GFP:ABD2 plants live imaged 4h post-gravistimulation every 30 min. The following key stages are highlighted: before cell division (Naïve), when nuclei migrate and swell (pre Div.1), right before the first division (Right before Div.1), first division (anticlinal) (Div.1) and second division (periclinal)((Div.2).

B) LRI originates form one single cell that creates two daughter cells, which undergo ACD. Second division is anticlinal (Div.2). Note that actin accumulates in the centre of the mother cell and is absent at the periphery. Both A and B: Yellow asterisks mark the position of the nuclei after division. White triangles mark new divisions. Purple-white asterisk highlight neighbouring non-dividing cells.

C) Schematic representation of actin (blue) reorganization during LRI. Long actin bundles can be observed in naïve cells; Right before division (R.b.Div1) the actin mesh accumulates around the nucleus. After the first division (Div.1) actin accumulates around the central part being absent at the periphery. Endodermis (En) and Xylem pole pericycle cells (XPP).

D) Quantification of actin disorganization in dividing cells (purple) and non-dividing cells (Yellow); the higher the score the more disorganized. Measurements done with FibrilTool. Different letters show significant differences among groups (Tukey Test; alpha=0.05, n=10).

3.1.9 Actin reorganization and asymmetric cell division are dependent on LBD16

We then tested whether perturbing the ability of founder cell to divide asymmetrically could influence the dynamics of actin network. For this, we crossed LBD16-SRDX with LBDD16pro::GFP:ABD2 and monitored actin dynamics in F1 seedlings, 8h post-gravistimulation.

According to our observations actin in LBD16-SRDX is organized in long bundles before cell division, as we previously described in wild type (Fig. 11 A). We detected that in LDB16-SRDX first division occurs approximately 10h after gravistimulation, compared to the 6-8h in wild type and this division is symmetric (Fig. 11 C). During the progression of mitosis actin accumulates at the pre-prophase band, as previously observed in wild type (Fig. 11 A and B). However, after division, the organization of the actin mesh is not maintained in LBD16-SRDX; in daughter cells actin bundles reappear, radiating towards the plasma membrane from the nucleus, which is located in the middle of each cell (Fig. 11 A).

We then quantified the organization of the actin mesh with FibrillTool (FiJi). In contrast with wild type, we cannot detect any difference in the organization of actin bundles between founder and non-dividing XPP cells after cell division (Fig. 11D).

Our results show that in LBD16-SRDX actin dynamics are changed in terms of polarity and organization. Together our observations suggest that absence of nuclei migration and symmetric cell division described in LBD16-SRDX could be a consequence of the defective actin dynamics observed in this line.

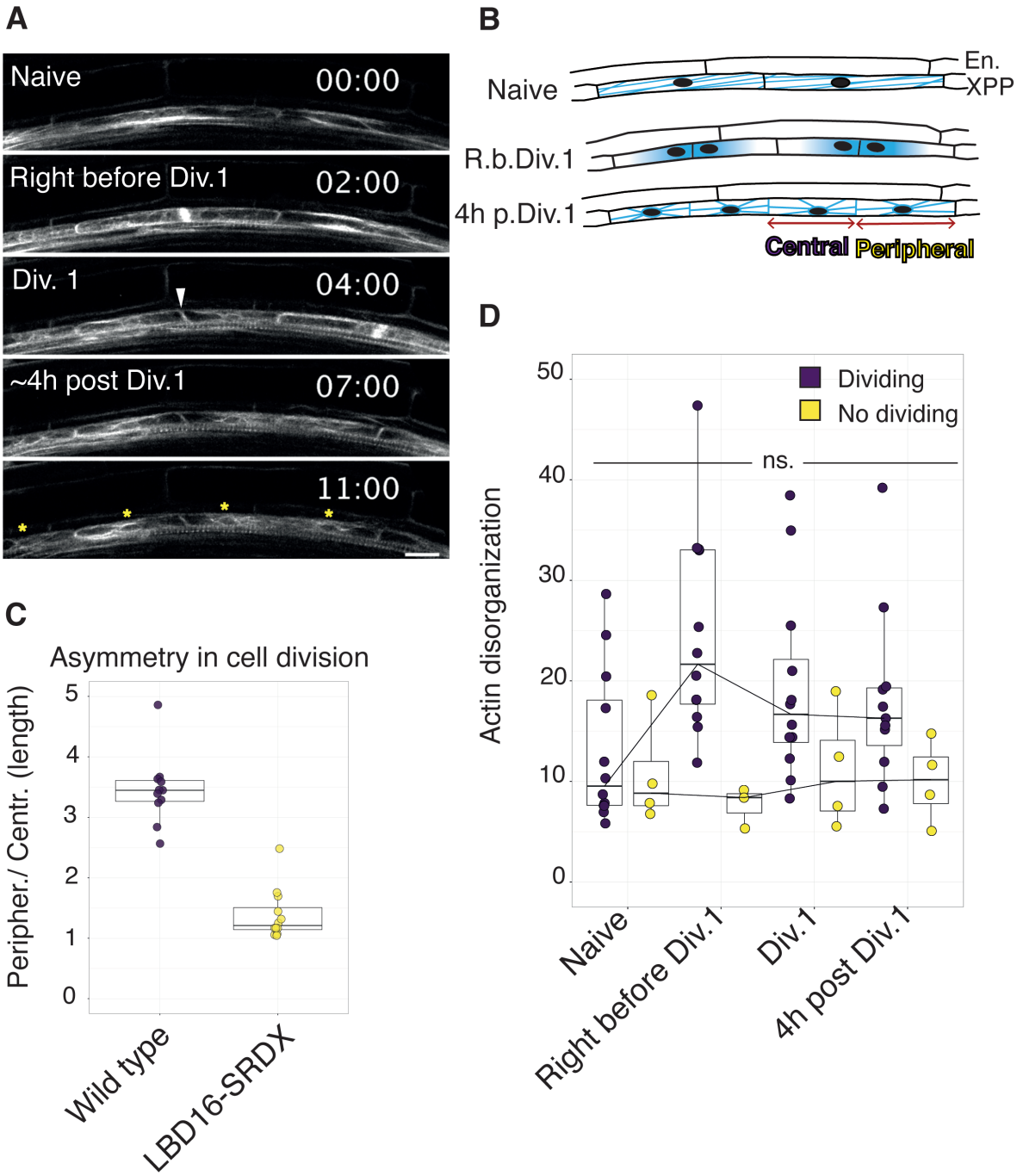
A
Naive
00:00
Right before Div.1
02:00
Div. 1
04:00
~4h post Div.1
07:00
11:00
B
Naive
En.
XPP
R.b.Div.1
4h p.Div.1
Central
Peripheral
C
Asymmetry in cell division
Peripher./ Centr. (length)
0
1
2
3
4
5
Wild type
LBD16-SRDX
D
Actin disorganization
0
10
20
30
40
50
Dividing
No dividing
ns.
Naive
Right before Div.1
Div.1
4h post Div.1

Fig. 11 Actin cytoskeleton organization and cell division are affected in LBD16-SRDX.

A) Two-photon confocal section after live imaging of LBD16pro::GFP:ABD2 marker in the LBD16-SRDX background 8h post-gravistimulation. Naïve cells show no obvious sings of initiation; Right before Div.1 actin accumulates at the pre prophase band; Cells divide once (Div.1) and nuclei can be observed in the centre of the cells; 4h and 8h after division actin bundles become more clear surrounding the nucleus and projecting towards the plasma membrane, but no actin mesh can be observed. White triangle marks cell division. Yellow asterisk mark the centred position of nuclei 8h after cell division. Scale bar 20μM.

B) Schematic representation of actin cytoskeleton (blue) organization and symmetric cell division depicted in A. In Naïve cells actin bundles line with the longitudinal cell axis. Right before division (R. b. Div1) actin disorganization increases but 4h after cell division actin bundles become visible again. Nuclei remain in the centre of the cells. Red arrows indicate the position where length was measured in the central and the peripheral cell. Endodermis (En) and Xylem pole pericycle cells (XPP) are indicated.

C) Ratio of daughter cells length after cell division in LDB16-SRDX and wild type. A ratio of 1 between the big daughter cell (peripheral) and the small daughter cell (central) in LBD16-SRDX indicates symmetric cell division. (N_{WT}=8; $N_{LBD16SRDX}$=8).

D) Quantification of actin disorganization in dividing cells (purple) and non-dividing cells (yellow) in the LBD16-SRDX background. The higher the score the more disorganized. Measurements done with Fibril Tool. Different letters show significant differences among groups (Tuckey Test; p-value<0.05,ndividing_cells=6).

3.1.10 Asymmetry is lost in the absence of a functional actin network

The previous results support the view that LBD16 controls polar nuclei migration and asymmetric expansion of founder cells by influencing the organization of the cytoskeleton. In our observations actin mesh is asymmetrically distributed in spatial association with the nucleus and the region of maximal expansion. Since pharmacological disturbance of the CMT network was instrumental to evidence its participation in the maintenance of asymmetric cell expansion, we decided to make use of the actin-depolymerizing compound Latrunculin B (LatB) and monitor the impact on founder cells expansion and division.

A concentration of LatB 500nM destabilizes actin bundles without completely abolishing cell division (Fig. 12 A). We observed that actin bundles disappear after pharmacological destabilization and depolymerized actin can be detected spreading along the cell or around the nucleus, which remain in the centre of cells (Fig. 12 A and B).

We then analysed cell expansion and cell division during LRI making use of the marker line sC111 in the presence of LatB 500nM or DMSO (Fig. 12 B and C). LatB strongly delays cell division and impairs nuclei migration. Consequently, in the presence of Lat B cells divide symmetrically in contrast with control conditions, where the ratio between daughter cells length is 1:4 (Fig. 12 D).

We also observed that the LatB treatment affects asymmetric cell expansion; In contrast with control conditions, in LatB no differences can be found on cell width between the two daughter cells (Fig. 12 E).

In summary, our observations indicate that polarization of cytoskeleton organization is instrumental for the maintenance of the asymmetry between the central region and the periphery during LRI. While CMT are necessary for controlling cell expansion, actin mainly controls the positioning on the nucleus and the cell division plane.

Actin mesh accumulates in the central domain, where maximal expansion occurs, and affecting actin dynamics has an influence on cell expansion. On the other hand, actin is excluded from the periphery, where CMT form transversal bundles. It seems also that the domains of actin accumulation and formation of CMT transversal bundles are mutually excluded.

To corroborate this hypothesis we monitored CMT dynamics during LRI under actin depolymerizing conditions. We took images of LRP in the marker line GATA23::GFP:MBD 20h post-gravistimulation in the presence of LatB 500nM.

Results

As previously described in the reporter line sC111, in the presence of LatB 500nM founder cells divide symmetrically at the bending. We observed that microtubules polymerization is not affected in the presence of LatB. Interestingly, microtubules tend to orient in parallel bundles with the same level of organization in the two daughter cells (Fig. 10 F).

This observation suggest that the loss of cell expansion asymmetry observed in the presence of LatB, could be derived from the homogeneous organization of CMT and implies a negative influence of actin in the organization of CMT in transversal bundles.

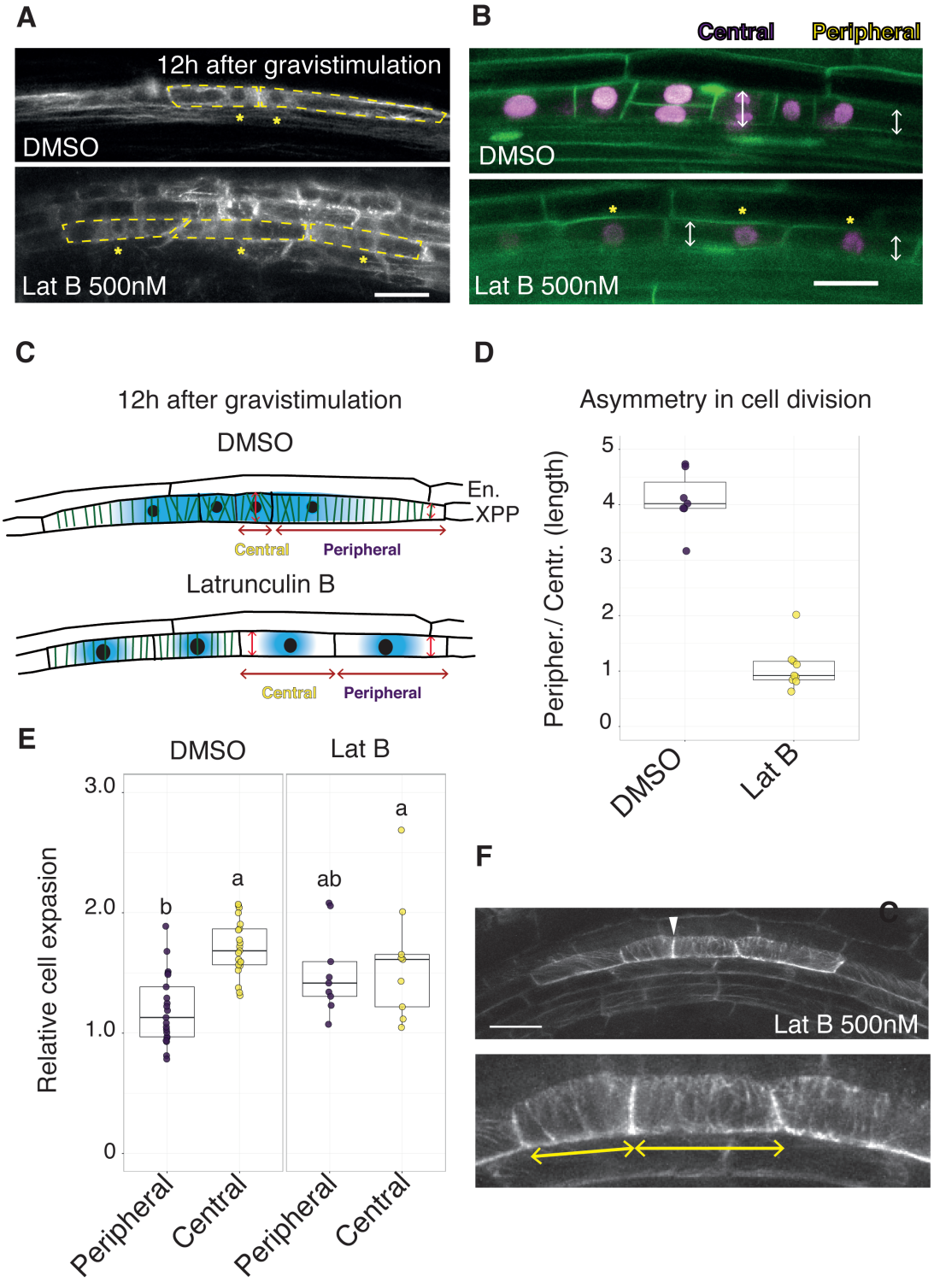

Fig. 12 Functional actin network is necessary for ACD and asymmetric cell expansion.

A) Confocal sections of LBD16pro::ABD2:GFP reporter in presence of 500mM Latrunculin B or control conditions (DMSO). Images were acquired 12h post-gravistimulation. The yellow boxes highlight the shape of cell at the bending in DMSO and LatB and the asterisk the position of the nuclei. Notice that in contrast to DMSO, in LatB treatment nuclei remain in the centre of the cells. Scale bar 20μM.

B) Confocal sections of the marker line sC111 12h post gravistimulation in LatB 500nM treatment. DMSO indicates control conditions. White arrows indicate the position where founder cell width was measured after division. The yellow asterisks highlight the position of the nuclei in the centre of cells on LatB treatment. Scale bar 20μM.

C) Schematic representation of the images in A, B and F. Actin is depicted in blue and microtubules are depicted in green in DMSO and LatB, Red arrows represent the measurements of cell length and cell width in the small/central and big/peripheral cell in DMSO and LatB.

D) Ratio of daughter cells length after founder cell division in presence of LatB. Ratio between the big daughter cell (peripheral) and the small daughter cell (central) was calculated. A ratio of 1 in LatB-treated roots indicates a symmetric cell division (n_{DMSO}=10, n_{LATB}=9).

E) Quantification of cell swelling 12h post-gravistimulation at the peripheral and the central domain in DMSO and LatB 500nM-treated roots. Cell width was normalized to cell width of non-dividing cells in the opposite xylem pole. Different letters indicate significant difference among groups (Tukey test; alpha=0.05, n_{DMSO}=23, n_{LATB}=9)

F) Two-photon image of GATA23pro::GFP:MBD in LatB 500nM 20h post-gravistimulation. The white arrow indicates the position of the division cell plane. Bellow there is a magnification, where yellow arrows highlight the similar size of daughter cells. Notice the organization of CMT in parallel bundles in both daughter cells.

3.2 Microtubule dynamics in the endodermis are auxin-signalling dependent

As the lateral root primordium develops it pushes against the overlying tissue. This process is called lateral root emergence and requires the activation of auxin-signalling-mediated processes, like loss of turgor pressure and activation of cell wall modifying enzymes in the three overlying tissues: the endodermis, the cortex and the epidermis [138, 156].

The endodermis differs from cortex and epidermis by the presence of the Casparian strip. This lignified and suberized structure seals endodermal cells together and makes the endodermal tissue a polarized barrier. Many transporters, as well as receptors are localized at either the outer or the inner side of the endodermis and gives each side different functions [157].

The inner side, in contact with the pericycle, is of special importance for lateral root development. Early auxin- but also mechanical signals between the pericycle and the inner side of the endodermis are essential to activate the first round of pericycle divisions [2, 128].

Because the Casparian strip is a lignified structure, endodermis cells cannot detach from each other. Consequently, in order to enable LRP emergence, the endodermis undergoes a dramatic local loss-of-volume until opposite membranes fuse together and form a gap to allow the growth of the LRP [2].

Cell shape in plants is largely controlled by cell wall. Its stiffness or elasticity is determined by the relative composition of its main components, cellulose, pectins and hemicelluloses and the chemical bounds between them [6, 16, 145].

CMT serve as intracellular rails that guide the deposition of cellulose at the cell wall by the cellulose synthase complex and thereby participate in the consolidation of cell shape [6, 37].

Although cell wall remodelling processes in the endodermis during the emergence of LRP have been described (Reviewed by [125]) little is known about CMT dynamics in the endodermis and their role during lateral root emergence.

3.2.1 Emergence through the endodermis is delayed in the katanin mutant *bot1-7*

To test whether microtubules dynamics contribute to the spatial accommodation of the endodermis we analysed lateral root emergence in the mutant, *bot1-7,* where CMT dynamics are impaired. Seedlings of *bot1-7* and wild type were simultaneously gravistimulated and fixed [147] after 18h to 42h. We compared LR emergence in both genotypes (Fig. 13). In *bot1-7*, remodelling of the endodermis is strongly delayed. Endodermal cells above the LRP remained almost unchanged in the mutant for longer time, causing emergence to be delayed.

This observation suggests that CMT dynamics are necessary to facilitate the spatial accommodation of the endodermis during LRP emergence.

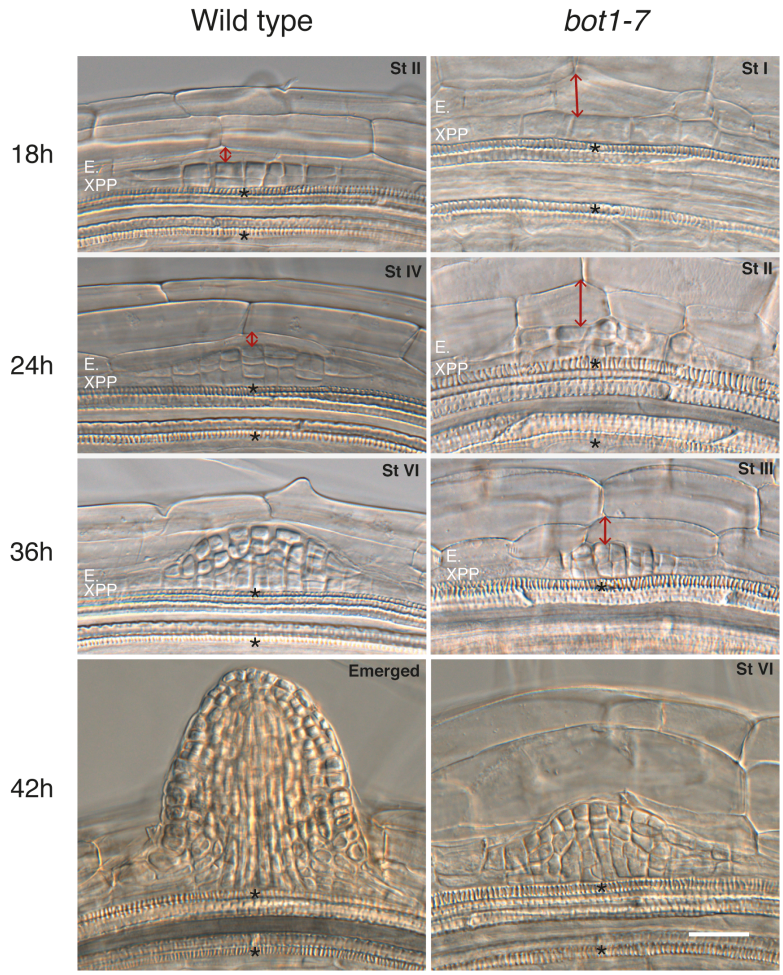

Fig. 13 Emergence through the endodermis is strongly reduced

Microphotographs of cleared 5 to 7 dag seedlings of Col-0 and *bot1-7* fixed at the indicated time post-gravistimulation. The stage of development (StI up to emerged) is indicated. Red arrows show the thickness of the endodermis at the highest point of the primordium. Black asterisks indicate the position of opposite xylem poles, taken as positional reference of the middle of the lateral root primordia in both genotypes. Scale bar 30μM. Endodermis (E), Xylem pole pericycle cells (XPP).

3.2.2 CMT reorganize in the endodermis and show intracellular heterogeneity

The microtubule-severing protein KATANIN is responsible of the organization of CMT in parallel bundles [139]. The defects in endodermal spatial remodelling observed in *bot1-7*, made us hypothesize that microtubule organization in parallel bundles could be necessary for endodermal spatial accommodation during emergence.

To test this hypothesis we first made use of the endodermis-specific microtubule marker CASP1pro::mVenus:MAP4 [2] to visualise CMT dynamics solely in the endodermis. As it is difficult to find young lateral primordia before they cross the endodermis, we induced LRI in all XPP cells by treatment with 10 μM IAA [11]. This enables us to analyse CMT orientation and cell shape in many endodermal cells simultaneously.

We observed that in absence of any treatment, endodermal cells are not tubular, but rather polygonal/ semi-cylindrical cells. If we divide endodermal cells along their longitudinal axis, we can observe that the outer half in contact with the cortex and the lateral sides between neighbouring cells are flat. In contrast, the inner half is convex to the vascular tissue (Fig. 14 A, DMSO).

For the analysis of CMT at different cell sides we did maximal projections of the inner (Vascular) and outer halves (Cortex and lateral) (Fig. 14 A, grey cells). Analysis of the CMT visualized with the CASP1pro::mVenus:MAP4 images revealed that the organization of CMT (Fig. 14 C, DMSO) is different between the inner and outer faces. While CMT in the vascular-side are oriented along the longitudinal axis, in the cortex-and lateral-sides show a rather chaotic organization.

Upon IAA treatment (24h, 10μM), pericycle cells divide and expand. In response to pericycle growth, the polygonal shape of the overlying endodermis is deformed and cells become flattened (Fig. 14 A and B, IAA). This change in endodermal cell shape is reflected in an increase of disorganization of the microtubule network, especially in the outer cell side (Fig. 14 C and E). CMT in the lateral sides reorganize in transversal parallel bundles to the longitudinal axis, which cannot be seen in the other cell sides.

Taken together, our observations indicate that CMT have different patterns of organization depending on the cell side. In response to IAA, pericycle cell start to grow and endodermal cell accommodate their shapes. This spatial accommodation originates patterns of CMT reorganization in the endodermis, which differ between cell-sides,

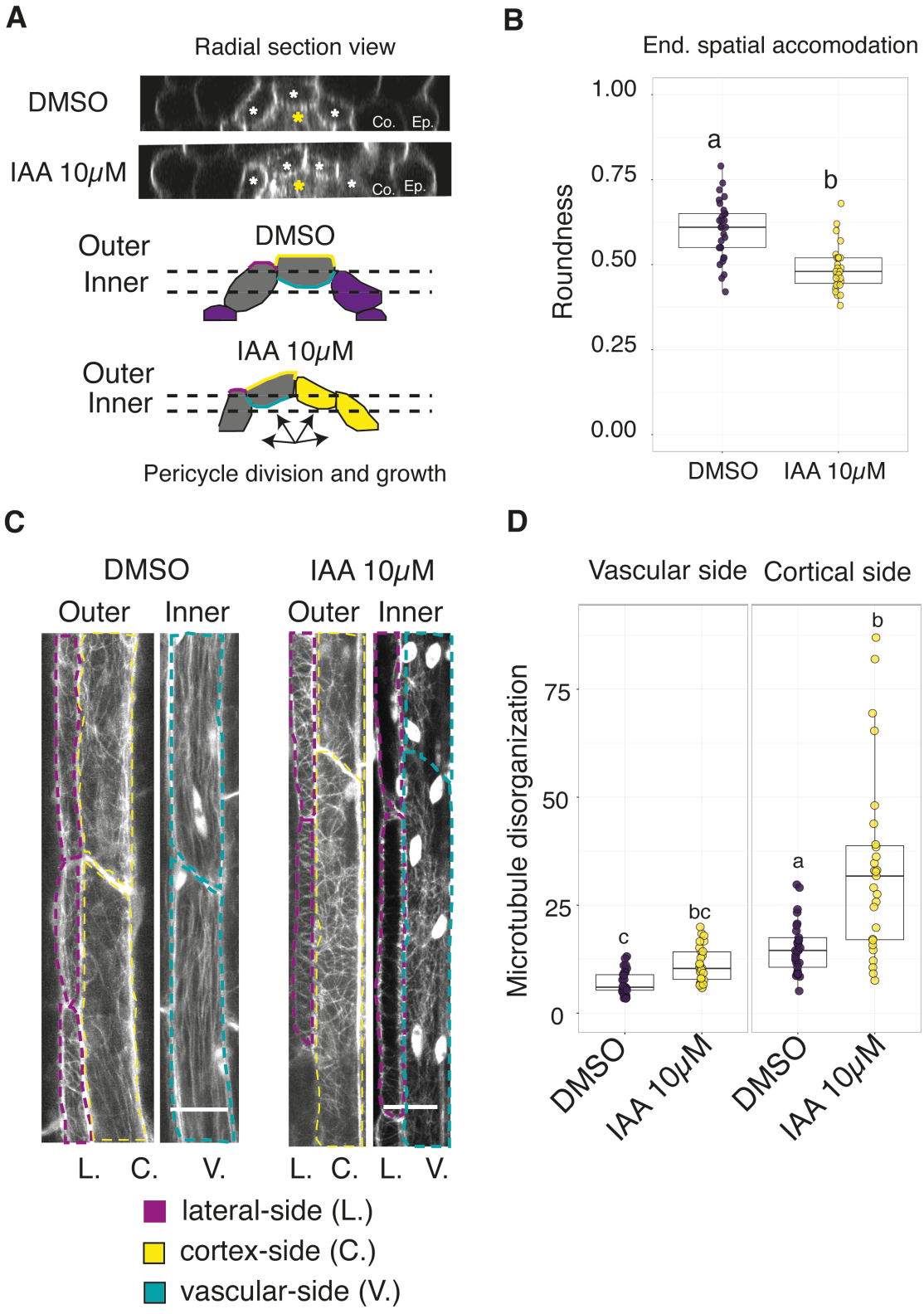
A
Radial section view
DMSO
IAA 10μM
Co.
Ep.
Outer
Inner
DMSO
IAA 10μM
Pericycle division and growth
B
End. spatial accomodation
Roundness
1.00
0.75
0.50
0.25
0.00
a
b
DMSO
IAA 10μM
C
DMSO
IAA 10μM
Outer
Inner
L.
C.
V.
lateral-side (L.)
cortex-side (C.)
vascular-side (V.)
D
Vascular side
Cortical side
Microtubule disorganization
75
50
25
0
c
bc
a
b
DMSO
IAA 10μM

Fig. 14. Cortical microtubules reorganize in the endodermis and show intracellular spatial heterogeneity.

A) Radial section of a Z-stack volume imaged with a two-photon laser in the marker line CASP1pro::MAP4:GFP. Concentric layers surrounding the vascular tissue (yellow asterisk) can be seen: Endodermis (white asterisk), Cortex (Co.) and Epidermis (Ep.) after 24h of DMSO and IAA 10μM treatment. The drawing shows the radial view of endodermal cells after 24h of DMSO (purple) and IAA 10μM (yellow) treatment. Dashed-lines indicate the limits of the maximal projections (C) done for the analysis of microtubule-organization in the outer and inner halves of the endodermal cells highlighted in grey. Lateral, vascular and cortical cell sides are indicated in different colours (See C).

B) Measurement of roundness of the radial section of the endodermis after 24h treatment with IAA 10μM (yellow) and DMSO (purple) (FiJi). Lower values indicate cell flattening during endodermal spatial accommodation.

C) Two-photon images of microtubule organization in the cross line: CASP1pro::MAP4:GFP x GATA23pro::nls:GFP. Inner and outer maximal projections show microtubule organization in the vascular- (cian), the cortex- (yellow) and lateral-sides (magenta). GATA23-positive nuclei can be appreciated in the inner maximal projection. Note how auxin treatment increases the number and the shape of GATA23-positive nuclei. Scale bar 20μm.

D) Measurement of CMT disorganization in the vascular and cortex side after 24h treatment with IAA10μM (Yellow) or DMSO treatment (purple). Higher values indicate more disorganization of CMT. Different letters indicate significant differences between groups (Tuckey Test; alpha=0.05,N_{DMSO}=58, N_{IAA}=54, at least 3individual replicates).

3.2.3 CMT reorganization in the endodermis is dependent on auxin signalling and partially controlled by SHY2

Auxin signalling is responsible of the spatial accommodation of the endodermis. The expression of the dominant negative version of *SHORT HYPOCOTYL2/IAA3* (*SHY2*) in the endodermis prevents cell shape remodelling and LRI cannot take place [2].

CMT are known to reorient in response to mechanical stresses [4, 9, 29]. Therefore, to determine to which extend the organization of CMT in the endodermis is responsive to auxin signalling or mechanical constrains, CASP1pro::mVenus:MAP4 was crossed with the mutant *slr1* or with CASP1pro::*shy2-2* [2], where a gain-of-function form of SHY2 is only expressed in the endodermis.

The rational for this experiment is that both lines lack lateral root initiation, however in *slr1* auxin signalling is exclusively blocked in the pericycle, whereas in CASP1*pro*::*shy2-2* auxin signalling is blocked only in the endodermis. This will allow us to disentangle whether the reorganization of CMT that we observe is a direct response to auxin or an indirect response to the initiation of the LRP and the induced mechanical changes.

After IAA treatment (10μM, 24h) we observed flattening of the endodermal cells in wild type; it was previously reported that prolonged IAA treatment can induce pericycle swelling and divisions in CASP1pro::*shy2-2* mutant [2]. We detected that endodermal cells in CASP1pro::*shy2-2* became less round after 24h of IAA10μM. However this occur to a lesser extend as in wild type. In contrast, in *slr1*, we could not observe any change in endodermis shape (Fig. 15 A and C), in accordance with the lack of LRI in this mutant.

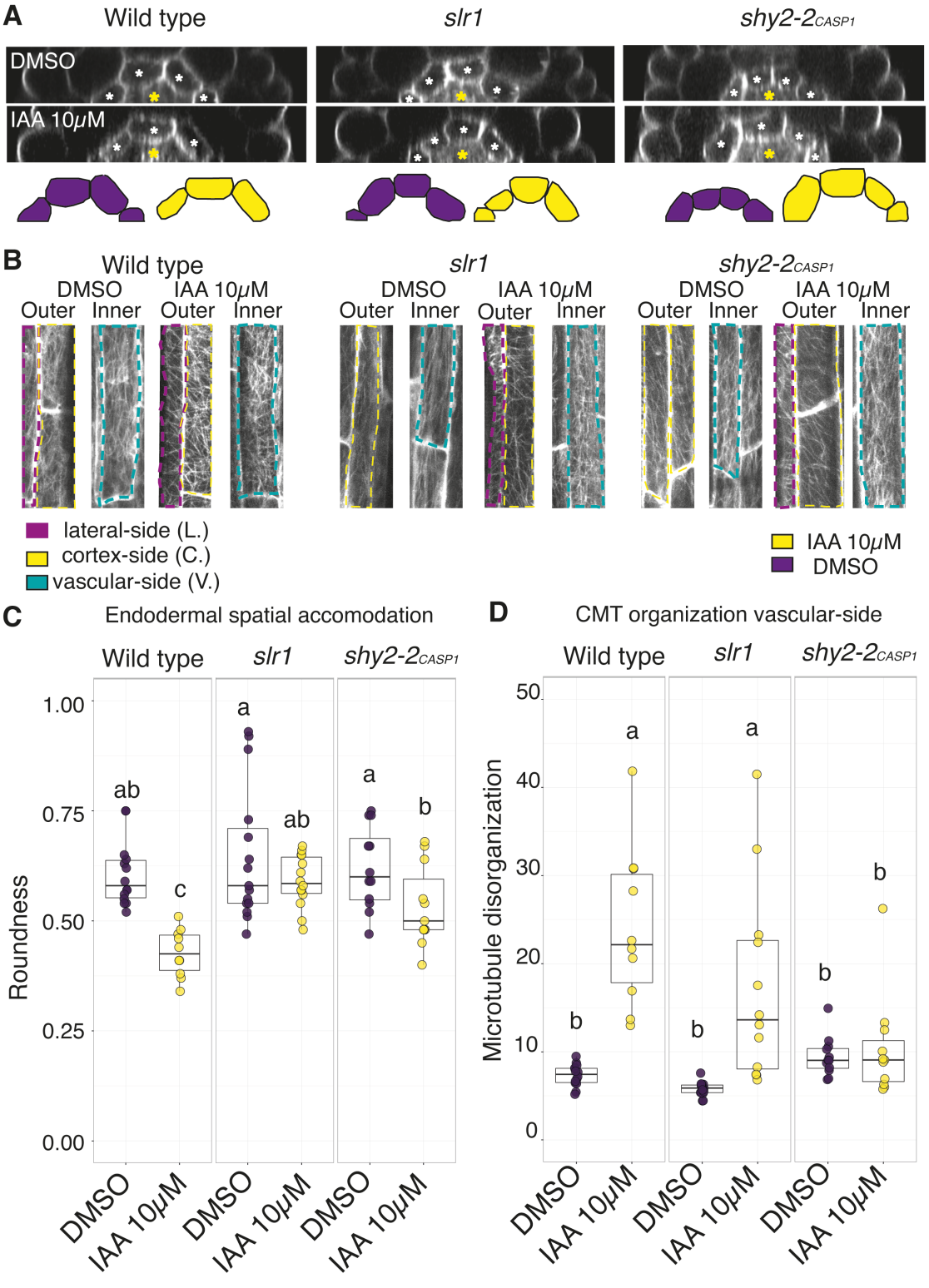
A
Wild type
slr1
shy2-2CASP1
DMSO
IAA 10µM
B
Wild type
slr1
shy2-2CASP1
DMSO
IAA 10µM
Outer
Inner
lateral-side (L.)
cortex-side (C.)
vascular-side (V.)
IAA 10µM
DMSO
C
Endodermal spatial accomodation
Roundness
1.00
0.75
0.50
0.25
0.00
ab
c
a
ab
a
b
D
CMT organization vascular-side
Microtubule disorganization
50
40
30
20
10
0
b
a
b
a
b
b

Fig. 15 Microtubule re-organization in the endodermis is SHY2- dependent.

A) Radial section of Z-stack volume taken with a two-photon laser in the marker line CASP1pro::mVenus:MAP4 crossed with Col-0, *slr1* and CASP1*pro*::*shy2-2* (*shy2-2* $_{CASP1}$). The endodermis (white asterisk) surrounding the vascular tissue (yellow asterisk) can be seen after 24h of DMSO or IAA 10μM treatment. The model shows radial view of endodermal cells in DMSO (purple) and IAA 10μM (yellow).

B) Two-photon images of microtubule organization in inner and outer maximal projections of CASP1pro::mVenus:MAP4 in wild type, *slr1* and CASP1pro::*shy2-2* (*shy2-2* $_{CASP1}$), after 24h of IAA 10μM treatment or control conditions (DMSO). In the inner maximal projection microtubule organization in the vascular-side (cyan) can be appreciated. In the outer maximal projection, microtubule organization at the lateral- (magenta) and cortex-side (yellow) of the endodermis is shown.

C) Measurement of roundness of the radial section of the endodermis after 24h treatment with IAA 10μM (yellow) and DMSO (purple) (FiJi) in Col-0, *slr1* and CASP1pro::*shy2-2* (*shy2-2* $_{CASP1}$). Lower values indicate cell flattening during endodermal spatial accommodation. Different letters indicate significant differences between groups (Tuckey Test; alpha=0.05, N_{cells_WT}=24, N_{cells_slr1}=29, $N_{cells\_CASP:shy2\_2}$=23).

D) Measurements of microtubule disorganization in the vascular-side after IAA (yellow) and DMSO treatment (purple) in Col-0, *slr1* and CASP1pro::*shy2-2* (*shy2-2*$_{CASP1}$). Higher values indicate more disorganization of CMT. Different letters indicate significant differences between groups (Tuckey Test; alpha=0.05, N_{cells_WT}=24, N_{cells_slr1}=29, $N_{cells\_CASP:shy2\_2}$=23).

We then analysed the organization of CMT. Although endodermal cells do not suffer any deformation in *slr1*, CMT reorganized similar as in WT (Fig. 15 B and D) indicating, that sensing of IAA alone, without mechanical deformations, is able to induce CMT re-organization in the endodermis.

In CASP1pro::*shy2-2,* where endodermal cells start flattening after 24h of IAA treatment, CMT at least in the inner side, remained similar as in control conditions (Fig. 15 D). In the lateral side, CMT transversal bundles could be also observed in CASP1pro::*shy2-2* and in the outer side CMT behave similar to wild type after IAA treatment.

Taken together, these results show that CMT organization in the endodermis is dependent on auxin signalling controlled by SHY2. Yet, as CMT organization in the outer and lateral sides of the CASP1pro::*shy2-2* mutant did not differ from wild type (Fig. 15 B), it seems that SHY2 controls CMT organization in the inner side.

3.2.4 CMT reorganization and cell-shape remodelling are delayed in the *bot1-7* mutant

The previous results suggest that CMT organization is responsive to exogenous IAA and/or the mechanical stress exerted by the growing primordium induced by auxin.

To test whether the reorganisation of CMT could be correlated in time with the spatial accommodation of the endodermis, we live-imaged endodermis-specific microtubule marker CASP1pro::mVenus:MAP4 during the emergence throw the endodermis in young LRP (Stage I-II); We performed a comparison between wild type and the mutant background *bot1-7* , were CMT dynamics are impaired.

In wild type, we measured the thickness of the endodermis over time until opposite membranes fuse together (Fig. 16 B). We observed that CMT first reorient up to 90° on the lateral side of the endodermis (highlighted in yellow), forming transversal parallel bundles (Fig. 16 A). As the cell progressively becomes thinner CMT bundles gradually depolymerize, starting from the edges (Fig. 16 B, wild type) to the centre of the cell. Notably, CMT depolymerize before the complete local loss-of-volume occur.

Similar to the observations made in presence of 10μM IAA, we did not observe formation of transversal parallel bundles on neither the internal nor external faces of the endodermis (green cell in Fig. 16A), yet we observe CMT depolymerisation before the fusion of the membrane. This rearrangement of CMT is specific of the endodermal cells above a LRP. Indeed, in an endodermis cell not directly abutting an LRP, CMT neither form parallel bundles nor undergo depolymerization (Fig. 16 A and B, green cell).

Results

In *bot1-7*, CMT are very disorganized and only local bundling can be detected in one of the cells overlying the growing primordium (highlighted in yellow, Fig. 16 A and B). As previously observed in cleared roots, the endodermis remains turgid in the mutant and loss-of-volume is very delayed compared to wild type.

Together these observations indicate that auxin induces reorganization of CMT, which seems to be necessary for the spatial accommodation of the endodermis during LRP emergence.

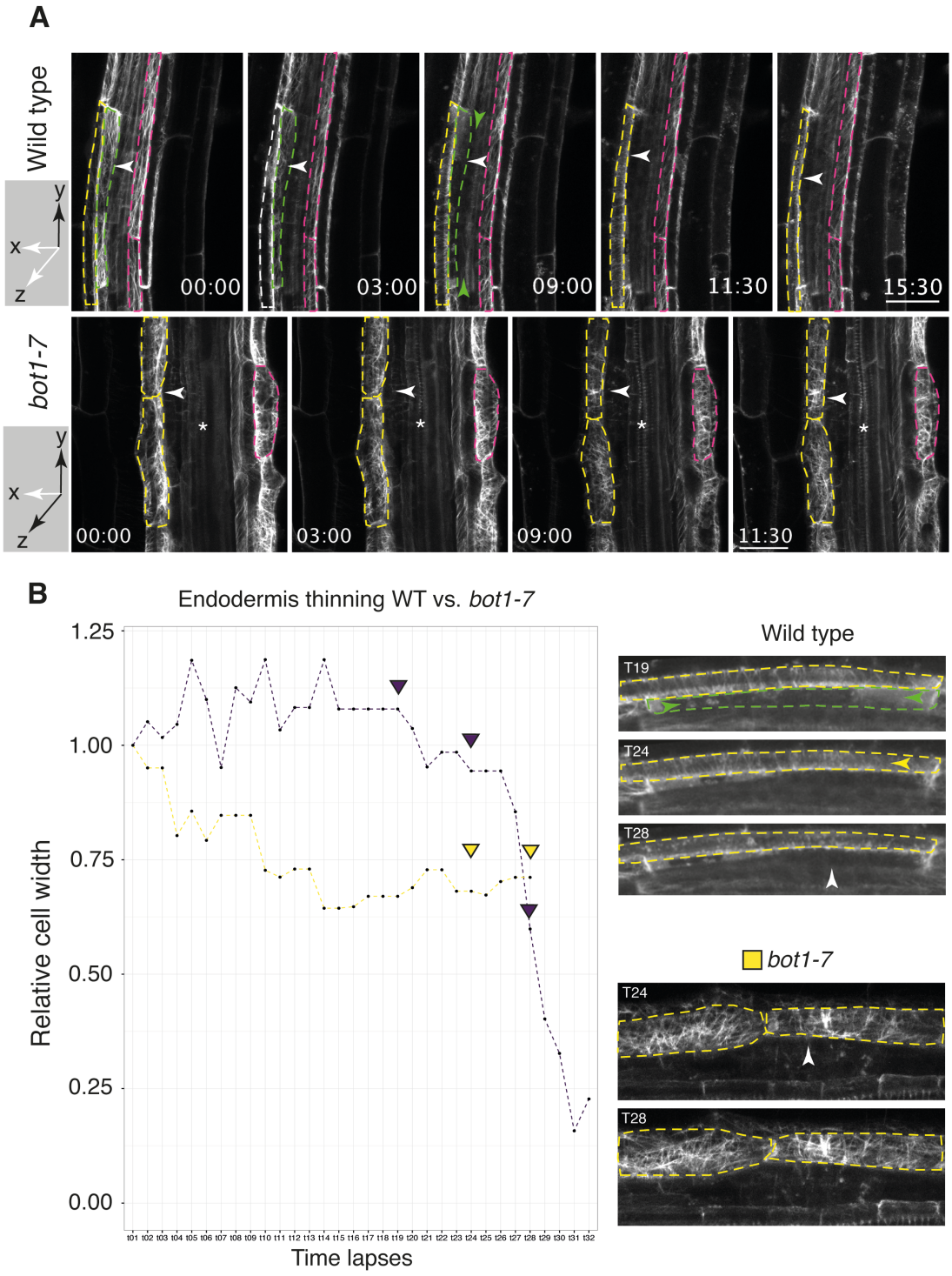

Fig. 16 Microtubules reorientation and cell shape remodelling are very delayed in the *bot1-7* mutant.

A) Two-photon confocal sections of CASP1pro::mVenus:MAP4 during LRP development in the Col-0 and the *bot1-7* background. Accommodating cells are highlighted in yellow (for the lateral view) and green (for the frontal view, only in wild type). Neighbouring cells opposite to the direction of the LRP growth are highlighted in magenta. In these cells no reorganization of CMT can be detected. White asterisk in the *bot1-7* indicate the position of the xylem pole. White arrows in the picture and the 3D coordinates indicate the growth direction of the LRP on each movie. In wild type the xylem pole cannot be seen because the LRP not only grows laterally (in X) but also frontally (in Z). Scale bar is 20 μm.

B) Measurement of local cell thinning in accommodating cells of Col-0 and *bot1-7* (Purple for wild type, Yellow for *bot1-7*). Cell width measurements are normalized to initial cell width for easy comparison between genotypes, where is 1 is the original cell width. Young LRP were imaged every 30min during 16h, for wild type and 13h for *bot1-7*, resulting in 32 time lapses for wild type and 28 for *bot1-7.* Time lapses T19 (only for wild type), T24 and T28 are highlighted with arrows in the graphic (purple for wild type and yellow for *bot1-7*) and correspond to the images on the right, where CMT organization in the accommodating cells can be appreciated. Green and yellow arrows (also A) show the depolymerizing wave. The white arrows indicate the direction of the growth of the lateral root primordium.

4 Supplementary figures

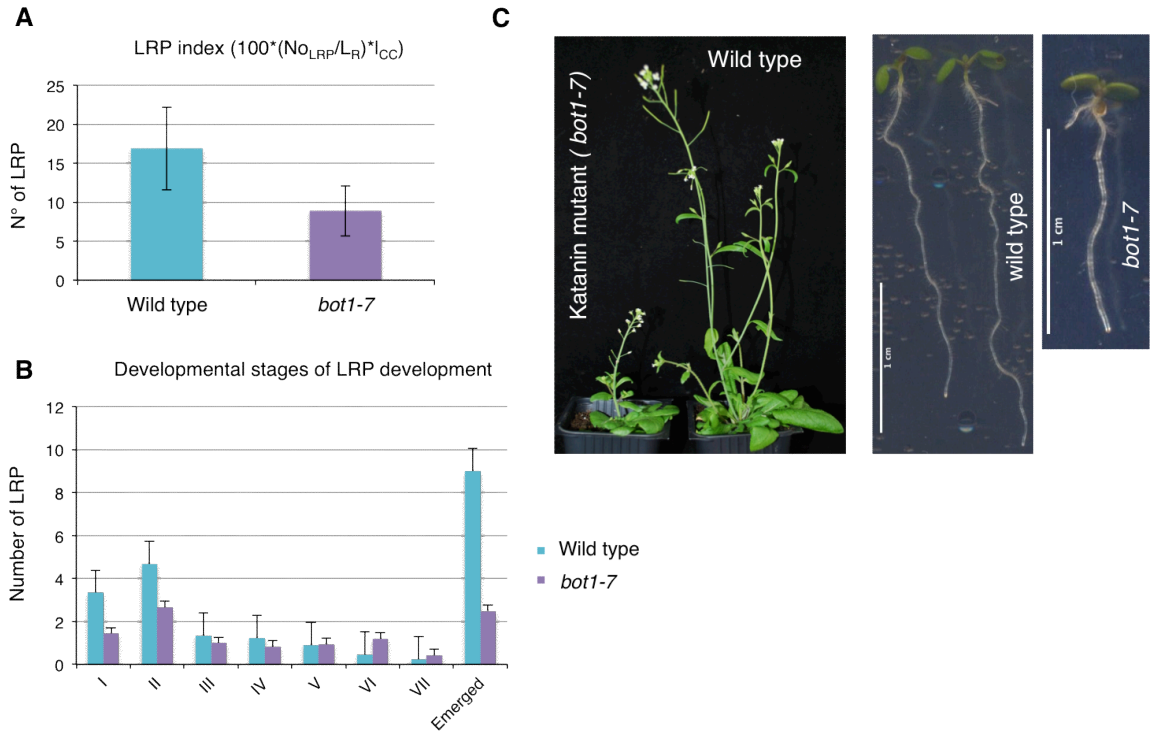

Fig.S 1. The *bot1-7* mutant is affected in cell growth and production of lateral roots

A) Quantification of lateral roots (LR) in wild type and the katanin mutant allele *bot1-7*. The lateral root primordia (LRP) index was used for accurate comparison between the both genotypes, due to the defects in cell expansion displayed by the mutant. No_{LRP}=Number of lateral root primordia; L_R= root length; I_{CC}= average length of cortex cells.

B) Quantification of the number of LRP at a specific developmental stage in wild type and *bot1-7*. The katanin mutant has less LRP than wild type in all stages from I to emerged status. This quantification allows determining at which developmental phase a genotype affects LRP development. The low number of LRP from stage I indicates problems from LR initiation (LRI) or earlier, during priming.

C) Images of the phenotype in shoots (left) and 7 day-old seedlings (right) of the katanin mutant and wild type.

Supplementary figures

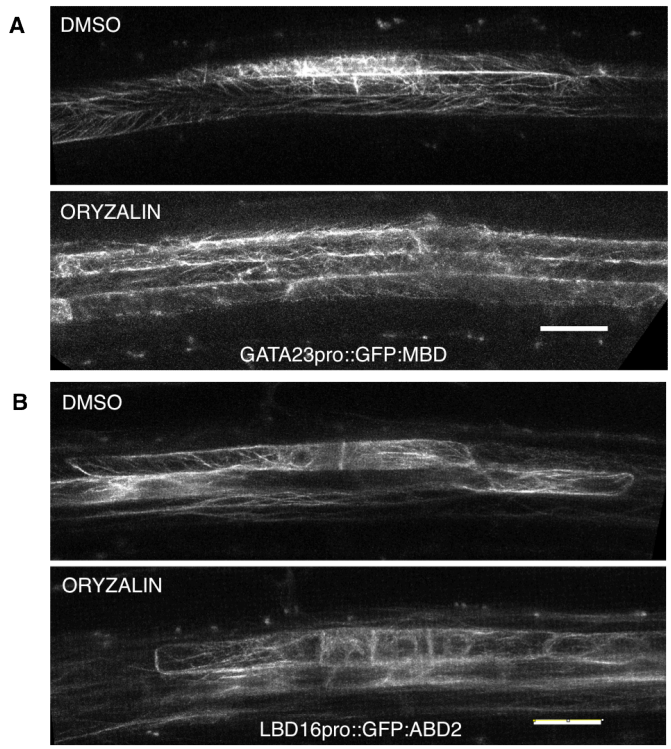

Fig.S 2 Low concentration of Oryzalin specifically depolymerizes CMT but has no effect on actin bundles

A) Images of the CMT marker line GATA23pro::GFP:MBD after 12h gravistimulation in the presence of oryzalin 320nM or DMSO. Although this concentration is low, bundles are affected at this concentration of Oryzalin. On B) the pattern of cell division is not affected, therefore the concentration of oryzalin was increased at 500nM for the rest the experiments. Scale bar 20μm.
Images of the actin marker line LBD16::GFP:ABD2 after 12h gravistimulation (DMSO or oryzalin 320nM). Bundles are visible in both treatments, showing that oryzalin specifically affects microtubules and not actin filaments.

Supplementary figures

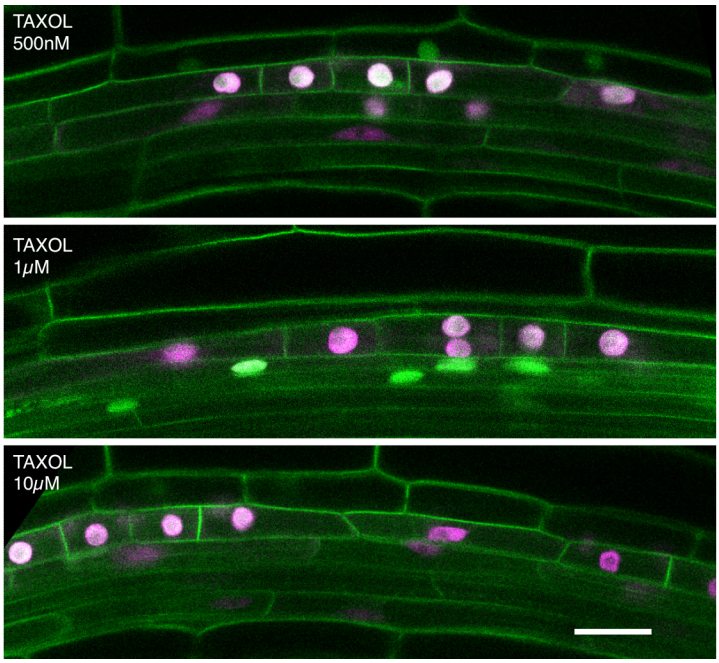

Fig.S 3. Taxol concentrations below 17μM did not induced any deffect on LRP phenotype

Images showing LRP after 12h gravistimulation in the marker line sC111. The experiments were done to see the effect of taxol on cell division and cell swelling. Starting with 500nM, increasing concentrations 1μM and 10μM did not induce defects on LRP development. Therefore, a final concentration of 17μM was used for the experiments, as 20μM completely abolished cell division.

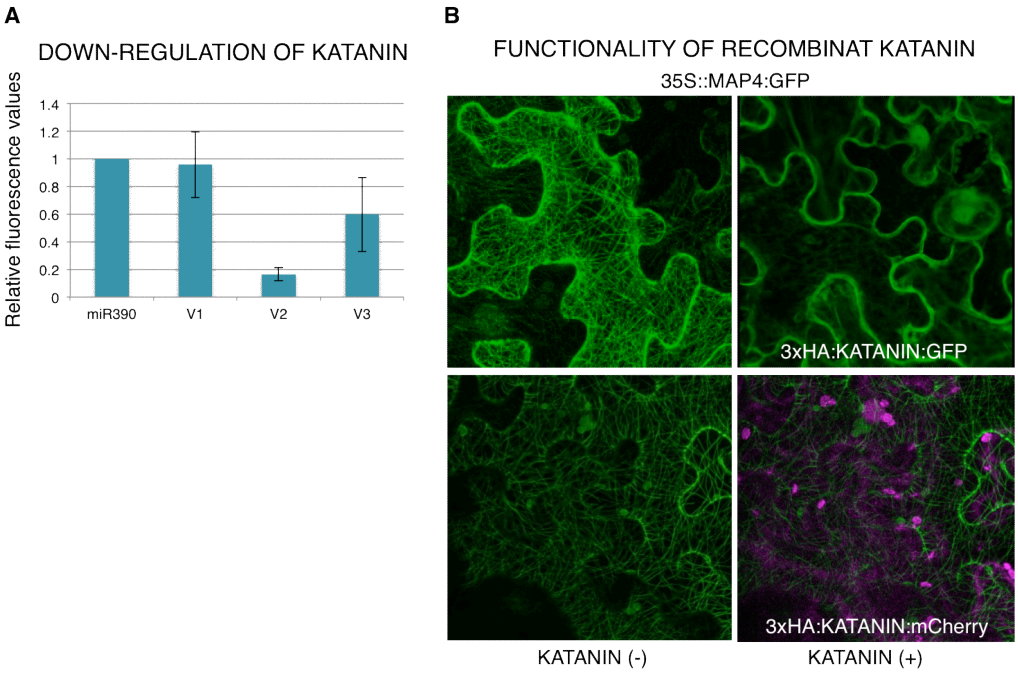

Supplementary figures

Fig.S 4 The ami$R_{KATANIN}$ (V2) can effectively down regulate KATANIN and recombinant KATANIN depolymerizes CMT in tobacco leaves.

A) Test of amiRNA specifically designed to down regulate KATANIN expression. Three versions of ami$R_{KATANIN}$ were co-infiltrated with the recombinant 3xHA:KATANIN-GFP on tobacco leaves. As control was used miR390. Infiltrated tobacco leaves were homogenized for protein extraction and GFP values were measured. GFP values are taken as readout of the expression level of 3xHA:KATANIN-GFP.Note that the second version of ami$R_{KATANIN}$ effectively reduces the level of KATANIN. This version was used for subsequent experiments. Values are an average of 4 individual repetitions and are normalized to expression, values in the control.

B) Confocal images of epidermis cells in tobacco after co-infiltration of two constructs of recombinant KATANIN, 3xHA:KATANIN-GFP and 3xHA:KATANIN-mCherry and the fluorescent microtubule marker 35S::MAP4:GFP. Note that the expression of 3xHA:KATANIN-GFP effectively induces severing and depolymerization of microtubules. In contrast 3xHA:KATANIN-mCherry did not show any effect on the organization of microtubules. 3xHA:KATANIN-GFP was used for subsequent experiments.

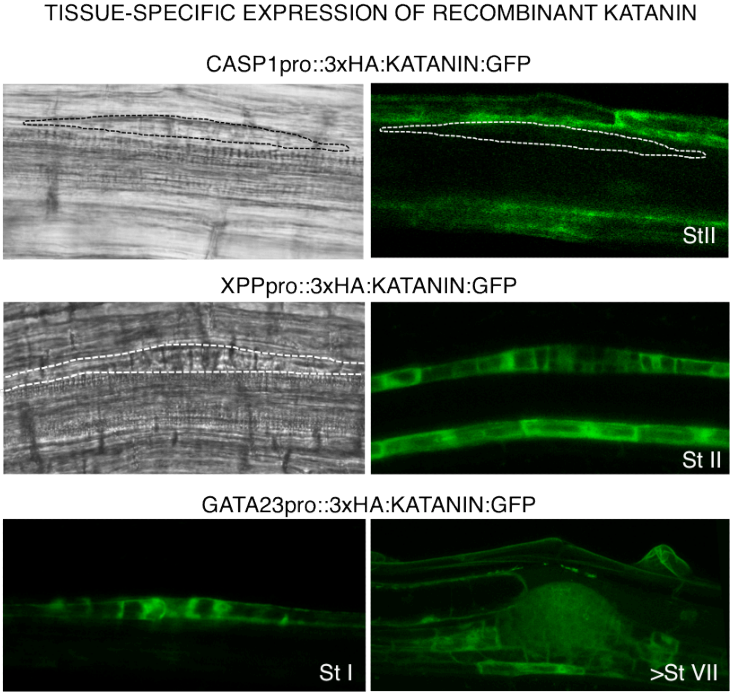

Fig.S 5 Expression of recombinant KATANIN under the control of tissue specific promoters

A) Confocal sections of three constructs generated for tissue specific expression of recombinant KATANIN. CASP1pro::3xHA:KATANIN:GFP is exclusively expressed in the endodermis. XPPpro:: 3xHA:KATANIN:GFP is expressed in XPP cells and LRP until stage II (StII). After stage II the promoter is silenced. GATA23pro:: 3xHA:KATANIN:GFP is exclusively expressed in founder cells even prior to LRI.

B) Expression is maintained during LRP development until emergence. The developmental stage is indicated as St.. Dashed lines indicate the position of the LRP. These tissue-specific promoters were cloned together with amiRN$A_{KATANIN}$ (V2) to generate tissue-specific down-regulation lines in Arabidopsis.

Supplementary figures

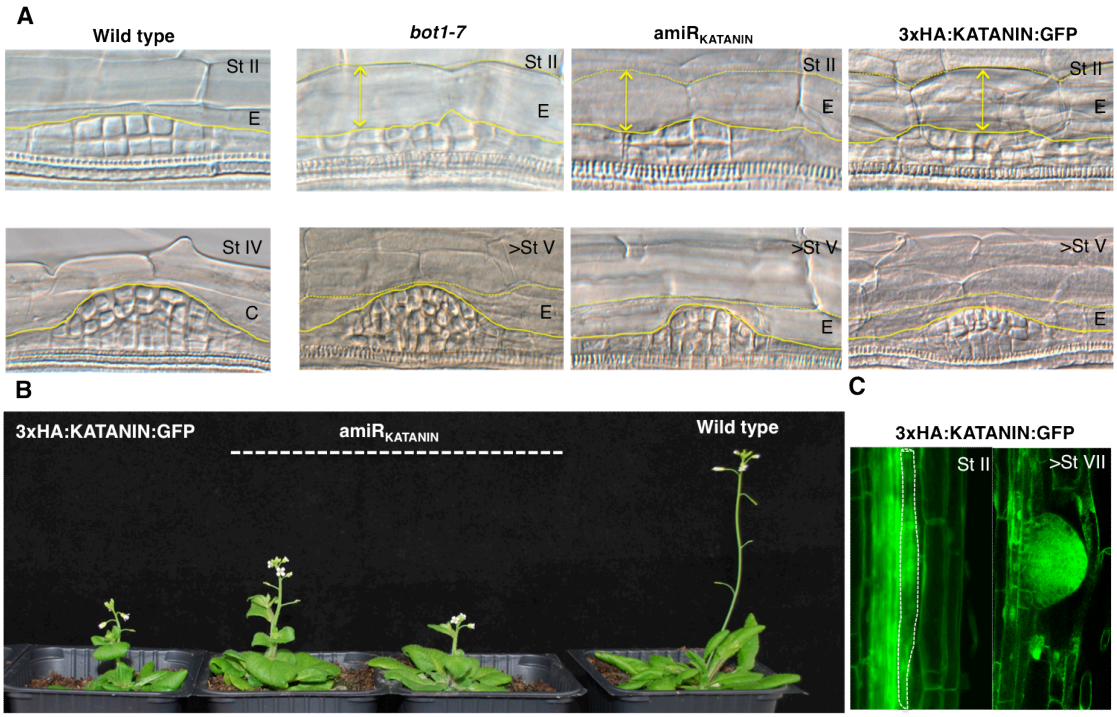

Fig.S 6 Lateral root primordia and shoot phenotype of the ubiquitous expression of amiR$_{KATANIN}$ and recombinant KATANIN are reminiscent to the *bot1-7* mutant phenotype.

A) Microscopic pictures of cleared roots showing LRP in: wild type, katanin mutant *bot1-7*, UBIQ10pro:: amiR$_{KATANIN}$ and UBIQ10pro:: 3xHA:KATANIN:GFP. In the upper row LRP in early stage II are depicted (St II). In the lower row older LRP (stage IV to V) are depicted. The yellow dashed line marks the perimeter of the LRP and the endodermis (E). Note that in wild type at stage IV the endodermis has been crossed and only the cortex (C) is visible. Note that the shape and the emergence through the endodermis are affected in the over-expression and knockdown lines, and show the similar phenotypes as the *bot1-7* mutant, especially in the younger stages.

B) Picture of Arabidopsis shoots of the katanin over-expression and knockdown lines and wild type. The constructs UBIQ10pro:: 3xHA:KATANIN:GFP and UBIQ10pro:: amiR$_{KATANIN}$ induce growth and plant development defects reminiscent to the mutant *bot1-7*.

C) Confocal sections showing the expression of UBIQ10pro:: 3xHA:KATANIN:GFP in root tissues and LRP (Stages II and >VII). The dashed white line shows the position of a stage II (StII) primordium.

Supplementary figures

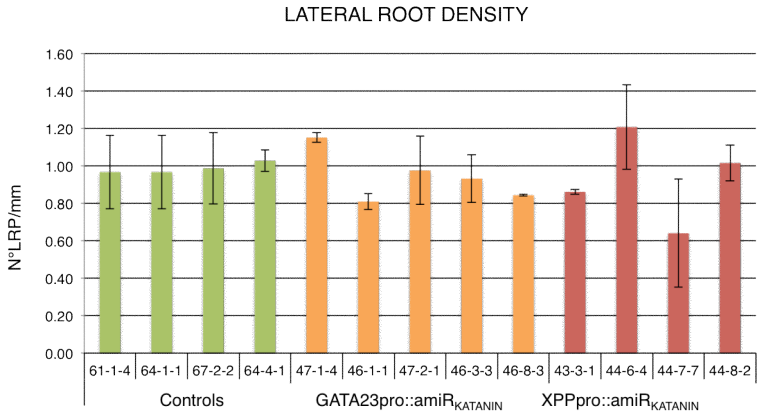

Fig.S 7 Tissue-specific expression of amiRNA$_{KATANIN}$ knockdown lines does not effectively reduce the number of LRP.

Average of lateral root density in 7 day old seedlings of control lines (Empty construct) and tissue-specific amiR$_{KATANIN}$ knockdown lines: GATA23pro:: amiR$_{KATANIN}$ and XPPpro:: amiR$_{KATANIN}$ At least three plants per line were analysed. Note the variability in the lateral root density shown in the knockdown lines compared to the controls. However, these results did not allow drawing any conclusion about the effect of katanin down regulation in the number of LRP.

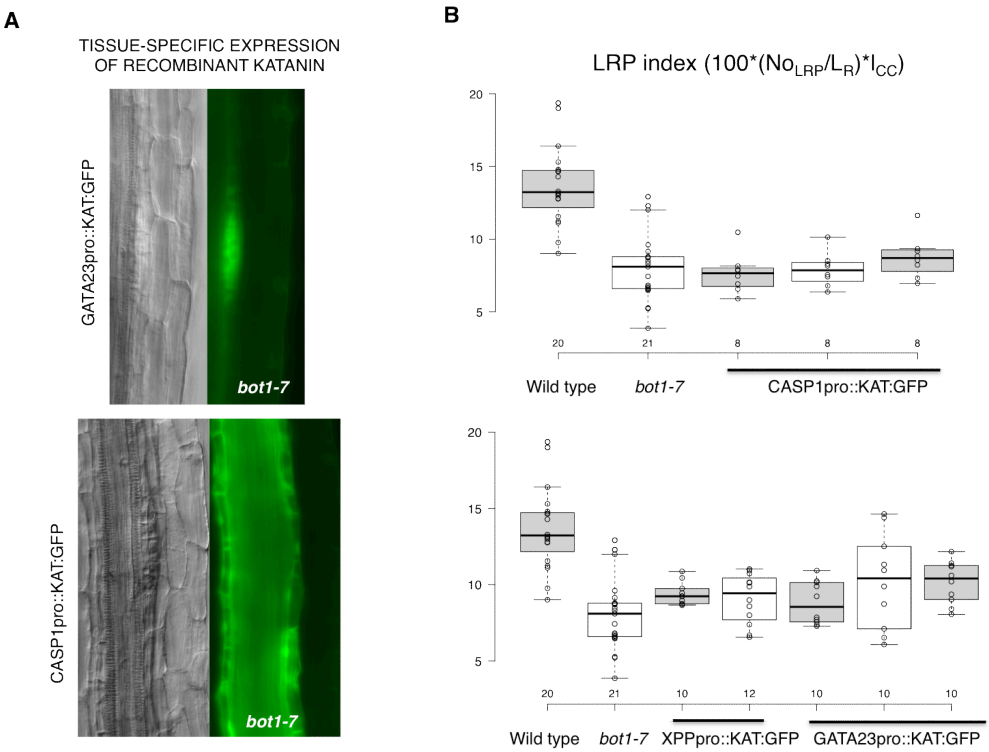

Fig.S 8 Tissue-specific expression of transgenic KATANIN did not rescue the LRP phenotype of the *bot1-7* mutant.

A) Confocal pictures (bright field and fluorescent) showing the tissue-specific expression of transgenic KATANIN in the lines CASP1pro::3xHA:KATANIN:GFP and GATA23pro:: 3xHA:KATANIN:GFP crossed with the mutant *bot1-7*. Arrows mark the position of the LRP.

B) Expression of either CASP1pro::3xHA:KATANIN:GFP, XPPpro:: 3xHA:KATANIN:GFP or GATA23pro:: 3xHA:KATANIN:GFP does not rescue the low number of LRP in the katanin mutant *bot1-7* compared to wild type. The lateral root primordia (LRP) index was used for accurate comparison between the different genotypes, due to the defects in cell expansion caused by the katanin mutation.

5 Discussion

5.1 Microtubule dynamics during lateral root initiation

5.1.1 CMT organization, cell wall and mechanics in founder cells during LRI

Lateral root initiation (LRI) is marked by synchronous expansion of two neighbouring founder cells and the migration of nuclei towards the common cell wall [2, 101]. Once nuclei are asymmetrically localized, founder cells divide asymmetrically originating two small daughter cells in the centre and two long daughter cells at the flanks. After division the expansion of the central domain is more pronounced than in the periphery. This asymmetric swelling prefigures the future dome shape of the primordium and is important for proper development of the lateral root [123].

In our analysis of LRI before asymmetric cell division (ACD) we found that, the nucleus migrate towards the common cell wall (central domain) and round up. Concomitantly, longitudinal bundles of cortical microtubule (CMT) disorganize and accumulate around the nucleus; at this point, we could detect asymmetry in cell swelling, where the region containing the nucleus expands more than the periphery.

Once cells have divided we detected that CMT arrange in organized transversal parallel bundles at the peripheral edge of the big daughter cell. In contrast in the small central daughter cells CMT become increasingly disorganized and these cells are constantly expanding. Hence, our observations show that during LRI, a typical pattern of CMT organization emerges. At the supra cellular levels (across the field of all founder cells), CMT are more disorganized in the centre where expansion is maximum than at the periphery where growth is minimal. At the single cell level (in a single founder cell), the graded organization is also visible.

Supra-cellular graded organization of CMT is important to guide growth of different plant organs. In dark-grown Arabidopsis hypocotyl and cells of the root-elongating zone, CMT are organized in transversal bundles that guide cell expansion along the shoot/root axis [23, 158]. CMT also contribute to the emergence of specific shape at single cell scale. At the sharp tip of the Arabidopsis petal cells, the supra-cellular reorganization of CMT at the edge constraints sepal growth and controls the final size of the organ (Ren, Dang et al. 2017). Similarly, after egg fertilization, CMT align in transversal rings to allow the elongation of the zygote, prior to ACD [65]. Indentations of leaf pavements cells or stomatal guard cells are other examples in which aligned transversal bundles of CMT are associated with anisotropic constriction of cell expansion, helping cells to acquire complex shapes (Eisinger, Ehrhardt et al. 2012[13]

During LRP formation the central domain expand faster after the first ACD. These cells undergo a new round of periclinal cell division and continue expanding faster than the flanking cells originating a dome-shape primordium [123]. We observed that CMT acquire an isotropic organization in these cells, which are more proliferative than the peripheral. This observation is reminiscent to examples of the shoot apical meristem (SAM), where disorganized pattern of CMT has been associated with being permissive for expansion and favoring the outgrowth of organs [159].

Discussion

What could trigger the fast expansion in the central domain and the isotropic organization of CMT?

Cell expansion is achieved by local increase of cell wall (CW) extensibility [12]. The extension of cell walls requires a change in the biochemical composition and arrangements of cell wall polysaccharides, which is partially achieved by the cell wall remodelling enzymes [16].

Auxin-driven acidification of the apoplast activates cell wall remodelling enzymes (CWR), like A-TYPE EXPANSINs (EXPA)[160]. Moreover, auxin is known to transcriptionally induce the expression of CWR enzymes during lateral root formation [130].

Right after the first asymmetric division the influx transporter AUX1 can be observed in the early lateral root primordium [103] and DR5 expression is confined in the central small cells, indicating a maximum of auxin-transcriptional response [11]. Hence its plausible that auxin accumulation in the central domain can induce the activity and expression of CWR enzymes, making these cells more prone to swell [12].

How is cell wall remodelling connected with the isotropic organization of CMT?
On the one hand, lowering hemicellulose levels in the *xxt1xxt2* mutant or treating plants with PECTIN METHYL ESTERASES (PME) induces disorganization of CMT and inhibits synthesis and deposition of cellulose on the primary cell wall [16, 161]. On the other hand, disorganization of CMT does not only lead to loss of uniformity in the deposition of cellulose [37] but it is also coupled with the activation of PME, EXPA and XYLOGLUCAN ENDO-TRANSGLUCOSULASE / HYDROLASE (XTH) [16]. It seems also, that there is positive feedback loop between CWR enzymes and CMT organization in SAM, that promotes cell wall expansion and outgrowth [16].

Back to our case of study it could be hypothesized that the softening of the CW in the small daughter cells could induce disorganization of CMT, which in turn would activate CW remodelling enzymes, making the CW of small daughter cells more expandable and prone to grow.

In this scenario local CMT dynamics could work as an amplifying factor, where disorganized CMT help to increase expansion in the central region and ordered transversal arrays constrain swelling in the periphery. This is supported by our results obtained after the chemical disturbance of microtubule polymerization. Homogeneous stabilization of microtubules with Taxol impairs swelling in the central region, whereas CMT depolymerization with Oryzalin enhances cell expansion in both central and peripheral regions.

Independently of the treatment, affecting CMT dynamics drastically reduces asymmetry in cell geometry. Therefore we conclude that functional CMT network is necessary for asymmetric cell expansion during LRI. This affirmation is reinforced by our observations in *bot1-7*, where CMT cannot organize in parallel bundles [139]. After live imaging of CMT in the *bot1-7* we observed that CMT are homogeneously disorganized in all pericycle cells and do not form transversal bundles. Consequently, we observed that in *bot1-7* the peripheral edge of the big daughter cell expands concomitantly with the central part and this lead to a loss of asymmetric swelling in the mutant. This observation is reminiscent with the results in the SAM, where growth heterogeneity between neighbouring cells is also impaired in the *KATANIN* mutant allele, *ktn-1* [28].

Although we could detect that depolymerization of microtubules with Oryzalin promotes cell expansion, we did not observed the same after tissue-specific depolymerization of CMT by LBD16>>PHS1ΔP (20h), where induction of LBD16>>PHS1ΔP lead only to a loss of asymmetric swelling. A possible explanation is that the pleiotropic effects of Oryzalin treatment could affect the stiffness of the endodermis, making it less able to counteract the growth of founder cells.

5.1.2 Auxin controls asymmetric organization of CMT: auxin transport, CMT and cell domains

Auxin transport and signalling controls every step of lateral root formation. Before the asymmetric division, the auxin influx transporter AUX1 mediates the accumulation of auxin in pericycle cells [104]. After ACD, AUX1 can be observed in the stage I primordium [103] and together with the polar localization of the efflux transporter PIN1 mediate the formation of an auxin maximum, which can be visualized as DR5pro::GUS expression [11]. Although DR5pro::GUS expression has been reported to be equally expressed in founder cells, once they divide asymmetrically, DR5 was confined in the two small daughter cells and later the auxin maximum accumulates at the tip of the primordium [11].

The difference in size and DR5 expression between the large and the small daughter cells are reflected in differential gene expression. For example, the receptor- like kinase ARABIDOPSIS CRINKLY4 (ACR4 [115]) is expressed in the small daughter cells once founder cells divide and give rise to a stage I LRP [92]; The differential expression of genes has been proposed to create to two domains in the LRP: the flanks (where cells barely divide) and the proliferative centre, where the expression of genes like MONOPTEROS (MP) and PLETHORA (PLT1/2/3/4) drive the formation of a new meristem [162].

In sum, the asymmetric cell division during LRI prefigures not only the future dome-shape primordium [123], but also establishes the definition of the central and the peripheral domains in terms of gene expression [162].

In our results we observe that the central and the peripheral domains are reflected in the different organization of CMT and levels of expansion. Blocking the transcriptional activity of LBD16, in the LBD16-SRDX line, abolishes polar localization of the nucleus and cells divide symmetrically [63]. We observed that in the two equal-sized daughter cells, CMT equally re-orient in transversal parallel bundles and swelling is symmetric between daughter cells.

In the light of our results, it could be said that blocking asymmetric division in LBD16-SRDX impairs the formation of the central and peripheral domain, at least in terms of microtubule organization and cell swelling.

The transcription factor *LATERAL ORGAN BOUNDARIES-DOMAIN16 /ASYMMETRIC LEAVES2_LIKE 18* (*LBD16/ASL18*) is directly regulated by ARF7 and ARF19, which in turn are de-repressed upon the degradation *SOLITARY-ROOT* (*SLR/IAA14*) [154]. A dominant mutation of SLR, *slr-1*, cannot be ubiquitinated upon auxin binding and constitutively represses ARF7 and ARF19. Concordantly the *slr-1* mutant fails to form lateral roots [69].

In the lab, a transcription analysis to find genes directly regulated by SLR in founder cells during LRI was performed similarly as previously published by [107] (Unpublished data). The peculiarity of our approach relies in the use of a dexamethasone (DEX) -inducible version of *slr-1* [69] exclusively driven in founder cells (GATA23pro::*slr-1*:GR). Using the lateral root-inducible system (LRIS) [108, 163] to synchronously induce LRI in the presence of DEX or DMSO, we could find genes exclusively regulated by SLR in founder cells during LRI before ACD, from 1 to 6h after IAA induction. An Internet platform created by Alexis Maizel facilitates the visualization of gene expression differences between DEX and DMSO in GATA23pro::*slr-1*:GR and its comparison with SHY2/IAA3 (GATA23pro::*shy2-2*:GR) (https://maizel-lab.shinyapps.io/mIAA_RNASeq_Candidate_Visualiser/).

LBD16 is specifically expressed in founder cells before ACD [63], 1h after IAA treatment (our results LRIS, GATA23pro::*slr-1*:GR) . Knowing its direct regulation by ARF7 and ARF19 it can be assumed that LBD16-SRDX drives an early inhibition of the SLR/ARF7/ARF19 signalling pathway in founder cells.

In accordance to the lack of asymmetry in LBD16-SRDX and subsequent disappearance of central and peripheral domains I search for genes directly controlled by SLR, whose inhibition could explain the loss in polar organization of cytoskeleton and nuclear

dynamics (For genes related with actin and nuclear migration and shape, see Discussion 5.2.).

Which molecular pathways mediate auxin regulation of the CMT organization? Several evidences show that auxin-dependent organization of cytoskeleton is mediated by plant RHO-like small GTPases, Rho Of Plants (ROPs) [13] [159]. These proteins act as molecular switches, changing between GTP-bound active form and the GDP- bound inactive form. Activation of ROPs is controlled by ROP-Guanine nucleotide Exchange Factor (ROP^{GEF}), whereas ROP-GTPase-Activating Protein (ROPGAP) mediates ROPs inhibition [38].

In the SAM it has been reported that accumulation of auxin promotes cell expansion and isotropic organization of CMT upon acting on the signalling pathway involving a ROP6, RIC1 and KATANIN [159]. Interestingly the same signalling pathway is involved in the auxin-mediated formation of CMT bundles at indentations in pavement cells (PC)[13].

ROP6 could be an interesting candidate for the control of CMT during LRI, as ROP6 is specifically expressed in LRP cells. The activation of ROP6 by GEF proteins determines its localization at anticlinal and periclinal plasma membranes in the LRP [164]. A possible regulator of ROP6 during LRI could be the ROP-activator, *ROPGEF14* (*GEF14*), which is significantly induced in founder cells after 2h of IAA treatment (Our results LRIS, GATA23pro::*slr-1*:GR). Interestingly, the connection between GEF14 and ROP6 has been recently published, positioning GEF14 as the linker between CW remodelling by PMEs and CMT organization driven by ROP6 [25].

In our observations we found a spatial correlation between CMT organization and maximal extensibility of the cell wall at the central domain. This central domain disappears when auxin signalling is blocked in the LBD16-SRDX background. Therefore the question arises, how does auxin-signalling interplay with cortical microtubules in the creation of local cell wall changes?

Polar auxin transport drives the accumulation of auxin, creating local auxin maxima, where auxin induces gene expression and acidification of the cell wall by activating H^+-ATPases [165, 166]. Acidification of the cell wall by auxin modifies the activity of CW remodelling enzymes, like EXPAs.

EXPAs mediate acid-induced cell wall loosening, breaking the connection between cellulose microfibrills and making them more accessible to cellulases [20]. EXPA1 is significantly activated in founder cells after 2h of IAA treatment (Our results LRIS, GATA23pro::*slr-1*:GR). Interestingly, the mutant *expa1* shows abnormal cell swelling and pattern of cell division during LRI [167]. According to the authors, EXPA1 is necessary for localized radial expansion of founder cells, which need to acquire a minimal cell width to undergo asymmetric cell division [167]. The connection between CMT isotropic organization and cell expansion, together with the recently discovered role of EXPA1 in founder cell swelling opens the possibility that CMT and EXPA1 act in the establishment and maintenance of the central domain during LRI.

The rapid auxin signalling processes are mediated by the activation of ion transporters at the plasma membrane (PM). The auxin influx transporter AUX1 drives the fast influx of auxin and protons, leading to the depolarization of the plasma membrane. Cytosolic auxin is perceived by SCFTIR1/AFB, which activates Ca^{+2} channels, increasing cytosolic Ca^{+2} levels [72]. Therefore, pH changes and Ca^{+2} influx count as fast auxin-induced responses [71]. Ca^{+2} is a common secondary messenger in eukaryotes, which sensed by calmodulin (CaM) participates in the regulation of cell polarity and cell-to-cell communication in developmental processes [168].

A recently characterized protein family, the IQ67 DOMAIN (IQD) [40] integrates auxin and Ca^{2+}-signalling for the regulation of microtubule organization [169]. According to the proposed mode of action, IQD would increase the stability of CMT bundles in low auxin and cytosolic Ca^{2+} concentrations and induce dynamicity of CMT when auxin and cytosolic Ca^{2+}

levels increase [169]. The IQD13 protein in coordination with ROPs and microtubules has been reported to create plasma membrane domains to induce local modifications in the secondary cell wall of xylem vessels [41].

IQD proteins could play an important role in the organization of CMT during LRI. The expression of two members of this family, IQD24 and IQD25, is significantly induced in founder cells after 2h of IAA treatment (Our results LRIS, GATA23pro::*slr-1*:GR). In light of the previous evidences, IQD24 and IQD25 could participate in the establishment and maintenance of the different CMT organization observed at the central and peripheral domains during LRI.

ROPs, GEFs and IQDs are parts of the signalling bridge between auxin and the organization of CMT, which in the last place is controlled by the action of microtubule associated proteins (MAPs). MAPs like KATANIN [139], CLASP[33] and MAP65 [34] are important for the formation and stability of organized parallel bundles.

Interestingly, MAP65-2 is activated in founder cells after 6h of IAA treatment (Our results LRIS, GATA23pro::*slr-1*:GR). The induction of MAP65 after 6h of IAA treatment coincides with the moment when first divisions can be detected in treated roots and with the observation that parallel bundles appear 6h after ACD. Analysis of the mutant *map65-2* will tell us whether MAP65 plays a role in the organization of CMT and the expansion constriction in the peripheral domain of the new LRP.

Our results show that transversal organization of CMT is characteristic of dividing cells. In adjacent non-dividing cells, CMT orientation barely changes even 6 hours after the first ACD. In contrast, we could observe that in LBD16-SRDX, CMT transversal bundles are also formed in non-dividing neighbouring cells.

A possible explanation is the higher number of cells expressing both DR5pro::GUS and LBD16pro::GUS in LBD16-SRDX [63]. It has been hypothesized that LBD16/ASL18 could control a feedback loop to inhibit LRI in neighbouring cells [63]. Presumably, the lack of inhibition-feedback loop in LBD16-SRDX might be responsible of the enhanced auxin-signalling response and the reorganization of CMT in neighbouring non-dividing cells.

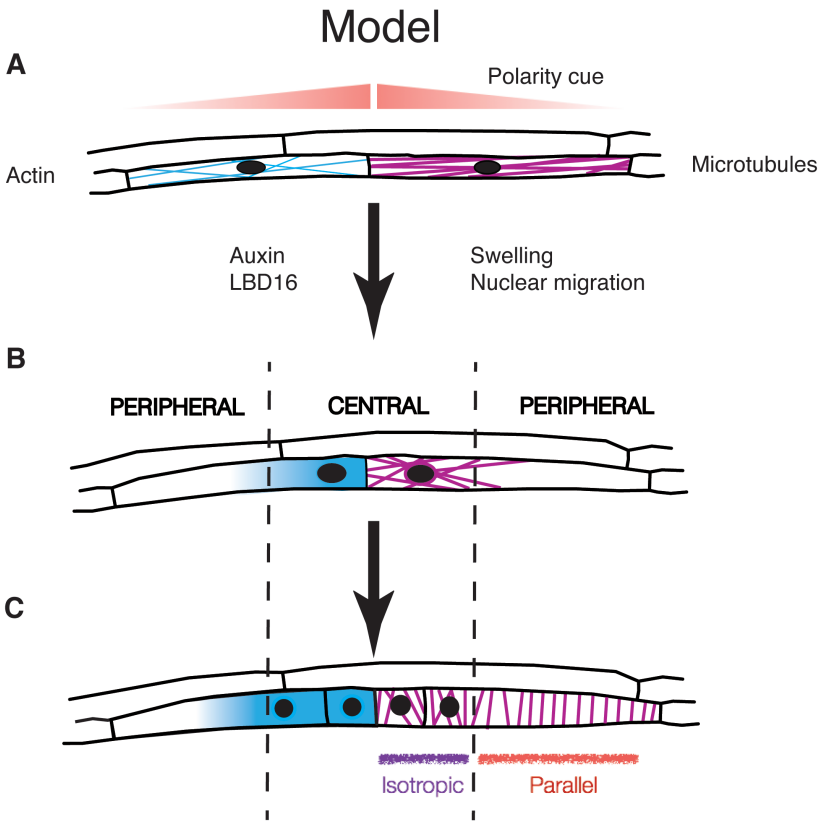

Fig. 17 The model depicts our observations of cytoskeleton dynamics during LRI

A) Naïve cells are depicted. Before asymmetric cell division, founder cells do not show any sign of LRI. Actin (blue) and CMT (Magenta) bundles line up with the longitudinal axis of the cells.

B) The early events of LRI are depicted: nuclei migrate to the common cell wall and round up, concomitantly, founder cells expand radially. At this stadium, the central and the peripheral domains can be distinguished. Nuclei are localized at the central domain, where cell expansion is more prominent than in the peripheral domains. The actin bundles reorganize in a polarized mesh around the nucleus. Microtubules bundles are also associated to the nucleus. Nuclear polar migration is regulated by auxin signalling and is LBD16-dependent [63].

C) Asymmetric division results in the formation of two small daughter cells at the central domain and two long daughter cells at the peripheral domain. The central domain expands faster than the peripheral domains. Actin mesh accumulates at the central domain. At the supra cellular levels (across the field of all founder cells), CMT are more disorganized in the centre (isotropic) where expansion is maximum than at the periphery where, CMT organize in parallel transversal bundles and growth is minimal. At the single cell level (in the long daughter cell), the graded organization is also visible.

5.2 Actin mediates auxin signalling and the establishment of cell polarity and asymmetric division.

5.2.1 Actin reorganization in a polarized meshwork surrounding the nucleus corresponds to the area of maximal expansion

Our analysis of actin dynamics during LRI show that before cell division, actin longitudinal bundles reorganize in a polarized mesh that surrounds the nucleus and is almost absent at the peripheral edge. Once cell divide, we observed that actin accumulates close to the nucleus and remains excluded from the periphery in the big daughter cell.

In the literature, longitudinal actin bundles have been reported to guide cytoplasmic streaming [43]. In our observations it is difficult to determine the association of actin with the

nucleus during polar nuclear migration. However, reorganization of actin in a polarized mesh occurs once the nuclei are asymmetrically localized in founder cells. This would suggest that longitudinal actin bundles act as tracks for nuclear movement and the actin mesh holds the nucleus at a specific position. Our observation that LatB has negative effects on nuclear migration and ACD seem to reinforce this idea.

We reported that after ACD, the actin mesh occupies the whole volume of the small daughter cell and in the big daughter cell actin accumulates close to the central domain, where cells expand faster.

The polar accumulation of actin at the region of maximal expansion is reminiscent of other developmental processes, like growth of root hairs and pollen tube [170]. In these examples, polar accumulation of fine actin at the growing end, serves for the delivery of vesicles to the expanding cell wall [43]. It is probable that the polar accumulation of actin during LRI corresponds with a region of localized exocytosis to the expanding CW.

We observed that asymmetric reorganization of actin occurs before ACD. In contrast, CMT reorientation in parallel bundles was detected approximately 6h after ACD. Interestingly, we found that maximal organization of CMT and accumulation of actin, are completely excluded from each other and are associated with either local constriction or expansion of growth, respectively.

The excluding distribution between actin and CMT bundles has been previously reported in pavement cells (PC) and tip growing cells [43] and ROP proteins are responsible of this antagonism (Reviewed by [44]. In PC characterized by their jigsaw-puzzle shape, two developmental phases has been proposed: First, ROP2 promotes actin diffusion leading to isotropic cell expansion at the growing lobe. Later, ROP6-dependent CMT transversal organization suppresses cell expansion and ROP2 activity at the indentation zones [43, 171].

Alike in PC, we observed to phases during LRI: first actin accumulates at the expanding domain before division and 6h after division CMT form transversal parallel bundles to constrain cell expansion at the periphery. Considering these observations, two questions arise;

(I) Could ROP2 and ROP6 coordinate these phases during LRI similar as in PC?

It is plausible that ROP2 and ROP6 participate in the organization of actin and microtubules during LRI, as the mutations on ROP2 and ROP6 show a LRP phenotype [172, 173]. Also ROP6 is localized at the plasma membrane of LRP cells [164]

(II) Could their antagonistic activities of ROP2 and ROP6 be responsible of the mutual avoidance between the actin mesh and the transversal CMT bundles during LRI?

The presumed reciprocal exclusion between actin and the transversal CMT bundles is also suggested by our observation on CMT organization in the presence of LatB; We detected that when actin network is disrupted by LatB treatment, CMT bundles homogeneously reorganize in parallel bundles in both daughter cells.

Together these observations suggest a model in which ROP-mediated accumulation of actin is associated with isotropic organization of CMT and cell expansion.

5.2.2 Auxin-dependent actin dynamics are necessary for polar nuclear migration, ACD and asymmetric swelling

As actin mesh accumulates around the nucleus, we observed at the periphery a black lumen, what we presumed to be the vacuole. According to the literature, actin is an important regulator of vacuole morphology, and together with myosin motor proteins controls the rapid morphological rearrangements of the vacuole strands [174]. Moreover, destabilization of actin by LatB has been reported to induce the formation of round and small vacuolar structures [175]

When we treated seedlings with LatB during LRI, nuclei remain in the centre of cells and cell expansion was symmetric. We hypothesize that the lost of asymmetry in cell expansion would involve actin-dependent vacuolar dynamics. Presumably, treatment with

LatB could induce fragmentation and homogeneous distribution of vacuolar structures in pericycle cells, originating a loss of asymmetric geometry.

In our results, treatment with LatB strongly delays cell division and impairs nuclei migration. Consequently ACD was completely abolished and cells divide symmetrically.

The effects of LatB on cell division and nuclear migration during LRI resemble previous observations in the zygote, where treatment with LatB abolished nuclei migration and prevents ACD [65]. Taken these results together we concluded that actin drives polar nuclear migration and ACD during LRI.

We observed that in LBD16-SRDX nuclear migration is impaired, cells divide symmetrically and nuclei remain in the centre of the daughter cells. Our analysis of actin dynamics in founder cells revealed that after ACD actin bundles disorganize and form a polarized mesh around the nucleus. However, in LBD16-SRDX actin bundles do not form a mesh; in contrast to wild type, after short disorganization during cell division actin bundles reappear radiating from the nucleus towards the plasma membrane.

We hypothesized that the defects on actin dynamics in LBD16-SRDX could explain the defects on cell division and nuclear migration. This presumption is based on the observation that disruption of actin network with LatB, leads to the same defects as expression of LBD16-SRDX.

Since actin bundles in LBD16-SRDX cannot reorganize in a polarized mesh, we speculate that LBD16 might control the expression of genes that act on actin polarity and stability or affect actin-nuclear interaction. Which genes could be involved in actin-mediated polar nuclear migration during LRI?

Apart of the possible role of ROPs in actin reorganization during LRI, another possible polarizing factor of actin dynamics could be the small peptide GOLVEN/root growth factor/CLE-like-6 (GLV6), which is exclusively expressed during LRP formation already at stage I. Altering GLV6 expression, delays the migration of nuclei and reduces the asymmetry of cell divisions [141].

Long actin bundles may act as tracks for nuclear migration during LRI. Actin-nuclear interaction is mediated by different protein-complexes present between the outer and the inner nuclear envelope (NE). The SUN (SAD1/UNC84) and KASH (Klarsicht/Anc/Syne-1 homology) domain protein complex is a well-known example of the interaction between the NE and the cytoskeleton [176]. The shape of the nucleus is affected in the KASH protein mutants: WIP, SINE and TOLL INTERLEUKIN RECEPTOR domain KASH protein (TIK), where nuclei are rounder than in wild type [177, 178].

Miosyn XI-I is a motor protein that associates actin filaments and WIT proteins. Mutations of Myosin XI-I, *kaku1-2* and *kaku1-4* as well as *wit1* and *wit2* (WPP domain-interacting tail-anchored protein (WIT1 and WIT2)) impair nuclear migration [177].
Interestingly, TIK is progressively down regulated upon auxin during LRI (Our results LRIS, GATA23pro::*slr-1*:GR). It could be hypothesized that TIK expression needs to be silenced during LRI to loosen the connection with actin and allow nuclei to round up.

5.3 Microtubules reorganization is controlled by auxin in the endodermis

5.3.1 Loss of CMT dynamics impairs spatial remodelling of the endodermis

Our analysis of lateral root emergence in *bot1-7* revealed that spatial accommodation in the endodermis is strongly delayed. We observed that in *bot1-7*, CMT are very disorganized and only local bundling could be detected in one of the cells overlying the growing primordium. As a consequence, endodermal cells adjacent to the LRP remained almost unchanged in the mutant for longer time, causing emergence to be strongly delayed. In contrast with wild type were a local sudden loss of volume occurs, emergence in the mutant through the endodermis takes place very progressively.

Discussion

Microtubules are known to reorient in response to mechanical stresses ant tensions [4, 9, 29]. Katanin activity increases the ability of plant cells to respond to mechanical forces generated by growth [28] and consequently in the katanin mutant, cell responses to mechanical stress are impaired [9]. These observations could explain the delay in endodermal spatial remodelling during lateral root emergence in the *bot1-7*.

Nonetheless, the pleiotropic effects in the mutant *bot1-7* should not be ignored and tissue-specific disturbance of microtubule organization in the endodermis will answer the question whether CMT organization are indeed needed for fast cell shape remodelling in the endodermis. So far, tissue-specific alterations of katanin expression did not lead to any significant changes during emergence. The results on the CASP1*pro*>>PSH1ΔP (experiments are currently being run in the lab) will shed more light on this question.

5.3.2 CMT reorganization in response to IAA treatment and spatial deformation shows intracellular heterogeneity

In this study, radial sections of images taken in the CASP1pro::mVenus:MAP4 marker line revealed that endodermal cells are polygonal-shaped cells: flat at the side to the cortex, convex towards the inside vascular tissue. Our results show that CMT are differently organized in the different cell sides of the endodermis: in the vascular-side CMT are oriented along the longitudinal axis with more thin dense and organized fibrils than in the cortex-and the lateral-sides where thin microtubules show a rather chaotic organization.

Swelling of founder cells needs to be coordinated with spatial accommodation of the overlying endodermis, which licenses the progression of LRI [2]. Later as the lateral root develops it pushes the endodermis.

As a consequence the endodermis undergoes a dramatic local loss-of-volume until opposite membranes fuse together and open a gap in the endodermis through which the primordium can grow [2]

Our analysis of CASP1pro::mVenus:MAP4 after IAA treatment revealed that the growth of the underneath dividing pericycle cells induces a loss of roundness of endodermal cells. This morphological change of the endodermis occurs concomitantly with a cell side-dependent reorganization of CMT: CMT in the lateral sides arrange in transversal parallel bundles, whereas in the vascular and cortex cell sides, the disorganization of the microtubule network increases, especially in the outer cell side.

A previous study analysed reorientation of CMT in response to hormones, IAA and gibberellin (GA), in light-grown hypocotyl cells [179]. These hormones induce the reorganization of CMT into transversal arrays in light-grown hypocotyl cells. Interestingly, reorganization of CMT in the hypocotyl shows differences among cell sides. Together with our results, these observations suggest that cell side-specific reorganization of CMT is common in different cell types. Auxin signalling controls reorganization of CMT independently of cell deformation and SHY2-signalling seems to be necessary.

Auxin signalling is responsible of the spatial accommodation of the endodermis. The expression of the dominant negative version of SHORT HYPOCOTYL2/IAA3 (SHY2) in the endodermis prevents cell shape remodelling and LRI cannot take place [2].

Since microtubules are known to change orientation in response to mechanical stresses [4, 9, 29] we wanted to determine to which extend the organization of CMT in the endodermis is responsive to auxin signalling or mechanical constrains.

To address this question CASP1pro::mVenus:MAP4 was crossed with mutant lines in which auxin signalling was either exclusively blocked in the endodermis or in the pericycle; The *slr-1* mutation only blocks the expression of DR5pro::GUS in the pericycle, cortex and epidermis, but does not affect auxin signalling in the endodermis. In contrast, auxin signalling in the endodermis is specifically controlled by SHY2/IAA3, which is expressed in few endodermis cells directly overlying the growing LRP [77].

Discussion

After treatment with IAA 24h, we observed that according to the absence of LRI in *slr1* [69] endodermal cells barely got deformed in *slr-1*. Interestingly, we could not observe any significant difference of CMT reorganization in *slr1* in comparison to wild type: in *slr-1* CMT form transversal arrays in the lateral side and increase disorganization in the other periclinal cell faces (cortical and vascular).

What could be extracted from this observation? In the light of our results in seems that the cell-side specific re-organization of CMT in the endodermis after IAA treatment does not only occur in response to cell deformations induced by mechanical stress. Our observations suggest that CMT in the endodermis are dependent on perception of IAA. This is hypothesis is supported by the results obtained in the CASP1pro::*shy2-2* line.

As previously reported, treatment with IAA induces swelling of the pericycle in CASP1pro::*shy2-2* [2]. However, in contrast with wild type and *slr1*, we observed that CMT organization in CASP1pro::*shy2-2* in the vascular-side was not influenced by exogenous treatment of IAA. Our results show that CMT organization in the endodermis is partially dependent on SHY2-regulation. As CMT organization in the outer and lateral sides did not differ from wild type after IAA treatment, we concluded that SHY2 controls CMT organization in the inner side.

The dominant negative regulator *shy2-2* blocks the expression of auxin-responsive genes [112]. Which auxin-responsive genes could participate in the organization of CMT in the endodermis?

CMT dynamics are dependent on the activity of different MAP proteins, like MAP65 [34], IQDs [180], KATANIN [139] and CLASPs [33]. These proteins are responsible of the stability of CMT bundles and their association with the plasma membrane [35]. SHY2 could control their expression in the endodermis and thereby induce changes in CMT organization.

Auxin also induces the expression of CW remodelling genes in the tissues overlying the growing LRP [77]. In fact, the expression of the cell wall remodelling enzymes: GLH17, PLA2, and EXPA17 is inhibited on *shy2-2*, which shows delayed emergence [77]. Knowing that biochemical changes in the cell wall are coupled with CMT organization [16] it could be hypothesized that the activation of CW remodelling enzymes, like EXPA14, EXPA17 and subtisilin-like protease (AIR3) by auxin at the site of emergence [133] can induce changes in the organization of CMT.

In our observations, CMT do not only change in orientation and organization. Indeed, upon IAA treatment we observed that microtubules fibers look less dense and thicker, what suggest microtubule bundling. Contrary, in *shy2-2* after IAA treatment CMT resemble thinner than in wild type. However, with the current parameters that we actually use, these differences cannot be quantified. Recently a quantitative pipeline has been published for describing bundling and other CMT dynamics in response to mechanical stresses [30]. Using their tools together with the change in orientation and anisotropy will help to better understand the behavior of CMT upon IAA treatment and compression and find new candidate genes to complete the model of CMT regulation in the endodermis.

6 Materials and Methods

6.1 Biological material

6.1.1 Arabidopsis thaliana

Arabidopsis thaliana ecotype Columbia (Col-0) was used as wild type.

6.1.1.1 Growth conditions for flowering

Plants were grown in soil, in long day conditions at 22°C in a growth chamber (Einheitserde CLT SM fein). These plants were used for propagation, crossing or transformation.

6.1.1.2 Crossing A.thaliana

Flowering plants were used to cross two different genotypes. Opened flowers were first removed from the plant serving as female. Then on the same plant one closed flower was opened, the anthers were removed and the remaining stigma was covered entirely with ripe pollen by gently touching it with anthers from the second genotype. At least three crosses were done per combination.

6.1.1.3 Transformation of A. thaliana with floral dip

Plants were grown until the first blots appear. To prepare the floral dip solution a 3-5 LB pre-culture of *A. tumefaciens* carrying the constructs of interest was grown at 28°C overnight. The next day 100*µ*l of pre-culture were used to incubate 250ml LB and the secondary culture was grown overnight at 28°. Cultures were pelleted and re-suspended in a solution of ½ MS, 5%sucrose and 50*µ*l/l of SilwetL-77. Re-suspended pellet was used to dip the inflorescence for max. 1 min. Plants remain one night under low light exposure and were brought back in the growing chamber.

6.1.2 Plant lines used in this study

Table 1. List of mutant alleles and transgenic lines

Name	Code	Source
pDR5v2pro::3xYFP:NLS x pRPS5Apro::dtTomato:NLS	SR251	[144]
UBQ10pro::GRP:3xPIP1,4 x GATA23pro::H2B:3xmcherry	stPVB003	Patrick von Born (Maizel Lab)
SR251x stPVB003-2-2	sC111	Marion Louveaux (Maizel Lab)
GATA23pro::GFP:MBD	stLB033	Lotte Bald (Maizel Lab)
bot1-7	sR190	Olivier Hamant [146]
pGreen179_GRP::CITRINE:TUA6:OCS	stAVB07-	Cloned by Joop Vermeer This study
UBIQ10pro::amiR$_{KATANIN}$	stAVB37	This study
CASP1pro::amiR$_{KATANIN}$	stAVB41	This study
XPPpro::amiR$_{KATANIN}$	stAVB43	This study
UBIQ10pro::3xHA:KATANIN:GFP	stAVB73	This study
CASP1pro::3xHA:KATANIN:GFP	stAVB76	This study

XPPpro::3xHA:KATANIN:GFP	stAVB86	This study
GATA23pro::3xHA:KATANIN:GFP	stAVB79	This study
LBD16pro::LhG4:GR:6xOP:PHS1ΔP:mCherry	stPRD057	Cloned by Lotte Bald (Maizel Lab)
stPRD57 in sC111	stPRD063	Paola Ruiz (Maizel Lab)
stPRD57 in stLB033-10-1	stPRD060	Paola Ruiz (Maizel Lab)
LBD16pro::GFP:ABD2	SR407	Tatsuaki Goh (Hidehiro Fukaki Lab) (Unpublished)
LBD16:SRDX	SR406	[63]
SR406 x stLB033-10-1		This study
SR406 x SR407		This study
pGreen179 CASP1pro::mVenus:MAP4	SR243	Joop Vermeer [181]
GATA23pro::NLS:GFP:GUS	SR106	Tom Beeckman [101]
SR106 xSR243	SCO64	This study
SR243 x *bot1-7*	sC055	This study
slr1	SR375	Hidehiro Fukaki [182]
SR243 x *slr1*	sC057	This study
CASP1pro::*shy2-2*	SR196	Joop Vermeer Niko Geldner [2]
SR243 x CASP1pro::*shy2-2*	SC068	This study

Codes from FileMakerPro database from Prof. Alexis Maizel's laboratory

6.1.3 Growth conditions for microscopy

Seeds were surface-sterilized with a sterilization solution (Ethanol 99%, SDS 0.1%) and air-dried to remove ethanol rest. The seed were sawn on agar squared agar plates with different media. Seeds were stratified at 4°C in dark for 48h. Seedling were grown vertically in long day conditions at 22°C in a Conviron A100.
For confocal microscopy experiments 4day old plants were transferred to a chambered cover glass as described by [183] and directly brought under the confocal.

6.1.4 Nicothiana benthamiana

6.1.4.1 Growth conditions

Nicotiana benthamiana was used for infiltration experiments. Plants were grown on soil in long day conditions at 25°C in a Conviron A1000 (Einheitserde CLT SM fein).

6.1.4.1.1 Infiltration

For testing the silencing efficiency of amiRNAs against KATANIN, young leaves of 5-week old plants were infiltrated with an *Agrobacterium tumefaciens* suspension carrying the $amiR_{KATANIN}$ V1, V2 and V3 candidates, the KATANIN reporter 3xHA:KATANIN:GFP and mCherry for normalization. Agrobacteria were grown overnight at 28°C in LB medium plus the appropriate antibiotics. After centrifugation, the pellet was re-suspended in water to reach an OD of 0.8. The infiltration mixes will contain one of the $amiR_{KATANIN}$ candidates or the negative control (miR390), the KATANIN reporter and mCherry.
Three days after infiltration, transformed leaf-disks were snap-frozen, grinded and proteins were extracted adding 300µl of protein extraction buffer (100mM Tris/HCl, pH 7.5, 150 mM NaCl, 0.1% Tween 20 and fresh 0.1 β-Mercaptoethanol). After centrifugation, the

supernatant was transferred into a 96-well plate to measure GFP and mCherry fluorescent values in the plate reader (TECAN Infinite M1000).

6.1.5 Bacteria strains and growth conditions

6.1.5.1 E.coli

Invitrogen™ TOP10 (DH10B) based electro competent cells were used. Temperature growth was at 37°C.

6.1.5.2 Agrobacterium tumefaciens

The electro competent strain ASE (KanR, CamR, pSoup+(TetR)) was used. Growth temperature was 28°C.

6.1.6 Media

6.1.6.1 Plant culture media and treatments

Standart ½ MS (Duchefa Biochemie Murashige & Skoog medium)[184]; 0.8% phyto agar (Duchefa Biochemie); 0.5g/l MES buffer (2-(N-Morpholino) ethanesulfonic acid)
pH was adjusted to 5.8 with KOH.

Table 2. Chemicals used for plant treatments and selections

Name	Description	Final working Co.
Auxin	Hormonal treatment	10μM
Oryzalin	Destabilizing microtubules	500nM
Taxol (Paclitaxel)	Stabilizing microtubules	17μM
Latrunculin B	Destabilizing actin	500μM
Dexamethasone	Glucocorticoid (Induction)	10μM
Glufosinate:Basta	Herbicide (Line selection)	10μg/ml
Hygromicin B	Antibiotic (Line selection)	50mg/ml (2000x stock)
Kanamycin	Antibiotic (Line selection)	50mg/ml (1000x stock)

6.1.6.2 Bacterial culture media

Lysogeny broth (LB) (Bertoni, 1951) with the appropriate antibiotic was used for liquid growing culture. For growing bacteria in Petri Dishes, LB medium was mixed with agarose (15g/l).

6.1.7 Recombinant DNA methods

6.1.7.1 Cloning Green Gate

The constructs generated in this study (ami$R_{KATANIN}$ and 3xHA:KATANIN:GFP) were generated using the Green Gate system. After cloning the sequences of interest in entry modules plasmids using BsaI restriction enzyme, six entry modules containing respectively promoter, N-terminal tag, CDS, C-terminal tag, terminator and the selection cassette were mixed with a final destination vector and successively digested by BsaI and ligated [185].
The constructs generated for this study were recorded on the FileMakerD database from Prof. Dr. Alexis Maizel's laboratory, Centre for Organismal Studies , Heidelberg University.

For the design of primers and in silico molecular biology the software Geneious was used [186].

6.1.7.2 amiRNA design

amiR$_{KATANIN}$ constructs were prepared according to the protocol by Rebecca Schwab, MPI for Developmental Biology, Tübingen, 2005 [187].
(http://wmd3.weigelworld.org/downloads/Cloning_of_artificial_microRNAs.pdf)

6.1.7.3 Primers used in this study

Table 3 Primers used in this study

Name	Sequence (5' to 3')	Purpose
GG-B-amiR-forward	AACAGGTCTCAAACACTGCAGCCCCAAACACACGC	miR319a (pRS300)
GG-E-amiR-reverse	AACAGGTCTCTGCAGCCCCATGGCGATGCC	miR319a (pRS300)
GG-primerI-amiR-katanin-variantI	GATTGAAAGTATTCGGGCAGCTATCTCTCTTTTGTATTCC	amiR-Katanin-Variant1
GG-primerII-amiR-katanin-variantI	GATAGCTGCCCGAATACTTTCAATCAAAGAGAATCAATGA	amiR-Katanin-Variant1
GG-PrimerIII-amiR-Katanin-Variant1	GATAACTGCCCGAATTCTTTCATTCACAGGTCGTGATATG	amiR-Katanin-Variant1
GG-PrimerIV-amiR-Katanin-Variant1	GAATGAAAGAATTCGGGCAGTTATCTACATATATATTCCT	amiR-Katanin-Variant1
GG-PrimerI-amiR-Katanin-Variant2	GATTAGTCAGATCGTCTCGACTCTCTCTCTTTTGTATTCC	amiR-Katanin-Variant2
GG-PrimerII-amiR-Katanin-Variant2	GAGAGTCGAGACGATCTGACTAATCAAAGAGAATCAATGA	amiR-Katanin-Variant2
GG-PrimerIII-amiR-Katanin-Variant2	GAGAATCGAGACGATGTGACTATTCACAGGTCGTGATATG	amiR-Katanin-Variant2
GG-PrimerIV-amiR-Katanin-Variant2	GAATAGTCACATCGTCTCGATTCTCTACATATATATTCCT	amiR-Katanin-Variant2
GG-PrimerI-amiR-Katanin-Variant3	GATTGATAAGAGCCTTACGCCTCTCTCTCTTTTGTATTCC	amiR-Katanin-Variant3
GG-PrimerII-amiR-Katanin-Variant3	GAGAGGCGTAAGGCTCTTATCAATCAAAGAGAATCAATGA	amiR-Katanin-Variant3
GG-PrimerIII-amiR-Katanin-Variant3	GAGAAGCGTAAGGCTGTTATCATTCACAGGTCGTGATATG	amiR-Katanin-Variant3
GG-PrimerIV-amiR-Katanin-Variant3	GAATGATAACAGCCTTACGCTTCTCTACATATATATTCCT	amiR-Katanin-Variant3
P-CASP1 A Fwd	AACAGGTCTCAACCTGGTACCTTAATCTGCATAAAAGTG	CASP1 promoter
P-CASP1 B Rev	AACAGGTCTCTTGTTTCTTGCAATTGGGGTTTAAAAG	CASP1 promoter
P-GATA23 A Fwd	AACAGGTCTCAACCTATAACTTTTCAATAATGGATCTCG	GATA23 promoter
P-GATA23 B Rev	AACAGGTCTCTTGTTGAGTCATCAAGAAAGGCTTAAG	GATA23 promoter
P-XPP(GRP) A Fwd	AACAGGTCTCAACCTGGTACCGTGTTTGGTTCG	XPP(GRP) promoter
P-XPP(GRP) B rev	AACAGGTCTCTTGTTGGAAATCTTCGTGTGTTAAGAC	XPP(GRP) promoter
Katanin CDs Eco31I C Fwd	AACAGGTCTCAGGCTCAACAATGGTGGGAAGTAGTAATTCG	Katanin (AT1G80350)
Katanin CDs Eco31I D Rev	AACAGGTCTCTCTGAAGCAGATCCAAACTCAGAGA	Katanin (AT1G80350)

6.1.8 DNA and RNA purification

6.1.8.1 Agarose gel

Electrophoresis in TAE buffer was used for DNA separation in 1-2% agarose gel. Ethidium bromide was used for detection of DNA under UV light.

6.1.8.2 Miniprep

QIAprep Spin miniprep kit (Qiagen) was used. Precipitation was done with Isopropanol 1:1.

6.1.8.3 DNA extraction kits from gels

DNA was isolated from gels according to the indications specified in GeneJet gel Extraction Kit (Thermo Scientific).

6.1.8.4 RNA extraction

mRNA was extracted according to the indications specified in GeneMATRIX Universal RNA Purification kit (Roboklon).

6.1.9 DNA and RNA amplification methods

6.1.9.1 PCR for cloning

For the amplification of promoters or coding sequences cloned in this study, the Q5 ® High-Fidelity DNA Polymerase (NEB) was used, following the producer indications.

6.1.9.2 cDNA preparation

cDNA was prepared using and according to the SuperScript TM II Reverse Transcriptase (Thermofisher) kit 2μg RNA were used as template .

6.1.9.3 Semi-quantitative PCR

For Semi-quantitative PCR, JumpStart^{TM} REDTaq® ReadyMix^{TM} ReactionMix (Sigma-Aldrich) was used according to the producer. 1μl cDNA was used as template.

6.1.10 Microscopy

6.1.10.1 Root clearing for DIC microscopy

Roots were cleared with a modified protocol from [147]. Seedlings were incubated in a solution of 4% HCl and 20% methanol for 15 min at 70°C. Then the solution was changed to 7% NaOH and 60% ethanol and incubated 15 min at room temperature. Plants were progressively rehydrated in 40, 20 and 10% ethanol changing the solutions every 5 min. The storage solution was 25%glycerol and 5% ethanol. Plants were placed on a glass slide with a solution of 50% glycerol and covered with a cover slide.

6.1.10.2 Lateral root quantification in the katanin mutants

LR initiation index (LRP density* average of cortical cell length*100) [188] was used to quantify lateral roots along the primary root. This parameter considers that some genotypes

or treatments affect the length of cell in the primary root and measuring simple density might hide important differences in lateral root initiation. For this reason, this parameter calculates the number of lateral root in a length of 100 cells, what enables comparisons of lateral root densities between wild type and genotypes with affected cell length, like the *katanin* mutant.

6.1.10.3 Image acquisition

For live imaging of lateral root initiation 4 dag were gravistimulated for 4h to 8h before imaging. Generally live imaging of was done overnight (14-16h) with a resolution of 1024x1024 pixels, 400 Hz speed, 30min to 1hour time lapses, maximum step size (Z-axis) of 1μm and 3 to 4 times line averaging.

6.1.10.3.1 Multiphoton (SP5) for cytoskeleton

Two-photon (2P) microscopy was used for live imaging of cytoskeleton (actin and microtubules). Images were taken with a Leica TCS SP5II microscope (Leica microsystems) equipped with a Spectra Physics MaiTai, DeepSee ultrafast pulsed laser system for multi-photon excitation. The microscope was further equipped with two hybrid photodetectors (HyDs, Leica HyD^{TM}). Images were taken with a HCX PL APO 63x/1.30 GLYC CORR CS 21 C objective. For excitation of GFP (Excitation wavelength 488nm-Emision wavelength 495nm-555nm), the excitation wavelength of the 2P laser was set at 800nm.

6.1.10.3.2 SP8

A Leica TCS SP8 SMD microscope (Leica microsystems) was used for live imaging of the sC111 line. Images were taken with a HCX PL APO 63x/1.30 GLYC CORR CS 21 C objective.

6.1.10.3.3 DIC microscopy

The microscope Zeiss Axio Imager M1 equipped with an AxioCamHR3_552 and DIC optics was used. The objective Plan-Apochromat 20x/0.8 M27 was used.

6.1.10.4 Image analysis of cell shape

6.1.10.4.1 Asymmetric swelling of cells on live imaging

To analyse swelling during lateral root initiation in wild type we made use of the SCO111 line. To catch the earliest events of lateral root initiation, live imaging started 4h after gravistimulation.

Five time points were selected for the analysis cell swelling during the following events:

Naïve, when cells have no sign of initiation.

Nuclei migration; Just after nuclei are asymmetrically localized in cells.

Nuclei rounding; when nuclei change their shapes an round up before division.

Div1; First asymmetric division.

Div2; the central cells undergo a periclinal division.

Single slices of the Z-stack were chosen, corresponding to the middle plane of the cells, which could be determined by the geometry of the nucleus, with the nucleolus in the centre.

Then two strait ROI line were drawn on the cell-width at the centre of the small daughter cell and at the periphery of the big daughter cell. Two ROIs were drawn per time point. Cell width was normalized to the initial cell width (Naïve) and plotted as a time line.

The same measurements were done using the marker line GATA23*pro*::MBD:GFP in the *bot1-7* and LBD-SRDX backgrounds. However, less time points were considered.

6.1.10.4.2 Asymmetric swelling after one-time point gravistimulation

Seedlings of the marker line SCO111 were gravistimulated for 12h in the presence of pharmacological treatments and cell swelling was analysed after the first cell division. In the induction line LBD16pro::LhG4:GR:6xOP:PHS1ΔP:mCherry (LBD16*pro*::>> PHS1ΔP), seedlings were gravistimulated for 20h. In all controls DMSO was at the same concentration (1:2000) for easy comparison between treatments.

Z-stacks were taken of lateral root primordia formed at the bending. Single slices of the stacks were selected corresponding to the middle of the dividing cells and the opposite XPP cells. Then four strait ROI line were drawn: one on the cell-width at the centre of the small daughter cell and at the periphery of the big daughter cell and other two on the cell width of an opposite non-dividing XPP cell. The cell width of the dividing cells was normalized to the cell width of the non-dividing cell.

6.1.10.4.3 Loss of asymmetry of cell division

For analysis of the asymmetry in cell division, the length of the two daughter cells was measured. Then the ratio between the big daughter cell and the small daughter cell was calculated.

6.1.10.4.4 Endodermis spatial accommodation after IAA treatment

For the analysis of endodermal spatial accommodation, a z-stack of the endodermis was taken in the marker line CASP1pro::mVenus:MAP4 after 24h treatment of IAA 10μM or DMSO. To see the cell contour we draw an orthogonal slice through the volume represented by the z-stack, using the Reslice plugin (FiJi). Then, maximal projections were done to increase the signal. Maximal projections only included cells in which microtubule organization was measured. Over these maximal projections, ROI were drawn along the cell contour. Shape descriptor analysis was performed for the ROIs. A PCA analysis determined that roundness could describe at best the differences in cell-contour shape between IAA and DMSO treatments. Roundness is the inverse of Aspect Ratio (AR), which is the ratio between the major and the minor axis of a fitted ellipse. Loss of roundness indicates, lower values of the minor axis of the fitted ellipse.

These measurements were done for CASP1pro::mVenus:MAP4 in wild type and the mutant backgrounds *slr1* and pCASP1::*shy2-2*. The contour of 24 cells (wild type), 29 cells (*slr1*) and 23 cells (pCASP1::shy2-2) was analysed.

6.1.10.4.5 Endodermis spatial accommodation during lateral root emergence

Local cell thinning was measured after live imaging of endodermis cells in Col-0 and *bot1-7* during lateral root development. A strait line ROI was drawn on the hyperstack (XYZT) at the position where the maximal reduction of volume was detected. Then the plugin Dynamic Reslice created an orthogonal slice through the volume represented by the stack (XYZ) along the ROI. For each time point an orthogonal view was drawn, in which the shrinking cell contour could be seen. The diameter of the cell contour was measured in each time point (T=29 for *bot1-7*; T=32 for wild type), normalized to the initial value at T=0 and plotted as a time line for comparison between genotypes. For this analysis only one live recording was used from wild type and one for *bot1-7*.

6.1.10.5 Image analysis of cytoskeleton organization

6.1.10.5.1 Fibril tool Image J/Fiji macro

Cytoskeleton organization was analysed with the Fiji Plugin Fibril Tool [28, 189, 190].

Marion Louveaux created an automated version, in which the user draws and save all ROI first and then let the macro compute automatically microtubule orientation on the set of ROI. Z-stacks were taken in the marker line decorating actin or microtubules. Maximal projections (2D) were done of the z-stacks. Then ROIs were drawn with the polygonal tool over the cell contour of the cells where the organization of the fibrils wanted to be measured. The macro took each ROI and computed fibril orientation. At the end it generated a Log.txt file containing information on microtubule orientation (angle (0°-90°) and quality) for each ROI (each cell contour) on each Max projection.
Quality is a measure of the anisotropy of the fibrils. If all fibrils are oriented in the same direction (highest anisotropy) quality will be 1. If fibrils have no directionality (lowest anisotropy) quality will be 0. Increasing disorganization of the fibril array was plotted as the inverse of anisotropy.

6.1.10.5.2 CMT orientation and organization in founder cells

Microtubule organization was analysed was analysed with the Fiji Plugin Fibril Tool. Life imaging was done on the microtubule marker line GATA23pro::MBD:GFP to detect microtubules in founder cells in wild type and LBD16-SRDX background.
To induce lateral root initiation, seedlings were gravistimulated for 4h in the case of wild type and 8h for LBD16-SRDX background, because initiation is delayed in this genotype.
Although only two time points were represented in the figures, 4 time lapses were selected for the analysis representing the following events:

Naïve, when cells have no signs of division;
Right before division, during the formation of the preprophase band and
Right after division, when two cells can be seen after the first division.
6h after Div1., when transversal bundles could be observed .
In the analysis of microtubules of LBD16-SDRX, another time point has added to the analysis, 12h after Div1., to show that microtubules organization did not change in time.

Polygonal ROIs were drawn on singe slice of the (Z-stack), where cortical microtubules of the dividing cell could be well appreciated. Four ROIs were drawn on each of the 4 time lapses, around the cell contour of each of the two daughter cells and other two non-dividing neighbouring cells.
Then Fibril Tool computed angle of orientation and quality (anisotropy) of the array.

6.1.10.5.3 Actin organization in dividing and non-dividing cells

Actin organization was analysed with the Fiji Plugin Fibril Tool. Life imaging was done on the actin marker line LBD16pro::ABD2:GFP to detect actin in founder cells in wild type and LBD16-SRDX background.
To induce lateral root initiation seedlings were gravistimulated for 4h in the case of wild type and 8h for LBD16-SRDX background, because initiation is delayed in this genotype.
Three time lapses were selected representing the following events:

Naïve, when cells have no signs of division;
Right before division, during the formation of the preprophase band and
Div1., when the cell divide for the first time.
In the analysis of actin of LBD16-SDRX, another time point has added to the analysis, 4h after Div1., to show that actin organization did not change in time.

For the analysis of actin organization ROIs were drawn on singe slice of the (Z-stack), where actin of the dividing cell could be well appreciated. Four ROIs were drawn on each of the 4 time lapses, around the cell contour of each the two daughter cells and other two non-dividing neighbouring cells. FibrilTool computed actin anysotropy on each of the ROIs. Disorganization (1/anysotropy) of actin fibrils in dividing and non-dividing cells was plotted.

6.1.10.5.4 Analysis of microtubule organization in the endodermis after IAA treatment

Microtubule organization was analysed with the Fiji Plugin Fibril Tool. Z-stacks of the endodermis were taken in the marker line CASP1pro::mVenus:MAP4, to detect microtubule fibrils in the endodermis. Maximal projections (2D) were done of the cell side adjacent to cortex cells (outer side) and the endodermal cell side adjacent to the vascular tissue (inner side). Then ROIs were drawn with the polygonal tool over the cell contour of the cells where the organization of the fibrils wanted to be measured. Disorganization of the fibril array in the vascular or cortex side of the endodermis after IAA treatment was plotted.
These measurements were done in wild type and the mutant backgrounds *slr1* and pCASP1::*shy2-2*.

6.1.11 Statistic analysis of the data

Significant differences were tested applying a one-factor analysis of variance (ANOVA) performing Tuckey-test as post-hoc analysis.

Charts and statistical analysis were performed using R. R Development Core Team (2008). R: A language and environment for statistical computing. R Foundation for Statistical Computing, Vienna, Austria. ISBN 3-900051-07-0, URL http://www.R-project.org.

7 List of abbreviations

ACD ..... *Asymmetric cell division*
bot1-7 ..... *katanin mutant*
CMT ..... *Cortical microtubules*
CW ..... *Cell wall*
CWR ..... *Cell wall remodelling*
DEX ..... *Dexamethasone*
DMSO ..... *Dimethyl Sulfoxide*
DR5 ..... *DIRECT REPEAT5*
IAA ..... *3-Indoleacetic acid*
LatB ..... *Latrunculin B*
LR ..... *Lateral root*
LRFC ..... *Lateral root founder cell*
LRI ..... *Lateral root initiation*
LRP ..... *Lateral root primordia*
MAP ..... *Microtubule associated protein*
PAT ..... *Polar auxin transport*
PHS1ΔP ..... *PROPYZAMIDE-HYPERSENSITIVE ΔP*
PM ..... *Plasma membrane*
PPB ..... *Preprophase band*
SAM ..... *Shoot apical meristem*
XPP ..... *Xylem pole pericycle*

8 References

[1] Sassi M, Traas J. When biochemistry meets mechanics: a systems view of growth control in plants. Current opinion in plant biology 2015;28:137-43.

[2] Vermeer JE, von Wangenheim D, Barberon M, Lee Y, Stelzer EH, Maizel A, et al. A spatial accommodation by neighbouring cells is required for organ initiation in Arabidopsis. Science 2014;343:178-83.

[3] Maeda S, Gunji S, Hanai K, Hirano T, Kazama Y, Ohbayashi I, et al. The conflict between cell proliferation and expansion primarily affects stem organogenesis in Arabidopsis. Plant & cell physiology 2014;55:1994-2007.

[4] Hamant O, Heisler MG, Jonsson H, Krupinski P, Uyttewaal M, Bokov P, et al. Developmental patterning by mechanical signals in Arabidopsis. Science 2008;322:1650-5.

[5] Sampathkumar A, Yan A, Krupinski P, Meyerowitz EM. Physical forces regulate plant development and morphogenesis. Current biology : CB 2014;24:R475-83.

[6] Paredez AR, Somerville CR, Ehrhardt DW. Visualization of cellulose synthase demonstrates functional association with microtubules. Science 2006;312:1491-5.

[7] Burk DH. Alteration of Oriented Deposition of Cellulose Microfibrils by Mutation of a Katanin-Like Microtubule-Severing Protein. The Plant Cell Online 2002;14:2145-60.

[8] Nakayama N, Smith Richard S, Mandel T, Robinson S, Kimura S, Boudaoud A, et al. Mechanical Regulation of Auxin-Mediated Growth. Current Biology 2012;22:1468-76.

[9] Heisler MG, Hamant O, Krupinski P, Uyttewaal M, Ohno C, Jonsson H, et al. Alignment between PIN1 polarity and microtubule orientation in the shoot apical meristem reveals a tight coupling between morphogenesis and auxin transport. PLoS biology 2010;8:e1000516.

[10] Hamant O, Meyerowitz EM, Traas J. Is cell polarity under mechanical control in plants? Plant signalling & behavior 2011;6:137-9.

[11] Benkova E, Michniewicz M, Sauer M, Teichmann T, Seifertova D, Jurgens G, et al. Local, efflux-dependent auxin gradients as a common module for plant organ formation. Cell 2003;115:591-602.

[12] Cosgrove DJ. Plant cell wall extensibility: connecting plant cell growth with cell wall structure, mechanics, and the action of wall-modifying enzymes. Journal of experimental botany 2016;67:463-76.

[13] Lin D, Cao L, Zhou Z, Zhu L, Ehrhardt D, Yang Z, et al. Rho GTPase signalling activates microtubule severing to promote microtubule ordering in Arabidopsis. Current biology : CB 2013;23:290-7.

[14] Chebli Y, Geitmann A. Cellular growth in plants requires regulation of cell wall biochemistry. Curr Opin Cell Biol 2017;44:28-35.

[15] Tameshige T, Hirakawa Y, Torii KU, Uchida N. Cell walls as a stage for intercellular communication regulating shoot meristem development. Front Plant Sci 2015;6:324.

References

[16] Armezzani A, Abad U, Ali O, Robin AA, Vachez L, Larrieu A, et al. Transcriptional induction of cell wall remodelling genes is coupled to microtubule-driven growth isotropy at the shoot apex in Arabidopsis. Development 2018.

[17] Bidhendi AJ, Geitmann A. Relating the mechanics of the primary plant cell wall to morphogenesis. Journal of experimental botany 2016;67:449-61.

[18] Lampugnani ER, Khan GA, Somssich M, Persson S. Building a plant cell wall at a glance. Journal of cell science 2018;131.

[19] Mcqueenmason SJ, Cosgrove DJ. Expansin Mode of Action on Cell-Walls - Analysis of Wall Hydrolysis, Stress-Relaxation, and Binding. Plant physiology 1995;107:87-100.

[20] Cosgrove DJ. Plant expansins: diversity and interactions with plant cell walls. Current opinion in plant biology 2015;25:162-72.

[21] Grebe M, Braybrook SA, Peaucelle A. Mechano-Chemical Aspects of Organ Formation in Arabidopsis thaliana: The Relationship between Auxin and Pectin. PloS one 2013;8:e57813.

[22] Hamant O, Meyerowitz EM, Traas J. Is cell polarity under mechanical control in plants? Plant signalling & behavior 2014;6:137-9.

[23] Peaucelle A, Wightman R, Hofte H. The Control of Growth Symmetry Breaking in the Arabidopsis Hypocotyl. Current biology : CB 2015;25:1746-52.

[24] Feng W, Kita D, Peaucelle A, Cartwright HN, Doan V, Duan Q, et al. The FERONIA Receptor Kinase Maintains Cell-Wall Integrity during Salt Stress through Ca(2+) Signalling. Current biology : CB 2018;28:666-75 e5.

[25] Lin W, Tang W, Anderson C, Yang Z. 2018.

[26] Hashimoto T. Microtubules in plants. Arabidopsis Book 2015;13:e0179.

[27] Muratov A, Baulin VA. Mechanism of dynamic reorientation of cortical microtubules due to mechanical stress. Biophys Chem 2015;207:82-9.

[28] Uyttewaal M, Burian A, Alim K, Landrein B, Borowska-Wykret D, Dedieu A, et al. Mechanical stress acts via katanin to amplify differences in growth rate between adjacent cells in Arabidopsis. Cell 2012;149:439-51.

[29] Sampathkumar A, Krupinski P, Wightman R, Milani P, Berquand A, Boudaoud A, et al. Subcellular and supracellular mechanical stress prescribes cytoskeleton behavior in Arabidopsis cotyledon pavement cells. Elife 2014;3:e01967.

[30] Louveaux M, Rochette S, Beauzamy L, Boudaoud A, Hamant O. The impact of mechanical compression on cortical microtubules in Arabidopsis: a quantitative pipeline. The Plant journal : for cell and molecular biology 2016;88:328-42.

[31] Wasteneys GO, Ambrose JC. Spatial organization of plant cortical microtubules: close encounters of the 2D kind. Trends in cell biology 2009;19:62-71.

References

[32] Dhonukshe P, Laxalt AM, Goedhart J, Gadella TW, Munnik T. Phospholipase d activation correlates with microtubule reorganization in living plant cells. The Plant cell 2003;15:2666-79.

[33] Ambrose JC, Shoji T, Kotzer AM, Pighin JA, Wasteneys GO. The Arabidopsis CLASP gene encodes a microtubule-associated protein involved in cell expansion and division. The Plant cell 2007;19:2763-75.

[34] Lucas JR, Courtney S, Hassfurder M, Dhingra S, Bryant A, Shaw SL. Microtubule-associated proteins MAP65-1 and MAP65-2 positively regulate axial cell growth in etiolated Arabidopsis hypocotyls. The Plant cell 2011;23:1889-903.

[35] Liu Z, Persson S, Zhang Y. The connection of cytoskeletal network with plasma membrane and the cell wall. J Integr Plant Biol 2015;57:330-40.

[36] Li SD, Lei L, Somerville CR, Gu Y. Cellulose synthase interactive protein 1 (CSI1) links microtubules and cellulose synthase complexes. Proceedings of the National Academy of Sciences of the United States of America 2012;109:185-90.

[37] Baskin TI, Beemster GT, Judy-March JE, Marga F. Disorganization of cortical microtubules stimulates tangential expansion and reduces the uniformity of cellulose microfibril alignment among cells in the root of Arabidopsis. Plant physiology 2004;135:2279-90.

[38] Yang Z, Lavagi I. Spatial control of plasma membrane domains: ROP GTPase-based symmetry breaking. Current opinion in plant biology 2012;15:601-7.

[39] Liang H, Zhang Y, Martinez P, Rasmussen C, Xu T, Yang Z. The microtubule-associated protein IQ67 DOMAIN5 modulates microtubule dynamics and pavement cell shape. Plant physiology 2018.

[40] Burstenbinder K, Mitra D, Quegwer J. Functions of IQD proteins as hubs in cellular calcium and auxin signalling: A toolbox for shape formation and tissue-specification in plants? Plant signalling & behavior 2017;12:e1331198.

[41] Oda Y. Emerging roles of cortical microtubule–membrane interactions. Journal of Plant Research 2017;131:5-14.

[42] Porter K, Day B. From filaments to function: The role of the plant actin cytoskeleton in pathogen perception, signalling and immunity. J Integr Plant Biol 2016;58:299-311.

[43] Fu Y. The ROP2 GTPase Controls the Formation of Cortical Fine F-Actin and the Early Phase of Directional Cell Expansion during Arabidopsis Organogenesis. The Plant Cell Online 2002;14:777-94.

[44] Chen X, Friml J. Rho-GTPase-regulated vesicle trafficking in plant cell polarity. Biochemical Society transactions 2014;42:212-8.

[45] Geldner N, Friml J, Stierhof YD, Jurgens G, Palme K. Auxin transport inhibitors block PIN1 cycling and vesicle trafficking. Nature 2001;413:425-8.

[46] Nagawa S, Xu T, Lin D, Dhonukshe P, Zhang X, Friml J, et al. ROP GTPase-dependent actin microfilaments promote PIN1 polarization by localized inhibition of clathrin-dependent endocytosis. PLoS biology 2012;10:e1001299.

References

[47] Dhonukshe P, Grigoriev I, Fischer R, Tominaga M, Robinson DG, Hasek J, et al. Auxin transport inhibitors impair vesicle motility and actin cytoskeleton dynamics in diverse eukaryotes. Proceedings of the National Academy of Sciences of the United States of America 2008;105:4489-94.

[48] Xu T, Wen M, Nagawa S, Fu Y, Chen JG, Wu MJ, et al. Cell surface- and rho GTPase-based auxin signalling controls cellular interdigitation in Arabidopsis. Cell 2010;143:99-110.

[49] Kleine-Vehn J, Dhonukshe P, Swarup R, Bennett M, Friml J. Subcellular trafficking of the Arabidopsis auxin influx carrier AUX1 uses a novel pathway distinct from PIN1. The Plant cell 2006;18:3171-81.

[50] Sampathkumar A, Lindeboom JJ, Debolt S, Gutierrez R, Ehrhardt DW, Ketelaar T, et al. Live cell imaging reveals structural associations between the actin and microtubule cytoskeleton in Arabidopsis. The Plant cell 2011;23:2302-13.

[51] Rasmussen CG, Bellinger M. An overview of plant division-plane orientation. The New phytologist 2018.

[52] Besson S, Dumais J. Universal rule for the symmetric division of plant cells. Proceedings of the National Academy of Sciences of the United States of America 2011;108:6294-9.

[53] Shao W, Dong J. Polarity in plant asymmetric cell division: Division orientation and cell fate differentiation. Dev Biol 2016;419:121-31.

[54] Pillitteri LJ, Guo X, Dong J. Asymmetric cell division in plants: mechanisms of symmetry breaking and cell fate determination. Cell Mol Life Sci 2016;73:4213-29.

[55] Sarkar AK, Luijten M, Miyashima S, Lenhard M, Hashimoto T, Nakajima K, et al. Conserved factors regulate signalling in Arabidopsis thaliana shoot and root stem cell organizers. Nature 2007;446:811-4.

[56] Schlereth A, Moller B, Liu W, Kientz M, Flipse J, Rademacher EH, et al. MONOPTEROS controls embryonic root initiation by regulating a mobile transcription factor. Nature 2010;464:913-6.

[57] Zhang Y, Dong J. Cell polarity: compassing cell division and differentiation in plants. Current opinion in plant biology 2018;45:127-35.

[58] Schaefer E, Belcram K, Uyttewaal M, Duroc Y, Goussot M, Legland D, et al. The preprophase band of microtubules controls the robustness of division orientation in plants. Science 2017;356:186-9.

[59] Spinner L, Gadeyne A, Belcram K, Goussot M, Moison M, Duroc Y, et al. A protein phosphatase 2A complex spatially controls plant cell division. Nat Commun 2013;4:1863.

[60] Dong J, MacAlister CA, Bergmann DC. BASL controls asymmetric cell division in Arabidopsis. Cell 2009;137:1320-30.

[61] Zhang Y, Wang P, Shao W, Zhu JK, Dong J. The BASL polarity protein controls a MAPK signalling feedback loop in asymmetric cell division. Developmental cell 2015;33:136-49.

[62] Yoshida S, Barbier de Reuille P, Lane B, Bassel GW, Prusinkiewicz P, Smith RS, et al. Genetic control of plant development by overriding a geometric division rule. Developmental cell 2014;29:75-87.

[63] Goh T, Joi S, Mimura T, Fukaki H. The establishment of asymmetry in Arabidopsis lateral root founder cells is regulated by LBD16/ASL18 and related LBD/ASL proteins. Development 2012;139:883-93.

[64] Liu P, Qi M, Xue X, Ren H. Dynamics and functions of the actin cytoskeleton during the plant cell cycle. Chinese Science Bulletin 2011;56:3504-10.

[65] Kimata Y, Higaki T, Kawashima T, Kurihara D, Sato Y, Yamada T, et al. Cytoskeleton dynamics control the first asymmetric cell division in Arabidopsis zygote. Proceedings of the National Academy of Sciences of the United States of America 2016;113:14157-62.

[66] Wang P HP. Interactions between plant endomembrane systems and the actin cytoskeleton. . Frontiers in Plant Science 2015;6.

[67] Casimiro I, Marchant A, Bhalerao RP, Beeckman T, Dhooge S, Swarup R, et al. Auxin transport promotes Arabidopsis lateral root initiation. The Plant cell 2001;13:843-52.

[68] Fukaki H, Tasaka M. Hormone interactions during lateral root formation. Plant molecular biology 2009;69:437-49.

[69] Fukaki H, Nakao Y, Okushima Y, Theologis A, Tasaka M. Tissue-specific expression of stabilized SOLITARY-ROOT/IAA14 alters lateral root development in Arabidopsis. The Plant journal : for cell and molecular biology 2005;44:382-95.

[70] Strader LC, Zhao Y. Auxin perception and downstream events. Current opinion in plant biology 2016;33:8-14.

[71] Monshausen GB, Miller ND, Murphy AS, Gilroy S. Dynamics of auxin-dependent Ca2+ and pH signalling in root growth revealed by integrating high-resolution imaging with automated computer vision-based analysis. The Plant journal : for cell and molecular biology 2011;65:309-18.

[72] Dindas J, Scherzer S, Roelfsema MRG, von Meyer K, Muller HM, Al-Rasheid KAS, et al. AUX1-mediated root hair auxin influx governs SCF(TIR1/AFB)-type Ca(2+) signalling. Nat Commun 2018;9:1174.

[73] Fendrych M, Akhmanova M, Merrin J, Glanc M, Hagihara S, Takahashi K, et al. Rapid and reversible root growth inhibition by TIR1 auxin signalling. Nat Plants 2018;4:453-9.

[74] Liu Y, Dong Q, Kita D, Huang JB, Liu G, Wu X, et al. RopGEF1 Plays a Critical Role in Polar Auxin Transport in Early Development. Plant physiology 2017;175:157-71.

[75] Vanneste S, Friml J. Auxin: a trigger for change in plant development. Cell 2009;136:1005-16.

[76] Overvoorde P, Fukaki H, Beeckman T. Auxin control of root development. Cold Spring Harb Perspect Biol 2010;2:a001537.

[77] Swarup K, Benkova E, Swarup R, Casimiro I, Peret B, Yang Y, et al. The auxin influx carrier LAX3 promotes lateral root emergence. Nature cell biology 2008;10:946-54.

[78] Marchant A. AUX1 Promotes Lateral Root Formation by Facilitating Indole-3-Acetic Acid Distribution between Sink and Source Tissues in the Arabidopsis Seedling. The Plant Cell Online 2002;14:589-97.

[79] Zhu J, Bailly Al, Zwiewka M, Sovero V, di Donato M, Ge P, et al. TWISTED DWARF1 mediates the action of auxin transport inhibitors on actin cytoskeleton dynamics. The Plant cell 2016:tpc.00726.2015.

[80] Friml J, Yang X, Michniewicz M, Weijers D, Quint A, Tietz O, et al. A PINOID-dependent binary switch in apical-basal PIN polar targeting directs auxin efflux. Science 2004;306:862-5.

[81] Geldner N, Anders N, Wolters H, Keicher J, Kornberger W, Muller P, et al. The Arabidopsis GNOM ARF-GEF mediates endosomal recycling, auxin transport, and auxin-dependent plant growth. Cell 2003;112:219-30.

[82] Richter S, Anders N, Wolters H, Beckmann H, Thomann A, Heinrich R, et al. Role of the GNOM gene in Arabidopsis apical-basal patterning - From mutant phenotype to cellular mechanism of protein action. European journal of cell biology 2010;89:138-44.

[83] Kleine-Vehn J, Leitner J, Zwiewka M, Sauer M, Abas L, Luschnig C, et al. Differential degradation of PIN2 auxin efflux carrier by retromer-dependent vacuolar targeting. Proceedings of the National Academy of Sciences of the United States of America 2008;105:17812-7.

[84] Salanenka Y, Verstraeten I, Lofke C, Tabata K, Naramoto S, Glanc M, et al. Gibberellin DELLA signalling targets the retromer complex to redirect protein trafficking to the plasma membrane. Proceedings of the National Academy of Sciences of the United States of America 2018;115:3716-21.

[85] Zazimalova E, Murphy AS, Yang H, Hoyerova K, Hosek P. Auxin transporters--why so many? Cold Spring Harb Perspect Biol 2010;2:a001552.

[86] Adamowski M, Friml J. PIN-dependent auxin transport: action, regulation, and evolution. The Plant cell 2015;27:20-32.

[87] Casimiro I, Beeckman T, Graham N, Bhalerao R, Zhang H, Casero P, et al. Dissecting Arabidopsis lateral root development. Trends in plant science 2003;8:165-71.

[88] Parizot B, Laplaze L, Ricaud L, Boucheron-Dubuisson E, Bayle V, Bonke M, et al. Diarch symmetry of the vascular bundle in Arabidopsis root encompasses the pericycle and is reflected in distich lateral root initiation. Plant physiology 2008;146:140-8.

[89] Dubrovsky JG, Rost TL, Colón-Carmona A, Doerner P. Early primordium morphogenesis during lateral root initiation in Arabidopsis thaliana. Planta 2001;214:30-6.

[90] Beeckman T, Burssens S, Inze D. The peri-cell-cycle in Arabidopsis. Journal of experimental botany 2001;52:403-11.

[91] Du YJ, Scheres B. Lateral root formation and the multiple roles of auxin. Journal of experimental botany 2018;69:155-67.

[92] De Smet I. Lateral root initiation: one step at a time. New Phytologist 2012;193:867-73.

References

[93] De Smet I, Tetsumura T, De Rybel B, Frei dit Frey N, Laplaze L, Casimiro I, et al. Auxin-dependent regulation of lateral root positioning in the basal meristem of Arabidopsis. Development 2007;134:681-90.

[94] Moreno-Risueno MA, Van Norman JM, Moreno A, Zhang J, Ahnert SE, Benfey PN. Oscillating gene expression determines competence for periodic Arabidopsis root branching. Science 2010;329:1306-11.

[95] Hofhuis H, Laskowski M, Du Y, Prasad K, Grigg S, Pinon V, et al. Phyllotaxis and rhizotaxis in Arabidopsis are modified by three PLETHORA transcription factors. Current biology : CB 2013;23:956-62.

[96] De Rybel B, Audenaert D, Xuan W, Overvoorde P, Strader LC, Kepinski S, et al. A role for the root cap in root branching revealed by the non-auxin probe naxillin. Nature chemical biology 2012;8:798-805.

[97] Xuan W, Audenaert D, Parizot B, Moller BK, Njo MF, De Rybel B, et al. Root Cap-Derived Auxin Pre-patterns the Longitudinal Axis of the Arabidopsis Root. Current biology : CB 2015;25:1381-8.

[98] Moller BK, Xuan W, Beeckman T. Dynamic control of lateral root positioning. Current opinion in plant biology 2017;35:1-7.

[99] Van Norman JM, Xuan W, Beeckman T, Benfey PN. To branch or not to branch: the role of pre-patterning in lateral root formation. Development 2013;140:4301-10.

[100] Dubrovsky JG, Sauer M, Napsucialy-Mendivil S, Ivanchenko MG, Friml J, Shishkova S, et al. Auxin acts as a local morphogenetic trigger to specify lateral root founder cells. Proceedings of the National Academy of Sciences 2008;105:8790-4.

[101] De Rybel B, Vassileva V, Parizot B, Demeulenaere M, Grunewald W, Audenaert D, et al. A novel aux/IAA28 signalling cascade activates GATA23-dependent specification of lateral root founder cell identity. Current biology : CB 2010;20:1697-706.

[102] Otvos K, Benkova E. Spatiotemporal mechanisms of root branching. Curr Opin Genet Dev 2017;45:82-9.

[103] Ditengou FA, Teale WD, Kochersperger P, Flittner KA, Kneuper I, van der Graaff E, et al. Mechanical induction of lateral root initiation in Arabidopsis thaliana. Proceedings of the National Academy of Sciences of the United States of America 2008;105:18818-23.

[104] Laskowski M, Grieneisen VA, Hofhuis H, Hove CA, Hogeweg P, Maree AF, et al. Root system architecture from coupling cell shape to auxin transport. PLoS biology 2008;6:e307.

[105] DiDonato RJ, Arbuckle E, Buker S, Sheets J, Tobar J, Totong R, et al. Arabidopsis ALF4encodes a nuclear-localized protein required for lateral root formation. The Plant Journal 2004;37:340-53.

[106] Bagchi R, Melnyk CW, Christ G, Winkler M, Kirchsteiner K, Salehin M, et al. The Arabidopsis
ALF4 protein is a regulator of SCF E3 ligases. The EMBO journal 2018;37:255-68.

[107] Vanneste S, De Rybel B, Beemster GT, Ljung K, De Smet I, Van Isterdael G, et al. Cell cycle progression in the pericycle is not sufficient for SOLITARY ROOT/IAA14-mediated lateral root initiation in Arabidopsis thaliana. The Plant cell 2005;17:3035-50.

[108] Himanen K. Auxin-Mediated Cell Cycle Activation during Early Lateral Root Initiation. The Plant Cell Online 2002;14:2339-51.

[109] Li X, Mo X, Shou H, Wu P. Cytokinin-mediated cell cycling arrest of pericycle founder cells in lateral root initiation of Arabidopsis. Plant & cell physiology 2006;47:1112-23.

[110] Marhavy P, Duclercq J, Weller B, Feraru E, Bielach A, Offringa R, et al. Cytokinin controls polarity of PIN1-dependent auxin transport during lateral root organogenesis. Current biology : CB 2014;24:1031-7.

[111] Berckmans B, Vassileva V, Schmid SP, Maes S, Parizot B, Naramoto S, et al. Auxin-dependent cell cycle reactivation through transcriptional regulation of Arabidopsis E2Fa by lateral organ boundary proteins. The Plant cell 2011;23:3671-83.

[112] Goh T, Kasahara H, Mimura T, Kamiya Y, Fukaki H. Multiple AUX/IAA-ARF modules regulate lateral root formation: the role of Arabidopsis SHY2/IAA3-mediated auxin signalling. Philos T R Soc B 2012;367:1461-8.

[113] De Smet I, Lau S, Voss U, Vanneste S, Benjamins R, Rademacher EH, et al. Bimodular auxin response controls organogenesis in Arabidopsis. Proceedings of the National Academy of Sciences of the United States of America 2010;107:2705-10.

[114] Benitez-Alfonso Y, Faulkner C, Pendle A, Miyashima S, Helariutta Y, Maule A. Symplastic intercellular connectivity regulates lateral root patterning. Developmental cell 2013;26:136-47.

[115] De Smet I, Vassileva V, De Rybel B, Levesque MP, Grunewald W, Van Damme D, et al. Receptor-like kinase ACR4 restricts formative cell divisions in the Arabidopsis root. Science 2008;322:594-7.

[116] Murphy E, Vu LD, Van den Broeck L, Lin Z, Ramakrishna P, van de Cotte B, et al. RALFL34 regulates formative cell divisions in Arabidopsis pericycle during lateral root initiation. Journal of experimental botany 2016;67:4863-75.

[117] Malamy JE, Ryan KS. Environmental Regulation of Lateral Root Initiation in Arabidopsis. Plant physiology 2001;127:899-909.

[118] Yu LH, Miao ZQ, Qi GF, Wu J, Cai XT, Mao JL, et al. MADS-box transcription factor AGL21 regulates lateral root development and responds to multiple external and physiological signals. Molecular plant 2014;7:1653-69.

[119] De Smet I, Signora L, Beeckman T, Inze D, Foyer CH, Zhang HM. An abscisic acid-sensitive checkpoint in lateral root development of Arabidopsis. Plant Journal 2003;33:543-55.

[120] Kong D, Hao Y, Cui H. The WUSCHEL Related Homeobox Protein WOX7 Regulates the Sugar Response of Lateral Root Development in Arabidopsis thaliana. Molecular plant 2016;9:261-70.

[121] Du Y, Scheres B. PLETHORA transcription factors orchestrate de novo organ patterning during Arabidopsis lateral root outgrowth. Proceedings of the National Academy of Sciences of the United States of America 2017;114:11709-14.

[122] Hirota A, Kato T, Fukaki H, Aida M, Tasaka M. The auxin-regulated AP2/EREBP gene PUCHI is required for morphogenesis in the early lateral root primordium of Arabidopsis. The Plant cell 2007;19:2156-68.

[123] von Wangenheim D, Fangerau J, Schmitz A, Smith RS, Leitte H, Stelzer EH, et al. Rules and Self-Organizing Properties of Post-embryonic Plant Organ Cell Division Patterns. Current biology : CB 2016;26:439-49.

[124] Lucas M, Kenobi, K., von Wangenheim, D., Voβ, U., Swarup, K., De Smet, I., … Bennett, M. J. . Lateral root morphogenesis is dependent on the mechanical properties of the overlaying tissues. . Proceedings of the National Academy of Sciences of the United States of America 2013; 110:5.

[125] Vilches-Barro A, Maizel A. Talking through walls: mechanisms of lateral root emergence in Arabidopsis thaliana. Current opinion in plant biology 2015;23:31-8.

[126] Stoeckle D, Thellmann M, Vermeer JE. Breakout-lateral root emergence in Arabidopsis thaliana. Current opinion in plant biology 2018;41:67-72.

[127] Marhavy P, Montesinos JC, Abuzeineh A, Van Damme D, Vermeer JEM, Duclercq J, et al. Targeted cell elimination reveals an auxin-guided biphasic mode of lateral root initiation. Genes & development 2016;30:471-83.

[128] Marhavy P, Vanstraelen M, De Rybel B, Zhaojun D, Bennett MJ, Beeckman T, et al. Auxin reflux between the endodermis and pericycle promotes lateral root initiation. The EMBO journal 2013;32:149-58.

[129] Orman-Ligeza B, Parizot B, de Rycke R, Fernandez A, Himschoot E, Van Breusegem F, et al. RBOH-mediated ROS production facilitates lateral root emergence in Arabidopsis. Development 2016;143:3328-39.

[130] Laskowski M, Biller S, Stanley K, Kajstura T, Prusty R. Expression profiling of auxin-treated Arabidopsis roots: toward a molecular analysis of lateral root emergence. Plant & cell physiology 2006;47:788-92.

[131] Kumpf RP, Shi CL, Larrieu A, Sto IM, Butenko MA, Peret B, et al. Floral organ abscission peptide IDA and its HAE/HSL2 receptors control cell separation during lateral root emergence. Proceedings of the National Academy of Sciences of the United States of America 2013;110:5235-40.

[132] Lee HW, Kim J. EXPANSINA17 up-regulated by LBD18/ASL20 promotes lateral root formation during the auxin response. Plant & cell physiology 2013;54:1600-11.

[133] Lee HW, Kim MJ, Kim NY, Lee SH, Kim J. LBD18 acts as a transcriptional activator that directly binds to the EXPANSIN14 promoter in promoting lateral root emergence of Arabidopsis. The Plant journal : for cell and molecular biology 2013;73:212-24.

[134] Lee HW, Kim NY, Lee DJ, Kim J. LBD18/ASL20 regulates lateral root formation in combination with LBD16/ASL18 downstream of ARF7 and ARF19 in Arabidopsis. Plant physiology 2009;151:1377-89.

[135] Peret B, Middleton AM, French AP, Larrieu A, Bishopp A, Njo M, et al. Sequential induction of auxin efflux and influx carriers regulates lateral root emergence. Molecular systems biology 2013;9:699.

[136] Porco S, Larrieu A, Du Y, Gaudinier A, Goh T, Swarup K, et al. Lateral root emergence in Arabidopsis is dependent on transcription factor LBD29 regulation of auxin influx carrier LAX3. Development 2016;143:3340-9.

[137] Peret B, Li G, Zhao J, Band LR, Voss U, Postaire O, et al. Auxin regulates aquaporin function to facilitate lateral root emergence. Nature cell biology 2012;14:991-8.

[138] Reinhardt H, Hachez C, Bienert MD, Beebo A, Swarup K, Voss U, et al. Tonoplast Aquaporins Facilitate Lateral Root Emergence. Plant physiology 2016;170:1640-54.

[139] Stoppin-Mellet V, Gaillard J, Vantard M. Katanin's severing activity favors bundling of cortical microtubules in plants. The Plant journal : for cell and molecular biology 2006;46:1009-17.

[140] Lavenus J, Goh T, Roberts I, Guyomarc'h S, Lucas M, De Smet I, et al. Lateral root development in Arabidopsis: fifty shades of auxin. Trends in plant science 2013;18:450-8.

[141] Fernandez A, Drozdzecki A, Hoogewijs K, Vassileva V, Madder A, Beeckman T, et al. The GLV6/RGF8/CLEL2 peptide regulates early pericycle divisions during lateral root initiation. Journal of experimental botany 2015;66:5245-56.

[142] Marmagne A, Rouet MA, Ferro M, Rolland N, Alcon C, Joyard J, et al. Identification of new intrinsic proteins in Arabidopsis plasma membrane proteome. Molecular & cellular proteomics : MCP 2004;3:675-91.

[143] Weijers D, Franke-van Dijk M, Vencken RJ, Quint A, Hooykaas P, Offringa R. An Arabidopsis Minute-like phenotype caused by a semi-dominant mutation in a RIBOSOMAL PROTEIN S5 gene. Development 2001;128:4289-99.

[144] Liao CY, Smet W, Brunoud G, Yoshida S, Vernoux T, Weijers D. Reporters for sensitive and quantitative measurement of auxin response. Nat Methods 2015;12:207-10, 2 p following 10.

[145] Peaucelle A, Wightman R, Hofte H. The Control of Growth Symmetry Breaking in the Arabidopsis Hypocotyl (vol 25, pg 1746, 2015). Current Biology 2015;25:1798-.

[146] Bichet A, Desnos T, Turner S, Grandjean O, Hofte H. BOTERO1 is required for normal orientation of cortical microtubules and anisotropic cell expansion in Arabidopsis. Plant Journal 2001;25:137-48.

[147] Malamy JE, Benfey PN. Organization and cell differentiation in lateral roots of Arabidopsis thaliana. Development 1997;124:33-44.

[148] Schuerholz A-K, Lopez-Salmeron V, Li Z, Forner J, Wenzl C, Gaillochet C, et al. 2018.

[149] Grefen C, Donald N, Hashimoto K, Kudla J, Schumacher K, Blatt MR. A ubiquitin-10 promoter-based vector set for fluorescent protein tagging facilitates temporal stability and native protein distribution in transient and stable expression studies. The Plant journal : for cell and molecular biology 2010;64:355-65.

[150] Roppolo D, De Rybel B, Tendon VD, Pfister A, Alassimone J, Vermeer JE, et al. A novel protein family mediates Casparian strip formation in the endodermis. Nature 2011;473:380-3.

[151] Fujita S, Pytela J, Hotta T, Kato T, Hamada T, Akamatsu R, et al. An atypical tubulin kinase mediates stress-induced microtubule depolymerization in Arabidopsis. Current biology : CB 2013;23:1969-78.

[152] Craft J, Samalova M, Baroux C, Townley H, Martinez A, Jepson I, et al. New pOp/LhG4 vectors for stringent glucocorticoid-dependent transgene expression in Arabidopsis. The Plant journal : for cell and molecular biology 2005;41:899-918.

[153] Dastidar MG, Jouannet V, Maizel A. Root branching: mechanisms, robustness, and plasticity. Wiley interdisciplinary reviews Developmental biology 2012;1:329-43.

[154] Okushima Y, Fukaki H, Onoda M, Theologis A, Tasaka M. ARF7 and ARF19 regulate lateral root formation via direct activation of LBD/ASL genes in Arabidopsis. The Plant cell 2007;19:118-30.

[155] Wang P, Hawkins TJ, Hussey PJ. Connecting membranes to the actin cytoskeleton. Current opinion in plant biology 2017;40:71-6.

[156] Roycewicz PS, Malamy JE. Cell wall properties play an important role in the emergence of lateral root primordia from the parent root. Journal of experimental botany 2014;65:2057-69.

[157] Alassimone J, Roppolo D, Geldner N, Vermeer JE. The endodermis--development and differentiation of the plant's inner skin. Protoplasma 2012;249:433-43.

[158] Panteris E, Adamakis I-DS, Daras G, Rigas S. Cortical microtubule patterning in roots ofArabidopsis thalianaprimary cell wall mutants reveals the bidirectional interplay with cell expansion. Plant signalling & behavior 2014;9:e28737.

[159] Sassi M, Ali O, Boudon F, Cloarec G, Abad U, Cellier C, et al. An auxin-mediated shift toward growth isotropy promotes organ formation at the shoot meristem in Arabidopsis. Current biology : CB 2014;24:2335-42.

[160] Cosgrove DJ. Catalysts of plant cell wall loosening. F1000Res 2016;5.

[161] Xiao C, Zhang T, Zheng Y, Cosgrove DJ, Anderson CT. Xyloglucan Deficiency Disrupts Microtubule Stability and Cellulose Biosynthesis in Arabidopsis, Altering Cell Growth and Morphogenesis. Plant physiology 2016;170:234-49.

[162] Lavenus J, Goh T, Guyomarc'h S, Hill K, Lucas M, Voss U, et al. Inference of the Arabidopsis lateral root gene regulatory network suggests a bifurcation mechanism that defines primordia flanking and central zones. The Plant cell 2015;27:1368-88.

[163] Himanen K, Vuylsteke M, Vanneste S, Vercruysse S, Boucheron E, Alard P, et al. Transcript profiling of early lateral root initiation. Proceedings of the National Academy of Sciences of the United States of America 2004;101:5146-51.

[164] Poraty-Gavra L, Zimmermann P, Haigis S, Bednarek P, Hazak O, Stelmakh OR, et al. The Arabidopsis Rho of plants GTPase AtROP6 functions in developmental and pathogen response pathways. Plant physiology 2013;161:1172-88.

[165] Takahashi K, Hayashi K, Kinoshita T. Auxin activates the plasma membrane H+-ATPase by phosphorylation during hypocotyl elongation in Arabidopsis. Plant physiology 2012;159:632-41.

[166] Fendrych M, Leung J, Friml J. TIR1/AFB-Aux/IAA auxin perception mediates rapid cell wall acidification and growth of Arabidopsis hypocotyls. Elife 2016;5.

[167] Ramakrishna P, Rance GA, Vu LD, Murphy E, Swarup K, Moirangthem K, et al. 2018.

[168] Hepler PK. Calcium: a central regulator of plant growth and development. The Plant cell 2005;17:2142-55.

[169] Wendrich J, Yang B-J, Mijnhout P, Xue H-W, De Rybel B, Weijers D. 2018.

[170] Fu Y, Wu G, Yang Z. Rop GTPase-dependent dynamics of tip-localized F-actin controls tip growth in pollen tubes. The Journal of cell biology 2001;152:1019-32.

[171] Fu Y, Gu Y, Zheng Z, Wasteneys G, Yang Z. Arabidopsis interdigitating cell growth requires two antagonistic pathways with opposing action on cell morphogenesis. Cell 2005;120:687-700.

[172] Li H, Shen JJ, Zheng ZL, Lin Y, Yang Z. The Rop GTPase switch controls multiple developmental processes in Arabidopsis. Plant physiology 2001;126:670-84.

[173] Lin D, Nagawa S, Chen J, Cao L, Chen X, Xu T, et al. A ROP GTPase-dependent auxin signalling pathway regulates the subcellular distribution of PIN2 in Arabidopsis roots. Current biology : CB 2012;22:1319-25.

[174] Zhang C, Hicks GR, Raikhel NV. Plant vacuole morphology and vacuolar trafficking. Front Plant Sci 2014;5:476.

[175] Scheuring D, Lofke C, Kruger F, Kittelmann M, Eisa A, Hughes L, et al. Actin-dependent vacuolar occupancy of the cell determines auxin-induced growth repression. Proceedings of the National Academy of Sciences of the United States of America 2016;113:452-7.

[176] Graumann K, Runions J, Evans DE. Characterization of SUN-domain proteins at the higher plant nuclear envelope. The Plant journal : for cell and molecular biology 2010;61:134-44.

[177] Tamura K, Iwabuchi K, Fukao Y, Kondo M, Okamoto K, Ueda H, et al. Myosin XI-i links the nuclear membrane to the cytoskeleton to control nuclear movement and shape in Arabidopsis. Current biology : CB 2013;23:1776-81.

[178] Poulet A, Probst AV, Graumann K, Tatout C, Evans D. Exploring the evolution of the proteins of the plant nuclear envelope. Nucleus 2017;8:46-59.

[179] Vineyard L, Elliott A, Dhingra S, Lucas JR, Shaw SL. Progressive transverse microtubule array organization in hormone-induced Arabidopsis hypocotyl cells. The Plant cell 2013;25:662-76.

[180] Burstenbinder K, Moller B, Plotner R, Stamm G, Hause G, Mitra D, et al. The IQD Family of Calmodulin-Binding Proteins Links Calcium Signalling to Microtubules, Membrane Subdomains, and the Nucleus. Plant physiology 2017;173:1692-708.

References

[181] Heisler MG, Ohno C, Das P, Sieber P, Reddy GV, Long JA, et al. Patterns of auxin transport and gene expression during primordium development revealed by live imaging of the Arabidopsis inflorescence meristem. Current Biology 2005;15:1899-911.

[182] Fukaki H, Tameda S, Masuda H, Tasaka M. Lateral root formation is blocked by a gain-of-function mutation in the SOLITARY-ROOT/IAA14 gene of Arabidopsis. Plant Journal 2002;29:153-68.

[183] Marhavy P, Benkova E. Real-time Analysis of Lateral Root Organogenesis in Arabidopsis. Bio Protoc 2015;5.

[184] Murashige T, Skoog F. A Revised Medium for Rapid Growth and Bio Assays with Tobacco Tissue Cultures. Physiol Plantarum 1962;15:473-97.

[185] Lampropoulos A, Sutikovic Z, Wenzl C, Maegele I, Lohmann JU, Forner J. GreenGate---a novel, versatile, and efficient cloning system for plant transgenesis. PloS one 2013;8:e83043.

[186] Kearse M, Moir R, Wilson A, Stones-Havas S, Cheung M, Sturrock S, et al. Geneious Basic: an integrated and extendable desktop software platform for the organization and analysis of sequence data. Bioinformatics 2012;28:1647-9.

[187] Schwab R, Ossowski S, Riester M, Warthmann N, Weigel D. Highly specific gene silencing by artificial microRNAs in Arabidopsis. The Plant cell 2006;18:1121-33.

[188] Dubrovsky JG, Forde BG. Quantitative analysis of lateral root development: pitfalls and how to avoid them. The Plant cell 2012;24:4-14.

[189] Boudaoud A, Burian A, Borowska-Wykret D, Uyttewaal M, Wrzalik R, Kwiatkowska D, et al. FibrilTool, an ImageJ plug-in to quantify fibrillar structures in raw microscopy images. Nat Protoc 2014;9:457-63.

[190] Schindelin J, Arganda-Carreras I, Frise E, Kaynig V, Longair M, Pietzsch T, et al. Fiji: an open-source platform for biological-image analysis. Nat Methods 2012;9:676-82.

9 Acknowledgements

First of all I want to thank Prof. Dr. Alexis Maizel for many, many things. Thanks for accepting me as your PhD student and give me this project, which in the end (finally!) turned up in a beautiful story. Also thanks for pushing me to give lots of presentations and send me to many conferences. I was in Chile, in France, in England… I enjoy all of these journeys. Thanks for teaching me to give good presentations and be less "Gaudi-style", I think I did some progress, but I keep on learning and I will always remember your tips. Thanks for the great parties that we organized and for being the best DJ in COS ;)

I want to thank my TAC members, Prof. Dr. Karin Schumacher, Dr. Sebastian Wolf and Dr. Markus Heisler for their support and advice all these years. Thank you Karin for giving me the opportunity to go to Japan! It was an amazing experience. And thanks to my fourth examiner Prof. Dr. Niko Geldner: it is an honour to have you in my thesis committee.

A very warm "Thank you!" to my lab members: Marion, Beatrice, Michi, Xao Zhue, Jazmin, Everardo, Lotte, Paola, Andrea and Mouli and the master students Maxito and Juan, for making the great atmosphere in the Lab and the nice costumes that we organized together for the "COS" party. Thank you Lotte for your help with the PC, because you always manage to solve all the problems (!) and for your help with all the paper work (!) and your cloning. And also to speak with me in German from the beginning!!

My sweet Mouli, thanks for being there with you "cow-walk": always calm, always ready to smile; it has been a pleasure to join you during your PhD. Thanks to Andrea and Paola, for the funny hours together and making every day bright. You know Andrea, how much I miss to annoy you ;). Endless "Thank you!" to you, Paola, for helping me so much, for being so patient with your "Gremlin", for feeding me (!), be my sister and for just being the sunshine every day.

Thanks to my "Beer hour" warriors, Anne-Laure (Ana Laura!!) and Francesca, my oldest friends in "COS". Thanks for the great moments we had together! We see "us" soon!

And thanks to the crazy French party animals: Cristophe and Slava. I admire your science and your perseverance Cristophe and it is great to go out with you. Together with Slava, you will never know how the night can end up…

I cannot forget here the "Wolfies"! Sweet Anka and Eli, thank you for the nice time! Thanks to "Tomato-Zhenni" and especial thanks to Borja, for being my "Coach" in many things ;) such us family planning and dress code. Thanks for being so patient these last days and give me a warm hug to cheer me up. Also thank you for your choreographies in the lab and bring me to laugh so many times.

Thanks to the "Schumachers"! Especially to the beautiful girls: Jana, Görken, Upendo and Zaida. I had a great time with you in "Bade-welt" and Venice and that unforgettable "Beer hour" with swimming pool, in which every one end up completely wet. And thanks of course to the boys: Fabian, Falco, Stephan, Raina and Noah for the nice conversations in the seminar room and the White Russians during the Movie Nights, Raina!

Thanks to the beautiful people in "COS". I feel very lucky to have done my PhD in this institute. Special thanks to Prof. Dr. Thomas Rausch, without him I would not be, where I am now, and the warm smile of Angelika, which always organizes every event so carefully.

I cannot forget my family: Gracias Mama por estar siempre ahí y darme los mejores consejos; por ser tan paciente y aceptar que viva en Alemania, aunque preferirías que estuviera en Madrid; por querer siempre ayudarme, calmarme, llevarme y traerme. Por tu risa y tu amor. Gracias Papa por apoyarme en esta locura de irme a Alemania y siempre enviarme ánimos cuando estaba triste y pensaba que no iba a poder mas. Y gracias por llevarme a conducir! . Y mi pollo, el verdadero, mi hermana del alma, Paula. Gracias hermana por las conversaciones, los viajes, las risas. Por venirme a visitar. Por escribirme siempre para enviarme ánimos. Os quiero muchísimo! Y no olvidar a los Vilches y por

supuesto las “Damnificadas”, por todas las comidas de navidad, las canciones, las bodas y las risas. Os quiero familia.

Back to English, thank to my “Nest-family”, Lydia and Norman. Thank you for your patience these last days. Lydia you know how much I am going to miss you the next year. How much you help me. You are just there every time I need you: bringing me calm when driving ;) or peeling carrots! Thank you for listening to me these days and try to make my life less miserable while writing the thesis. GRACIAS!!

And thanks to my best half, my love, Norman. Thanks for your love, our beautiful nest, your jokes… te adoro!

Thanks to my “Niens-Cioutsoucis-family”, for accepting me in the family and become my family here. Thanks for your love and the beautiful hours together.

Thanks to “Mis chicas”, in Heidelberg Nuria, Rocio e Ixil and out of Heidelberg, the “Uni-girls” Maria, Ari, Violeta and Alba. I love you girls!! And thanks to the “Españolada” for the great moments together! Thank to Juan Manuel and Silvia for the Chocotorta and your warm friendship.

And thanks to my oldest friends, “Los del Parque Avenidas”: Victor, Zusta, Jaime, Pinillos, Padilla, Torres and Begoña. I am what I am, thanks to you.

This 5-year journey is close to the end and I have to admit, that I feel very sad about it. As I always said, “I would have done a 10-year PhD!” And the reason for this is because I have been extremely happy these years. There was difficulties, specially the last three exhausting months, but the overall feeling is that making a PhD is the best decision I have ever taken in my life and if I could, I would start right again from the beginning.